Impacts of Climate Change on Water Resources of Fitzroy River and Tigris River Basins and Identification of Adaptation Measures

Nahlah Abed Abbas

Thesis

Submitted in Fulfilment of the
Requirements for the Degree of
Doctor of Philosophy

the School of Engineering and Technology

Central Queensland University

03/08/2020

CANDIDATE'S STATEMENT

By submitting this thesis for formal examination at CQUniversity Australia, I declare that it meets all requirements as outlined in the Research Higher Degree Theses Policy and Procedure.

STATEMENT AUTHORSHIP AND ORIGINALITY

By submitting this thesis for formal examination at CQUniversity Australia, I declare that all of the research and discussion presented in this thesis is original work performed by the author. No content of this thesis has been submitted or considered either in whole or in part, at any tertiary institute or university for a degree or any other category of award. I also declare that any material presented in this thesis performed by another person or institute has been referenced and listed in the reference section.

COPYRIGHT STATEMENT

ACKNOWLEDGEMENT OF PROFESSIONAL SERVICES

Professional editor, Jeffrey Keddie, provided copyediting and proof-reading services, according to the guidelines laid out in the University-endorsed national guidelines, 'The editing of research theses by professional editors'.

ACKNOWLEDGEMENT OF FINANCIAL SUPPORT

I gratefully acknowledge the funding received from the Australian Commonwealth Government through the Research Training Program which has supported this research.

DECLARATION OF CO-AUTHORSHIP AND CO-CONTRIBUTION

Abbas, N., Wasimi, S.A., Al-Ansari, N., & Baby, S. (2018). Recent trends and long-range forecasts of water resources of northeast Iraq and climate change adaptation measures, Water, *10*(11), p.1562. doi: 10.3390/w10111562.
Status: Published
In conducting the study, I was responsible for collecting data, software setup, management and analysis of electronic data. This publication was written by me. I formed the research question, collated the literature, analysed the data and interpreted the results. (80%)
My co-authors, Professor Saleh, Professor Al-Ansari and Mrs Nasrin critically reviewed the manuscript with questions, comments and criticism. They assisted also provided guidance in editing and preparing the manuscript for submission (20%)

Abbas, N., Wasimi, S.A., Al-Ansari, N., & Baby, S. (2018). Water resources problems of Iraq: Climate change adaptation and mitigation. *Journal of Environmental Hydrology*, *26*. Paper 6, pp. 1-11.
Status: Published
In conducting the study, I was responsible for collecting data, software setup, management and analysis of electronic data. This publication was written by me. I formed the research question, collated the literature, analysed the data and interpreted the results. (80%)
My co-authors, Professor Saleh, Professor Al-Ansari and Mrs Nasrin critically reviewed the manuscript with questions, comments and criticism. They assisted also with guidance in editing and preparing the manuscript for submission (20%)

Abbas, N., Wasimi, S. A., Bhattarai, S., & Al-Ansari, N. (2017). The Impacts of climate change on Fitzroy River basin, Queensland, Australia. *Journal of Civil Engineering and Architecture*, *11*(1), pp. 38-47. doi: 10.17265/1934-7359/2017.01.005.
Status: Published
In conducting the study, I was responsible for collecting data, software setup, management and analysis of electronic data. This publication was written by me. I formed the research question, collated the literature, analysed the data and interpreted the results. (80%)
My co-authors, Professor Saleh, Professor Al-Ansari and Dr. Surya Bhattarai critically reviewed the manuscript with questions, comments and criticism. They assisted also provided guidance in editing and preparing the manuscript for submission (20%)

Abbas, N., Wasimi, S. A., & Al-Ansari, N. (2016). Model-based assessment of climate change impact on Isaac River catchment, Queensland. *Engineering*, *8*(7), pp. 460-470; doi: 10.4236/eng.2016.87043.

Status: Published

In conducting the study, I was responsible for collecting data, software setup, management and analysis of electronic data.
This publication was written by me. I formed the research question, collated the literature, analysed the data and interpreted the results. (80%).

My co-authors, Professor Saleh, Professor Al-Ansari critically reviewed the manuscript with questions, comments and criticism. They assisted also provided guidance in editing and preparing the manuscript for submission (20%)

Abbas, N., Wasimi, S. A., & Al-Ansari, N. (2016). Impacts of climate change on water resources in Diyala River basin, Iraq. Journal of Civil Engineering and Architecture, 10(9), pp.1059-1074; doi: 10.17265/1934-7359/2016.09.009.

Status: Published

In conducting the study, I was responsible for collecting data, software setup, management and analysis of electronic data.
This publication was written by me. I formed the research question, collated the literature, analysed the data and interpreted the results. (80%)

My co-authors, Professor Saleh, and Professor Al-Ansari critically reviewed the manuscript with questions, comments and criticism. They assisted also provided guidance in editing and preparing the manuscript for submission (20%)

Abbas, N., Wasimi, S. A., & Al-Ansari, N. (2016). Climate change impacts on water resources of Greater Zab River, Iraq. *Journal of Civil Engineering and Architecture, 10*(12), pp. 1384-1402; doi: 10.17265/1934-7359/2016.12.009.

Status: Published

In conducting the study, I was responsible for collecting data, software setup, management and analysis of electronic data.
This publication was written by me. I formed the research question, collated the literature, analysed the data and interpreted the results. (80%)

My co-authors, Professor Saleh, and Professor Al-Ansari critically reviewed the manuscript with questions, comments and criticism. They assisted also provided guidance in editing and preparing the manuscript for submission (20%)

Abbas, N., Wasimi, S. A., & Al-Ansari, N. (2016). Assessment of climate change impact on water resources of Lesser Zab, Kurdistan, Iraq using SWAT model. Engineering, 8(10),697-715; doi: 10.4236/eng.2016.810064.

Status: Published
In conducting the study, I was responsible for collecting data, software setup, management and analysis of electronic data. This publication was written by me. I formed the research question, collated the literature, analysed the data and interpreted the results. (80%)
My co-author, Professor Saleh, Professor Al-Ansari critically reviewed the manuscript with questions, comments and criticism. They assisted also provided guidance in editing and preparing the manuscript for submission (20%)

Abbas, N., Wasimi, S. A., & Al-Ansari, N. (2016). Assessment of climate change impacts on water resources of Al-Adhaim, Iraq using SWAT model. Engineering, 8 (10), pp. 716-732; doi: 10.4236/eng.2016.810065.
Status: Published
In conducting the study, I was responsible for collecting data, software setup, management and analysis of electronic data. This publication was written by me. I formed the research question, collated the literature, analysed the data and interpreted the results. (80%)
My co-author, Professor Saleh, Professor Al-Ansari critically reviewed the manuscript with questions, comments and criticism. They assisted also provided guidance in editing and preparing the manuscript for submission (20%)

Abbas, N., Wasimi, S. A., & Al-Ansari, N. (2016). Assessment of climate change impacts on water resources of Khabour in Kurdistan, Iraq using SWAT model. Journal of Environmental Hydrology, 24, Paper 10, pp.1-21; doi: 10.4236/eng.2016.810064.
Status: Published
In conducting the study, I was responsible for collecting data, software setup, management and analysis of electronic data. This publication was written by me. I formed the research question, collated the literature, analysed the data and interpreted the results. (80%)
My co-author, Professor Saleh, Professor Al-Ansari critically reviewed the manuscript with questions, comments and criticism. They assisted also provided guidance in editing and preparing the manuscript for submission (20%)

Abbas, N., Wasimi, S.A. and Al-Ansari, N. (2017). Climate change impact assessment on Greater Zab and Lesser Zab using SWAT model. Proceedings of the 19th International Conference on Water Engineering (ICWE 2017), October 26-27, Istanbul, Turkey. Paper No. 17TR100043. Won the best paper award
Status: Published

In conducting the study, I was responsible for collecting data, software setup, management and analysis of electronic data. This publication was written by me. I formed the research question, collated the literature, analysed the data and interpreted the results. (80%)
My co-author, Professor Saleh, Professor Al-Ansari critically reviewed the manuscript with questions, comments and criticism. They assisted also provided guidance in editing and preparing the manuscript for submission (20%)

Abbas, N. and Wasimi, S.A. (2016). Model-based climate change impact assessment on water resources of Kurdistan, Iraq. Proceedings of the Sixth IASTED International Conference Environment and Water Resource Management (AfricaEWRM 2016), September 5 - 7, Gaborone, Botswana. pp. 79-86. doi: 10.2316/P.2016.836-006.
Status: Published
In conducting the study, I was responsible for collecting data, software setup, management and analysis of electronic data. This publication was written by me. I formed the research question, collated the literature, analysed the data and interpreted the results. (80%)
My co-author, Professor Saleh critically reviewed the manuscript with questions, comments and criticism. He assisted also provided guidance in editing and preparing the manuscript for submission (20%)

Abstract

Australia and Northeast Iraq have scarce water resources which are vulnerable to climate change. Analyses of historical data have revealed that these two regions are experiencing climate change to a degree higher than generally reported elsewhere.

To date the relationship between climate change and its effect on water resources of Australia and Northeast Iraq has been sparsely addressed in the published literature, and almost no attention has been paid to climate change-related water resources issues.

In order to fill that gap, this research work first investigates if there has been a significant change in climate in these two regions, and this has been found to be true. The relationship between climate change and its impact on water resources is explored through the application of the widely used ‘white box’ model SWAT. The model depicts the availability of water resources, classified separately as blue and green waters, for short-term and distant futures for the two regions. Some of the findings are foreboding and warrant urgent attention of planners and decision makers for certain places where (in both regions) the results show that climate change will have major impacts on water resources. The Fitzroy River Basin will experience hotter and wetter weather, while the Iraqi Basin will see hotter and drier weather in the near and distant futures, near being up to 2046-2064 and distant being up to 2080-2100. The research makes some projections of future water resource distributions in the two regions based on climatic scenarios from some widely used General Circulation Model (GCM) ensembles.

The research further investigates how the population is adapting to already changed climates and how it is expected to cope in the future when the shift in climate is expected to be much greater.

ACKNOWLEDGMENTS

I express my profound gratitude and sincere thanks to my principal supervisor, Professor Saleh A Wasimi, my first supervisor, Professor Nadhir Al-Ansari, and my second supervisor, Dr. Surya Bhattarai, for their assistance and guidance. I am indebted to them for the enormous amount of time, effort and support they have given me during the course of this research. Without them it would not have been possible to complete my study.

My heart-felt thanks go to Mr Aun Dhaib, Mr Hussien Baka and Mr Mohamed Saleh, who helped me in collecting different types of data for Iraq, which was not an easy task given the socio-political climate of the country.

My deep appreciation goes to my family, especially my late mother and my late uncle Hameed, who have made me the person I am now. I am grateful also to my friends Haider, Jameel, Hawraa, Lammia, Haifaa and Nasrin for their support and love.

DECLARATION OF AUTHORSHIP AND ORIGINALITY

I, the undersigned author, declare that all of the research and discussion presented in this thesis is original work performed by the author. No content of this thesis has been submitted or considered either in whole or in part, at any tertiary institute or university for a degree or any other category of award. I also declare that any material presented in this thesis performed by another person or institute has been referenced and listed in the reference section.

Nahlah Abed Abbas 26/01/2019

…………………………………….. ……………………………….

(Name of Candidate) Date

Table of Contents

List of Figures

List of Tables

List of Abbreviations

BCM:	Billion Cubic Metres
CMIP:	Coupled Model Intercomparison Project
CMIP3:	The model ensemble for the IPCC’s Fourth Assessment Report (AR4)
CMIP5:	The model ensemble for the IPCC’s Fifth Assessment Report (AR5)
CN:	Curve number (used to estimate direct runoff)
DEM:	Digital elevation model
ENC:	Nasch-Sutcliff efficiency
ENSO:	El Niño Southern Oscillation
ET:	Evapotranspiration
GCM:	General Circulation model
GIS:	Geographic information system
HRUs:	Hydrologic Response Units
MUSLE:	Modified universal soil loss equation
PDO:	Pacific Decadal Oscillation
R^2:	Coefficient of determination
SCS:	Soil conservation service
SUF1-2:	Sequential uncertainty fitting algorithm version 2
SWAT:	Soil water assessment tool
WCRP:	World climate research program

CHAPTER 1

INTRODUCTION

1.1 Background

Climate change occurs naturally, but during the last century global warming has been so rapid that it cannot be attributed to natural causes alone (Ammann et al. 2007; IPCC5 2014). It is now believed that anthropogenic activities such as burning of fossil fuel and land cover conversion (e.g., deforestation) have led to increase in greenhouse gases: elevated CO_2 concentrations and other greenhouse gases (e.g., CH_4, N_2O, etc.) have the potential, by modifying radiative forcing, to cause global warming, which is assumed to have started since the industrial revolution of the 1850s. Many studies indicate that global warming is highly likely to cause climate shifts (Wu and Johnston 2007). Based on observed and modelled data, it has been established that elevated CO_2 concentration and climate shifts would impact considerably hydrological cycles mainly through the alteration of evapotranspiration and precipitation (Mimikou et al. 2000; Ragab and Prudhomme 2002; Yu et al. 2002; Pechlivanidis et al. 2011; Winter and Eltahir 2012; Coffey et al. 2014; Xuan and Chang 2014). Changes in rainfall intensity and volume from the historical normal have been observed since the last century, and, if the trend continues, there will be more frequent manifestations in the future of precipitation extremes, both dry and wet, which are of major concern due to their potential to cause hardship (Pruski and Nearing 2002; Delpla et al. 2009). The dry or wet extremes often cause severe droughts or major floods, respectively, imparting greater variability in river discharge and soil moisture (Owor et al. 2009) with far-reaching environmental consequences. A further ramification of climate change is the modification of water quality (Wilson and Weng 2011). Any increase in rainfall, whether in size of raindrops or storm intensity may directly exacerbate soil erosion, which, in turn, could increase the loads of sediment yields, suspended solids and *E. coli* (Delpla et al. 2009; Whitehead et al. 2009), and all of these influence surface water qualities. Droughts are also thought to affect water quality (Yu et al. 2002). In drought events, long residence time and reduction in water volume occur, leading to increased water temperatures and salinity, lower dissolved oxygen concentration, and increased algal blooms (Somville and De Pauw 1982; Murdoch et al. 2000; Van Vliet and Zwolsman 2008; Pechlivanidis et al. 2011; Van Vliet et al. 2011; Mosley et al. 2012).

Australia and MENA (Middle East and North Africa) regions are highly vulnerable to climate change and variability (IPCC 2014). Australia has a highly variable dry climate, along with weather induced catastrophes such as bushfires, floods and droughts – all of which could be aggravated by climate change (Keenan and Cleugh 2011). The MENA region in most parts is semi-arid to arid, typically with less than 150 mm of annual rain and high evaporation rates (IPCC 2014), which will be impacted significantly with any slight change in climate. Water scarcity has recently emerged in large parts of both regions (Australia and MENA) and could get worse due to changing climate (IPCC 2014). Arguably, climate change is one of the greatest challenges confronting these regions: it could have significant adverse effects on water resources and hence the environment and economy, particularly in the agricultural sector. Thus, there is an imperative for predicting the potential impacts of climate change, specifically on the duration and magnitude of precipitation, that have ramifications for sustaining and managing water resources appropriately. Already it has been reported for some regions that water scarcity has become significantly worse (Chowdhury et al. 2014; Al-Ansari et al. 2014). Unfortunately, however, todate water issues related to climate change have not been well addressed within climate change analyses and climate policy construction (IPCC 2014) and, particularly in Australia and MENA, very little attention has been paid to climate change-related water resources issues (Government of Queensland 2014; Issa et al. 2014). Given this perspective, the main objective of this research is to develop suitable tools for long-term predictions of the changes in basin characteristics due to an altered nature's forces and processes, particularly climate change, and to identify water availability in two forms – blue water, which is directly accessible water to humans, and green water which is not directly accessible such as soil water content – and also to identify potential impacts due to climate change in the Fitzroy River basin in Australia, the largest river basin on the Australian east coast (Lough 2007), and in the five tributaries of the Tigris River basin in Iraq, which contributes 80% of Tigris flow (Issa et al. 2014).

1.2 Problem outline

Australia and MENA are highly vulnerable to climate change due to their geographical and hydrological uniqueness (Hughes 2003; Issa et al. 2014). Australia is the driest inhabited continent in the world and is recognised as one of the most vulnerable to climate change (Hughes 2003; Rotstayn et al. 2007; Timbal and Jones 2008; Keenan and Cleugh 2011; Cai et al. 2014; Chowdhury et al. 2014). The continent has a high degree of rainfall variability and extreme weather events, such as floods and droughts, which are likely to appear more often in the future due to climate change (Nicholls et al. 1997). The MENA region, by contrast, is an enormous zone of generally varied climatic conditions categorized by a high degree of aridity and highly variable and very low annual rainfall (Medany 2008) that could experience major environmental changes due to any climatic shift. Most of the MENA region lands are classified as arid to semiarid due to the typical annual precipitation being below 150 mm (Al-Ansari et al. 2014).

Climate shift has been significant since the last century, in both regions (Australia and MENA), mainly through observed increases in surface air temperature (IPCC 2014). In Australia, during the period of 1950 to 2010, mean surface air temperature increased by 0.9°C, greater than the global average of 0.7°C, and the rising trend is continuing (Keenan and Cleugh 2011). In the MENA region, since the 1950s the average temperature has increased by 0.2°C to 0.3°C per decade (Zakaria et al. 2013) and it is projected to increase by 3°C to 5°C by the end of this century (Elasha 2010). As a consequence of increases in mean air temperature, changes are occurring in fundamental hydrological processes such as rainfall, runoff and evaporation (Chowdhury et al. 2014). Australia and MENA have experienced significant changes in rainfall since the 1900s, in particular after the 1950s, leading to changes in water availability and quality (IPCC 2014). Changes in water quantity have caused water shortage problems and a disruptive modification in the utilization of water resources such as water allocation systems and hydropower sites (Medany 2008). Water quality also has degraded in response to climate change (IPCC 2014). Therefore, analysis of potential impacts of climate change on watersheds is important for Australia and MENA.

1.3 Aims and objectives

The proposed research is an attempt to better understand the hydrological characteristics of the basins and their vulnerability to climate change. This will require development and application of suitable mathematical tools that can be used for long-term predictions of the changes in the two basins. These tasks are envisaged within the framework of the use of a geographic information system (GIS), the calibration of a physics-based, spatially distributed watershed model, SWAT, the incorporation of climate forecasts from General Circulation Models (GCMs), and statistical analyses.

The specific objectives of this research are to investigate the alteration of blue and green water regimes as a function of changes in rainfall volume and intensity, as well as evapotranspiration due to climate change, and to examine possible opportunities and challenges of sustainable utilization of water resources in climate adaptation strategies in the Fitzroy and the Tigris river basins.

The following main objectives are addressed:

1. Determination of the performance and suitability of the three tools – GIS, SWAT and statistical analyses.
2. Improved understanding of the existing hydrological systems and investigation as to how changes in climate (rainfall and temperature) may affect and alter streamflow regimes and other hydrological processes under different climatic scenarios.
3. Identification and understanding of the various aspects of implications of climate change in these regions.
4. Development of suitable tools which could be used by organizations to account for climate change impacts, adaptations and vulnerability in their planning and management strategies.

1.4 Organization of the thesis

This thesis comprises eight chapters to address the specific objectives. The second chapter describes the study areas of the Fitzroy and Tigris River basins in detail, including the location, climate, soil and land use types. The third chapter describes the software and method used in this thesis, which include GIS software, the SWAT model, the SUFI-2 technique and general circulation models (GCMs). The fourth chapter presents statistics on several variables such as temperature, precipitation, sea level, etc., as historically observed, as well as trends for both regions. The fifth chapter addresses the calibration, validation and sensitivity analysis aspects for the discharge stations in both regions (Tigris and Fitzroy). Chapter six presents and discusses the results. Chapter seven considers possible adaptation and mitigation measures that could be undertaken in response to climate change. Chapter eight draws the thesis work to a conclusion. The importance of the research and future research prospects are also discussed in the final chapter.

CHAPTER 2

STUDY AREAS

2.1 Fitzroy Basin

The Fitzroy River basin is the largest river basin on the east coast and the second largest seaward-draining catchment in Australia. It extends from the city of Rockhampton to Carnarvon Gorge National Park in the west, and drains an area of approximately 142,645 km^2 (approximately 10 percent of Queensland's land area) to the southern end of the Great Barrier Reef (GBR) (Cobon et al. 2007). Originally, most of the catchment was dominated by Brigalow (Acacia harpophylla) forest and other ecosystems such as eucalypt forests, grasslands, and riparian communities, but these were mostly cleared in the 1960s and 1970s (Yu et al. 2013).

The basin comprises the catchment of the Fitzroy River and its major tributaries: the Nogoa, Comet, Connors-Isaac, Dawson, and Mackenzie Rivers (Rolfe et al. 2004) (Figure 2.1). The Nogoa River is in the far west of the basin, flowing through Emerald, and it later links with Theresa Creek that comes from the northwest around Clermont. The Comet drains the south-central part of the basin and then combines with the Nogoa, forming the Mackenzie River. The Connor-Isaac drains the northern part of the basin and then is joined by the Mackenzie just upstream of the Tartaeus Weir. The Dawson drains the southern part of the basin and joins the Mackenzie further downstream. The combined stream is referred to as the Fitzroy, debouching into the southern Pacific Ocean approximately 60 km downstream of Rockhampton (Dougall 2014).

The climate of the Fitzroy Basin is tropical to sub-tropical, ranging from semi-arid inland to humid near the coast, with wet summers and mild to dry winters (Government of Queensland 2014). The mean annual temperature varies between 19.2°C in the south and 22.6°C in the north. There is a high level of rainfall variability within the catchment due to climatic drivers such as the El Niño Southern Oscillation (ENSO) and the Pacific Decadal Oscillation (PDO) (Lough 2007). Mean annual rainfall ranges from greater rainfall areas close to the coast, with up to 1800 mm in the east and up to 600 mm in the west. Rainfall is mostly linked to the tropical monsoon, with occasional widespread heavy rainfall from tropical cyclones from the Coral Sea off the east coast of Queensland (Yu et al. 2013). Flows are highly variable within and between years: greater than 90% of flow occurs in the wet season from December to May (Lough 2007).

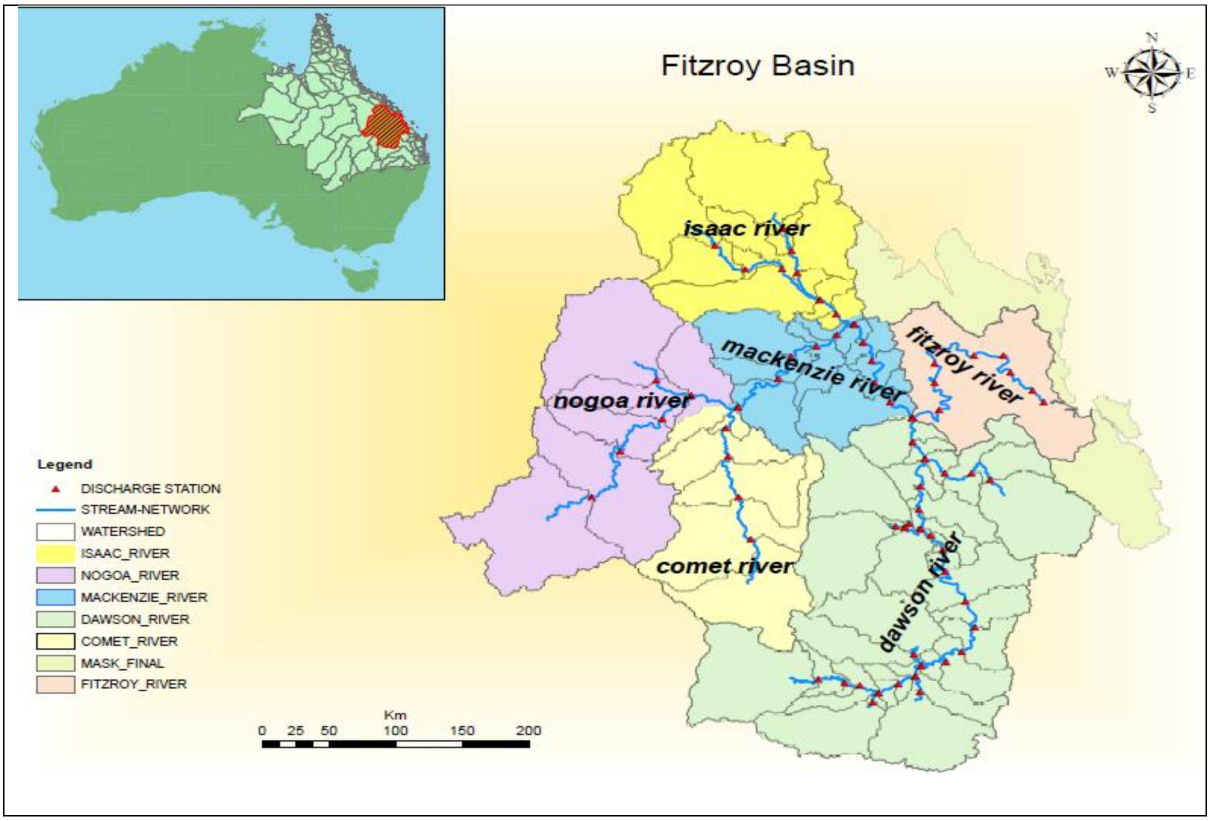

Figure 2.1: Stream network, location of major reaches and sub-catchments of the Fitzroy River basin (Source: original work created for this thesis)

The soils of the Fitzroy Basin are diverse owing to large variations in lithology, climate and geomorphic processes. More than 100 soil types are recorded in the catchment and no one soil group is dominant (Dougall 2014) (Figure 2.2).

The most common land use in the catchment is grazing. Large areas of dry-land cropping are present in the western part of the basin, whereas irrigated cropping occurs in the towns of Emerald, Theodore and Biloela. Extensive coal mining is occurring in the Bowen Basin, especially around the towns of Moranbah, Dysart, Blackwater and Moura (Dougall 2014) (Figure 2.2).

The Fitzroy Basin is of significant importance to Queensland, and considered one of the richest areas in the state due to its land, minerals and water resources; it supports industry sectors such as grazing, agriculture, mining, forestry and tourism. It contains approximately 10% of the state's agricultural land and 95% of the catchment is under agricultural land-use, comprising about 87% grazing and 13% cropping (Cobon et al. 2007). This basin is the main source of fresh water to approximately 185,000 people or 5.3% of the state's population (Rolfe et al. 2004). Water demand is expected to increase as population is projected to grow rapidly (Australian Bureau of Statistics 2014). Climate change is projected to enhance discussion, debate and dialogue on water issues in this region (Cobon et al. 2007).

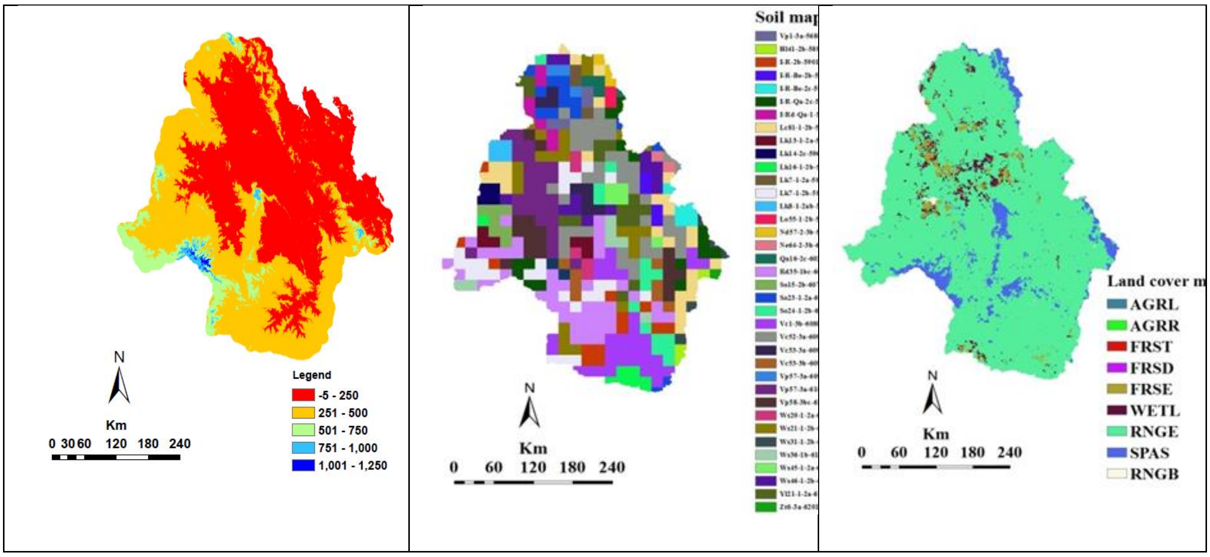

Figure 2.2: From left to right DEM, soil and land cover map of Fitzroy Basin (Source: original work created for this thesis)

The Fitzroy River basin was selected as a study area for following reasons. Firstly, the region is highly vulnerable to climate change and variability (Yu et al. 2013), which made this area a hot spot for research in terms of climate change. Secondly, although extensive research exists on the basin, to the best of our knowledge no climate change-related water issues studies have been conducted before this study. This study is envisaged to fill the gap of lack of knowledge of climate change-related water issues. This would support decision makers in planning relevant adaptation and mitigation measures, and thus decrease the adverse impacts on water resources in the basin. In addition, the Fitzroy Basin is located in a sub-tropical environment: there is a high level of rainfall variability within the catchment due to climatic drivers. Consequently, flows are highly variable within and between years. Recently, Fitzroy basin is experiencing more frequent extreme rainfall and heat waves.

2.2 Tigris Basin

The Tigris River has five major tributaries: the Khbour, Greater Zab, Lesser Zab, Al-Adhiam and Diyala Rivers (Figure 2.3). These tributaries are located in the left bank of the Tigris River and make a significant contribution to Tigris flow. These tributaries are shared between Iraq and Turkey or Iraq and Iran, except for the Al-Adhiam River.

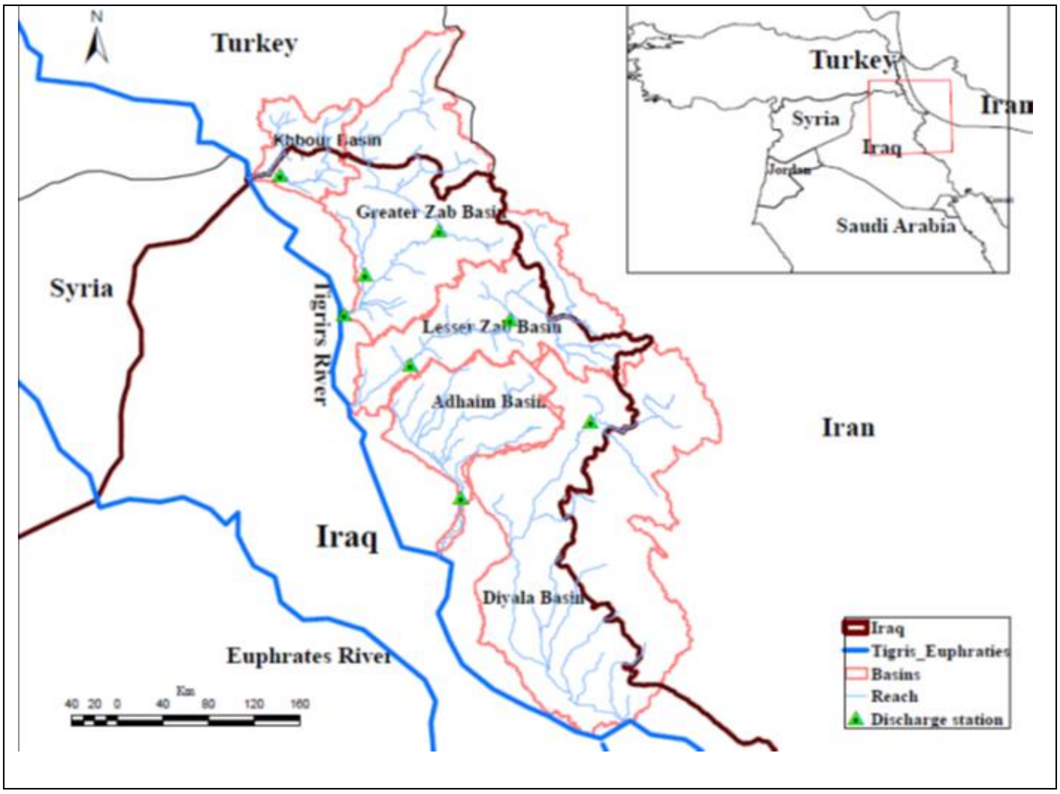

Figure 2.3: Location map of the study area in MENA (Source: original diagram created using data from (Al-Ansari et al., 2014)

2.2.1 Khbour sub-basin

The Khbour (Figure 2.4, Table 2.1) rises from the Eastern Anatolia Region in Turkey, flows to the south crossing Turkey-Iraqi border and then to the west through Zakho City, and finally joins the Tigris River a small distance to the south. The mean annual flow of the Khbour is 68 m^3/sec and its length is 181 km (UN-ESCWA and BGR 2013). The basin is highly mountainous, with various elevations ranging from 300 to 3300 m above the sea level. Many springs rise in the basin. The mean annual temperature is 10°C and mean annual rainfall 780 mm. About 60% and 25% of precipitation, including snowfall, occurs in winter and spring, respectively. In autumn and summer, 14% and 1% of precipitation, respectively, falls as rain. The flow regime of the Khbour River demonstrates highly seasonal flow, with peak flow occurring in May and low seasonal flow from July to December (Figure 2.5). This is a typical near-natural nival regime, in which winter precipitation in the form of snow and snow-melt in the spring is dominant. Approximately 46% of the watershed is covered by forest, 30% by wetland (forested) and 23% of the land is used for agriculture. Up-to-date information on water use in the basin is very limited and no water resources management study is available for this basin (UN-ESCWA and BGR 2013).

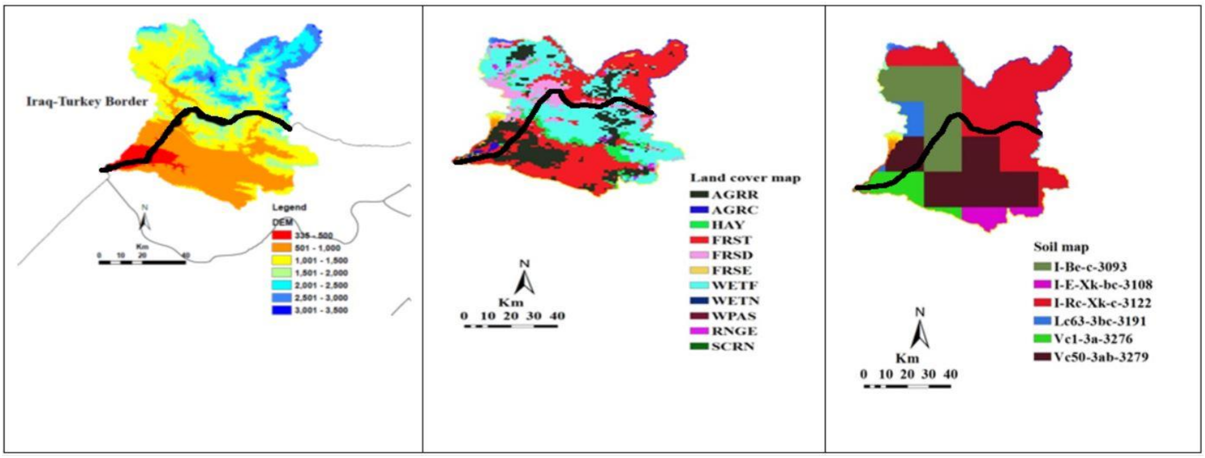

Figure 2.4: From left to right DEM, land cover and soil map of the Khbour sub-basin (Source: original work created for this thesis)

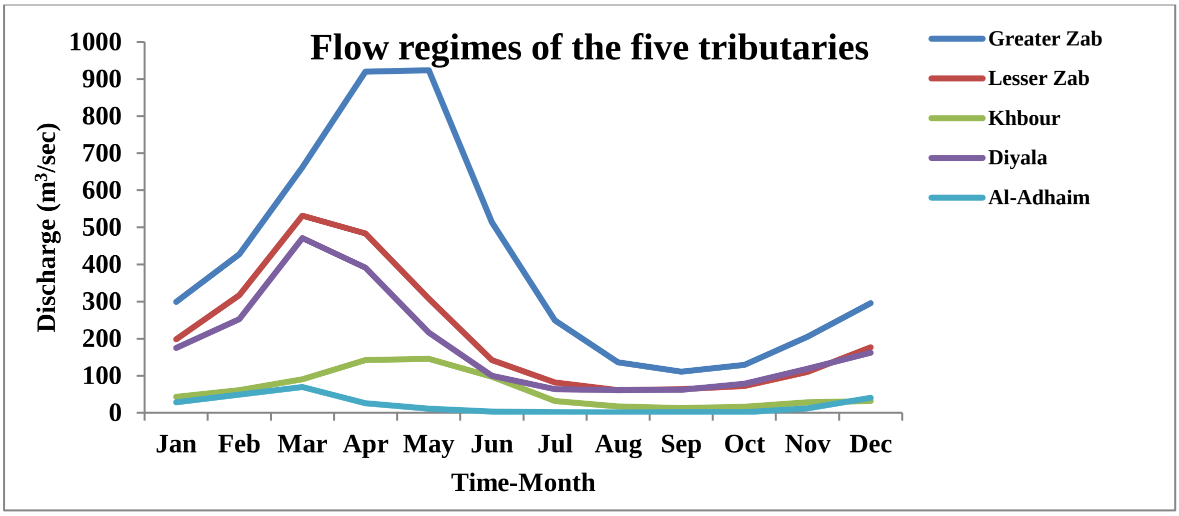

Figure 2.5: Average monthly flow regimes of the main Tigris River tributaries at different discharge stations (at Zakho station in Khbour sub-basin, at Eski Kalak station in Greater Zab, at Dukan station in Lesser Zab, at Injana station in Al-Adhaim and Derbendikh station in Diyala) for the period 1960 to 1990 (Source: original work created for this thesis)

2.2.2 Greater Zab sub-basin

The Greater Zab (Figure 2.6, Table 2.1) is the major Tigris tributary in terms of water harvest. It originates from the Ararat Mountains in Turkey and runs through the central northern part of Iraq and then links with the Tigris River south of Mosul city. This basin is situated between latitudes 36^0N and 38^0N, and longitudes 43.3^0E and 44.3^0E. It comprises four main tributaries: the Shamdinan, Haji Beg, Rawandooz and Khazir-Gormal Rivers (Kafia et al. 2009). Based on some estimates, the Greater Zab contributes about 35% of Tigris flow (UN-ESCWA and BGR 2013). Similar to the Khbour sub-basin, the Greater Zab sub-basin is mountainous, with many springs and most of the precipitation, including snow falls in winter and spring (Abdulla and Al-Badranih 2000). The mean annual temperature is 14.3^0C and mean annual precipitation is 570 mm. Similar to the Khbour flow pattern, rainfall and snow melt lead to a typical nival flow pattern with a distinct high flow season in spring and a peak flow in May (Figure 2.5). Seventy nine percent of the watershed is covered by pasture, and 21% of the land is used for varying agriculture.

Table 2.1: Description of the basins of the five tributaries of the Tigris River (UN-ESCWA, BG R 2013)

River	Khbour	Greater Zab	Lesser Zab	Al-Adhaim	Diyala
Basin area (Km^2)	6143	26473	15600	13,000	33240
Basin area shares (%)	Iraq 43%	Iraq 65%	Iraq 80%	Iraq 100%	Iraq 75%
	Turkey 57%	Turkey 35%	Iran 20%		Iran 25%
River length (Km)	181 km	462 km	302 km	230	574 km
Maximum annual flow (BCM)	4.3	23.6	15.1	1.2	14.4
Minimum annual flow (BCM)	0.9	3.7	1.7	0.4	1.2
Mean annual flow (BCM)	2	12.7	7.8	0.80	4.6
Dams	Unregulated	Unregulated	2	1	3

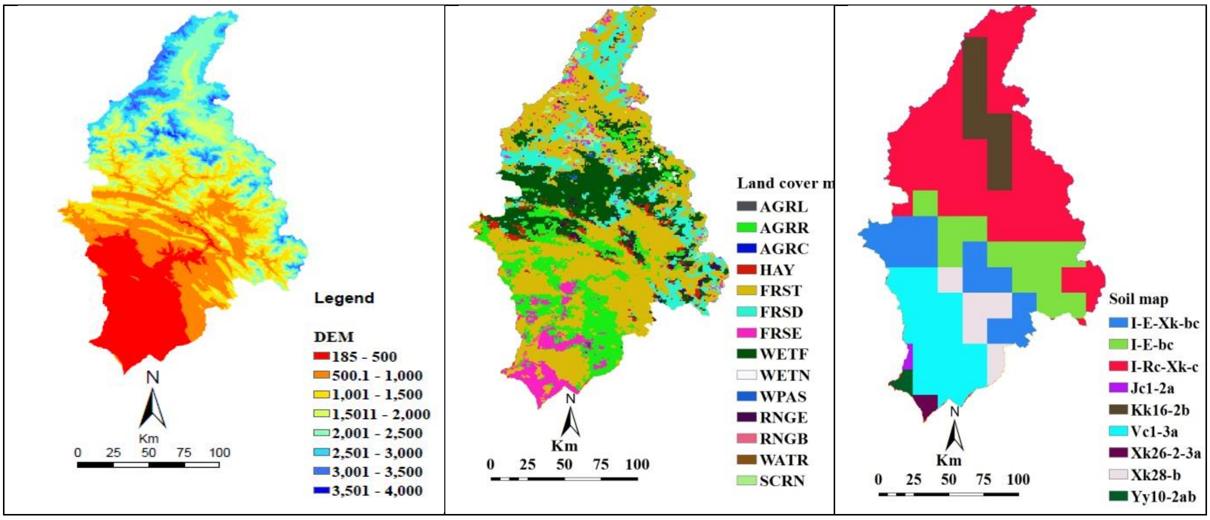

Figure 2.6: From left to right DEM, land cover and soil map of Greater Zab sub-basin (Source: original work created for this thesis)

2.2.3 Lesser Zab sub-basin

Further south of Mosul, the Lesser Zab (known also as little or lower Zab) (Figure 2.7, Table 2.1) links with the Tigris River. It originates from north-eastern Zagros Mountains in Iran adjacent to the Iraqi border. The Lesser Zab watershed is located approximately between latitudes 35.16^{0}N and 36.79^{0}N and longitudes 43.39^{0}E and 46.26^{0}E (Saeedrashed and Guven 2013). The Lesser Zab joins the Tigris River at Fatah (Al-Ansari and Knutsson 2011). Its average discharge contribution to the Tigris River is about 191 m^3/s (UN-ESCWA and BGR 2013). Al-Ansari et al. (2014) state that the main contribution to Tigris discharge originates from the Greater and Lesser Zab Rivers, which is estimated at about 40-60% of total Tigris flow. The mean annual temperature is 16°C and mean annual precipitation is 670 mm, most of which falls in winter and spring, with less snowfall compared to the Greater Zab River. The Lesser Zab streamflow shows similar dynamics and seasonal variations to other tributaries of Tigris. Peak flows of the Lesser Zab occur in early spring (April) (Figure 2.5), generally due to the low snowfall level and early snowmelt. Approximately 70% of the watershed is covered by pasture and 30% of the land is used for agriculture.

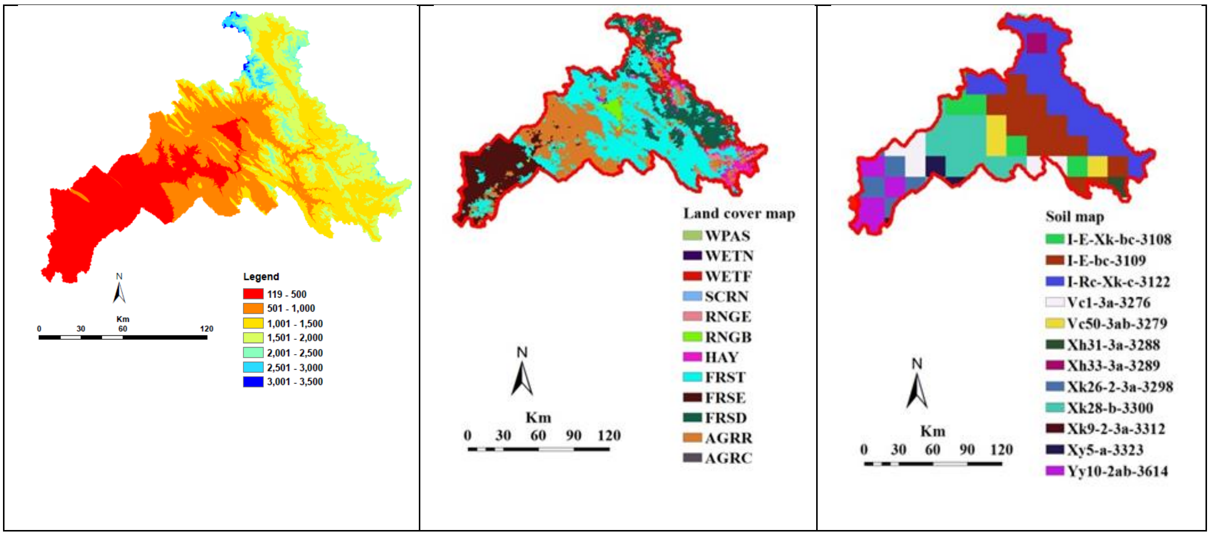

Figure 2.7: From left to right DEM, land cover and soil map of Lesser Zab sub-basin (Source: original work created for this thesis)

2.2.4 Al-Adhaim sub-basin

Al-Adhaim or Nahr Al Uzaym (Figure 2.8, Table 2.1) is located in northeast Iraq, and rises from the hilly and mountainous areas in Iraq. The basin is characterised by limited rainfall and no snowfall. The basin is fed by rainfall only, and therefore the occurrence of effective flow is during the wet season (Al-Kadhimi et al. 2013; Abdulla and Al-Badranih 2000). It links with the Tigris River approximately 13 km downstream of Balad city (UN-ESCWA and BGR 2013). The annual precipitation for the Al-Adhaim sub-basin ranges from 80 to 330 mm, and temperatures vary between 2^0C and 48°C. The Al-Adhaim flow system is classified as an irregular flow system that depends greatly on precipitation (Abdulla and Al-Badranih 2000). This river runs dry in summer from May to October and high flow occurs during November to May (Figure 2.5). Accordingly, the Al-Adhaim can be classified as an arid basin. Approximately, 71% of the basin is covered by forest and 29% by agricultural land.

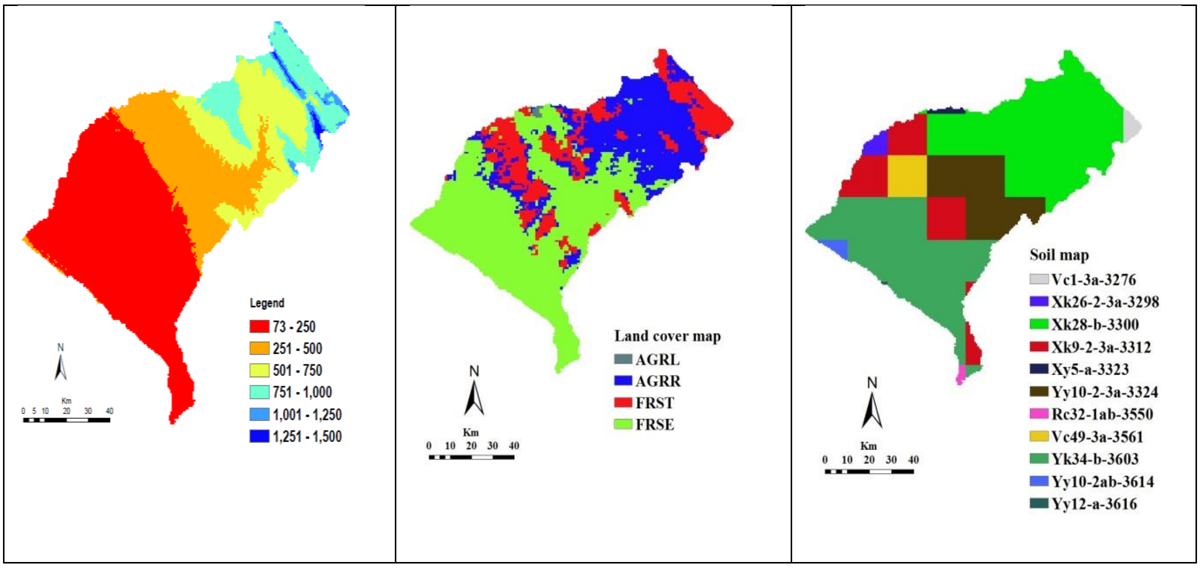

Figure 2.8: From left to right DEM, land cover and soil map of Al-Adhaim sub-basin (Source: original work created for this thesis)

2.2.5 Diyala sub-basin

The Diyala sub-basin (Figure 2.9, Table 2.1) originates in the Zagros Mountains in Iran, shaping the Iran-Iraq border for more than 30 km (Al-Ansari et al. 2014). The basin is situated between latitude 33.22^{0}N and 35.83^{0}N, and longitude 44.50^{0}E and 46.83^{0}E. Its main tributaries are the Sirwan, Tanjeru and Wand Rivers (Al-Faraj and Scholz 2014). The Diyala River links with the Tigris River 15 km south of Baghdad. More dams have been built along the Diyala River compared to other Tigris tributaries. Three dams have been built within Iraqi part (Derbendikhan Dam, Hemrin Dam, Diyala Weir) for multipurpose uses. In spite of the construction of these dams, no significant influence on flow volumes and flow regime have been detected (UN-ESCWA and BGR 2013). Mean annual temperature is 36°C and mean annual precipitation is 420 mm. The Diyala flow regime is very similar to the Lesser Zab streamflow (Figure 2.5). The peak flows occur in April and low flows from July to November. Approximately 77% of the watershed is covered by forest and 23% of the land is used for agriculture. Due to unavailability of data for the whole sub-basin, the upper part of the sub-basin was studied only.

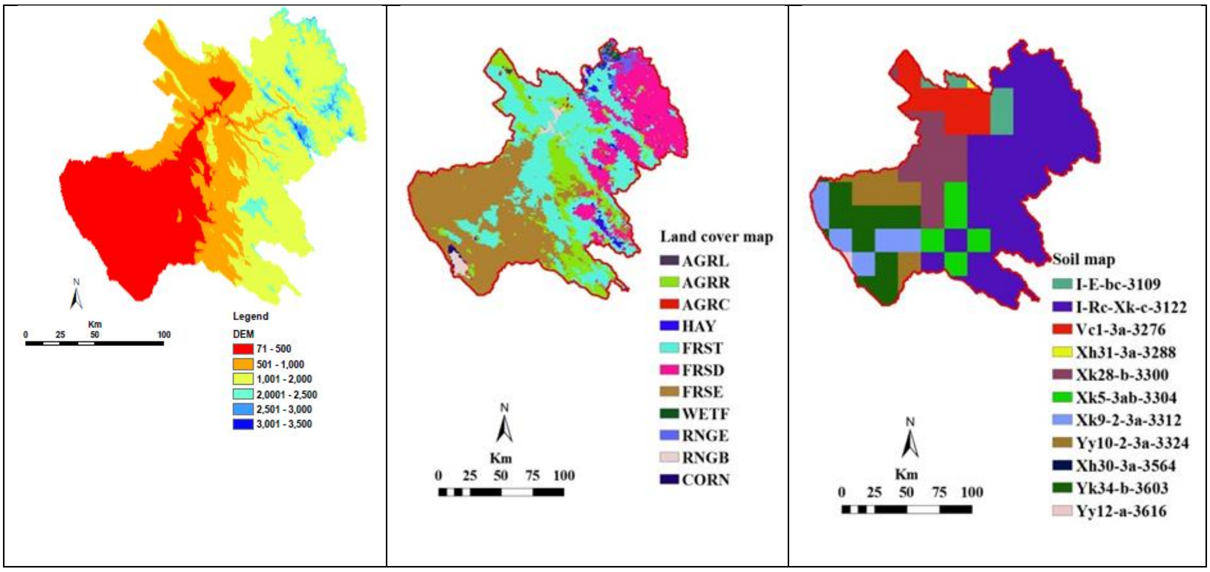

Figure 2.9: From left to right DEM, land cover and soil map of Diyala sub-basin (Source: original work created for this thesis)

The Tigris basin was selected for the following reasons. The Tigris River is the main fresh water source for two-thirds of Iraq's population. It is in a semi-arid to arid region, typically with less than 150 mm annual rain and high evaporation rate (IPCC 2014), which would be influenced considerably with any slight change in climate. Water scarcity has recently emerged in large parts of the region and could become worse due to changing climate (IPCC 2014). Climate change is one of the greatest challenges confronting this region: it could have significant adverse effects on water resources and hence the environment and economy, particularly in the agricultural sector (Al-Ansari et al. 2014). Unfortunately, due to ongoing war, social unrest and insecurity very little attention has been paid to climate change-related water resources issues (Issa et al. 2014). Thus, there is an imperative for predicting the potential impacts of climate change. This study would be the first initiative to study these impacts scientifically based on modelling.

To summarise, the Fitzroy River is located in a sub-tropical area that is rich in resources, minerals and economic activities, and supports industry sectors such as grazing, agriculture, mining, forestry and tourism. The Tigris River basin is arid to semi-arid; it rises in the mountains of Anatolia, Turkey and flows through Iraq. Although the Tigris River is considered the most important river for Iraq and the only water source for Baghdad, capital of Iraq, it is plagued by poverty and exhibits low economic activities. These two rivers have been selected because of their known effects due to climate change: the Fitzroy basin is experiencing more frequent extreme rainfall and heat waves, while the Iraqi basin is experiencing more frequent droughts and high air temperatures. Table 2.2 shows a comparison between the two basins.

Table 2.2: Comparison between Fitzroy basin, Australia, and Tigris basin, Iraq

Basin	Size\ km^2	Length\ km	Sub-basin	Topography	Land use	Soil types	Weather	Flow
Fitzroy	142,645	480	5	Hilly to flat	87% grazing, 30% is cropping, mining forest	100	tropical to sub-tropical, high level of rainfall variability	highly variable
Tigris	70.471	1300 within the study area, total length 1850	5	highly mountainous to flat	North of the basin 70%is pasture 30% different agriculture activities while the south 70 % forest and 30% land activities	12	arid to semiarid with less than 150 mm annual rainfall	seasonal

CHAPTER 3

MATHEMATICAL MODELS

3.1 Geographic Information Systems (GIS)

Geographic Information Systems (GIS) are computer-based systems comprising an integrated hardware, software and data system that can capture, store, manage, visualise, question, analyse and demonstrate all forms of topographical or spatial data so that trends, patterns and relationships in complicated data sets can be revealed (Wieczorek and Delmerico 2009). Recently, GIS has been used as a great tool to function a superior decision support system to prepare, manage and implement water resources (Setegn et al. 2008). GIS was developed in the 1960s by Roger Tomlinson in Canada and was called Tomlinson's Canada Geographic Information System (CGIS) (Wieczorek and Delmerico 2009). CGIS was initially developed to record natural resources such as soil and timber, but the usage of GIS worldwide began in the 1970s (Wieczorek and Delmerico 2009).

The major aspects related to GIS are GIS base design, critical concepts of geographic data and spatial analysis. The definition of GIS has changed over time based on the broad applications for which GIS has been used. The definition can also change based on the growth of GIS together with other technical expansions such as computer information systems, software, and analytical algorithms (Wieczorek and Delmerico 2009). This has resulted in changing the target definitions over time. Following are some examples of GIS definitions:

- “Set of tools for collecting, storing, retrieving at will, transforming and displaying spatial data from the real world for a particular set of purposes” (Burrough 1986, in Klosterman 1991).
- “…an organized collection of computer hardware, software, geographic data, and personnel designed to efficiently capture, store, update, manipulate, analyze, and display all forms of geographically referenced information” (ESRI 1990, in Wieczorek and Delmerico 2009).
- “Automated systems for the capture, storage and retrieval of spatial data” (Clarke 1997 in Wieczorek and Delmerico 2009).
- “ … system for input, storage, manipulation, and output of geographic information; a class of software; a practical instance of a GIS combines software with hardware, data, a user, etc., to solve a problem, support a decision, help to plan…” (Goodchild 1992).

Geography is of importance in GIS application, because nearly every aspect or decision has a geographic element (Wieczorek and Delmerico 2009). Geographic information has connections to spatial features of the earth. This includes all of the spheres linked with earth such as the biosphere, lithosphere, atmosphere and hydrosphere (Tait 2005). Geographic data are saved and analysed in GIS using different methods. The major two applied methods to store and analyse geographic data are vector and raster illustrations. Vector data represent particular locations of geographic features such as points, lines and areas. Raster data are imageries symbolized by the number of cells (or pixels) in a row-and-column format comprising the image (Tait 2005). The number of cells is often reasonably large, particularly for a high-resolution image (Higgins et al. 2007). By contrast, vector data storage is generally parsimonious, as the geographic characteristics are characterized by nodes (points) that can be linked with lines which create the features (Tait 2005).

Spatial analysis demands facilities for the input, management and display of spatially-based data. All these facilities are currently available within existing GIS packages (Goodchild et al. 1992).

3.2 Hydrological models

Hydrological models offer a framework in which the relationships between climate and water resources can be generated and examined. Hydrological models are important for water resources management, flood prediction and design, water quality assessment and climate. They are meant to accurately predict the apportioning of water among different pathways of the hydrological cycle (Leavesley 1994). This apportioning is estimated by the water balance equation:

$$Q = P - ET \pm \Delta S \qquad (1)$$

where Q is runoff, P is precipitation, ET is evapotranspiration, and ΔS is the change in system storage.

According to Pechlivanidis et al. (2011), hydrological models are classified into three categories: empirical (black box), conceptual (grey box) and physics-based (white box), depending on the amount of detailing of the hydrological processes that exist in a watershed. Empirical models are built by empirically observed data that only capture the relationship between input and output; conceptual models contain hypothetical elements which simulate to some degree the internal working of the real-world process; and physics-based models use the laws of physics to describe the hydrological processes.

Empirical models are beneficial for predicting hydrology and soil erosion, based on the definition of the significant factors via field observations, measurements, experiments and statistical methods; however, they are site-specific and require long-term data (Leavesley 1994; Nearing et al. 1994). An early example of an empirical model is the unit hydrograph theory for event-based catchment scale simulation that was developed by Sherman in 1932 (Jakeman et al. 1990); this model was applied with ease for ungauged catchments. Some more recent empirical models that have been developed are Data Based Mechanistic (DBM) modelling (Young 1998) and Artificial Neural Networks (ANN) (Lange 1999). DBM has "been developed as an empirical transfer function model based on the available input-output data" (Young 1998); therefore, factors can be assessed from input-output data only. ANN is able to calculate a complete hydrograph for any rainfall distribution. Furthermore, this method has been developed to develop a hydrograph out of a neural network which can be compared to a unit hydrograph.

Conceptual models are based on two criteria. Firstly, the structure of the model should be specified before conducting any modelling, and, secondly, not all of the model parameters have a direct physical interpretation (Leavesley 1994). They are useful in representing all of the component hydrological processes recognized as important in catchment scale input-output relationships (Pechlivanidis et al. 2011). However, they are unable to fully describe other physical processes such as sediment movement (Elliot and Hall 1997). TANK (Sugawara 1974) and NAM (Nedbør Affstrømnings Model) (Nielsen and Hansen 1973) are examples of conceptual models. The TANK model is a simple model, composed of three tanks placed one above the other in sequence (Jeong and Kim 2005). The runoff from the tank model can be evaluated by the sum of the discharges from the several tanks; streamflow routing is conducted by using an additional tank (Tingsanchali and Gautam, 2000). In the NAM model the overland flow and interflow are directed via two linear reservoirs in series and ground water flow via a single linear reservoir (Tingsanchali and Gautam 2000).

Physics-based models are major tools for analysing the effects of land management practices on water, sediment and water quality in large complex watersheds (Pechlivanidis et al. 2011). They are based on identifying the essential physical processes and invoking the conservation laws of mass, momentum and energy (Petter 1992). Most of these models attempt to account for the watershed heterogeneity and spatial distribution of topography, soil characteristics, land use, rainfall, and evaporation (Setegn 2010).

Recently, some of the physics-based watershed models developed and which have gained popularity are Chemicals Runoff and Erosion from Agricultural Management Systems (CREAMS) (Knisel 1980), Agricultural Non-Point Source Model (Young et al. 1989), Water Erosion Prediction Project (WEPP) (Nearing et al. 1989), European Soil Erosion model (EUROSEM) (Morgan et al. 1998) and Soil and Water Assessment Tool (SWAT) (Arnold et al. 1998). Among these models, SWAT, a physics-based distributed model, is well-recognised for the analysis of the impacts of land management practices on water, sediment, agriculture, and non-point pollution in large complex watersheds (Schuol and Abbaspour 2007). The SWAT model is also capable of assessing the impacts of climate change on hydrological and biochemical cycles on a long-term basis (Nietsch et al. 2005). After a review of models, the SWAT model was adopted for this study because it was deemed the most appropriate.

3.2.1 SWAT Model Applications and literature review

The SWAT (Soil Water Assessment Tool) was originally developed by the United States Department of Agriculture (USDA) and the Agricultural Research Service (ARS) at the Grassland, Soil and Water Research Laboratory in Temple, Texas (Nietsch et al. 2005). The SWAT model is a watershed-scale, semi-distributed streamflow model. It is used to analyse hydrological characteristics and water quality at various sub-watershed scales with different soils, land use and management conditions on a long-run basis (Arnold et al. 1998). To fulfil this objective, the model –

- is physics-based discrete time (daily computational time step) analytical, rather than regression type equations that describe the relationships between input and output data. SWAT requires data about climate, topography, soil properties, land use/cover and land management practices occurring in a watershed. The physical processes related to water movement, sediment movement, plant growth, nutrient cycles, etcetera are directly simulated by SWAT model using the input data (Arnold et al. 1998).

- uses available hydro-meteorological data: SWAT requires a certain minimum amount of data to run which is normally accessible from government agencies.

- has capability of simulating large basins or basins with different management practices.

- allows users to simulate long-term impacts such as the impacts of climate and land change.

The SWAT model has been successfully applied for watershed analysis studies worldwide. One of the earliest studies is by Bingner (1996) in northern Mississippi, where SWAT was validated for streamflow in various sub-catchments on daily and annual scales. Another is by

Arnold et al. (1998), where the SWAT model was successfully applied for several watersheds in Texas using a large number of stream discharge stations. Santhi et al. (2001) applied the SWAT model satisfactorily in a large watershed, Hico and Valley Mills, along the north Bosque River in Texas. White and Chaubey (2005) used various discharge stations to calibrate and validate their model successfully in Illinois. Wu and Johnston (2007) successfully calibrated the model in a watershed of northern Michigan. Luo et al. (2013) applied the model under different field conditions of nine headwater drainage basins in the Coastal Ranges and Sierra Nevada of California.

In China, Xiuwan (2004) applied the SWAT model to Suomo Basin to simulate the rainfall-runoff relationship and identify the impacts of climate and land change on the basin. Huang and Zhang (2004) applied the model to a high altitude, cold, semi-arid Yingluoxia catchment located on Heihe River basin, north-western China, to simulate the hydrological characteristics of the watershed. Zhang et al. (2007) were also successful in applying the model to predict the hydrological response to climate change in the Luohe River basin. Luo et al. (2013) used the model to simulate precipitation and streamflow in the Sanchuan River catchment located in the middle reaches of the Yellow River basin with an arid and semi-arid climate. Li et al. (2009) used the SWAT model in a runoff simulation in the upper reaches of the Yihe River. Cheng et al. (2009) applied the model to the Kuye River basin, one of the typical watersheds with plentiful coarse sand in the middle reaches of the Yellow River, to simulate streamflow and baseflow. Guo et al. (2008) applied the model to the Xinjiang River basin of the Poyang Lake to simulate the hydrological characteristics of this basin. More recently, Zhou et al. (2013) used the model to identify and measure how hydrological characteristics of the watershed respond to land use and land cover changes in the Yangtze River delta, one of the most developed regions in China.

In Iran the SWAT model was applied to simulate runoff and sediment in the Beheshtabad and Vanak watersheds in the northern Karun catchment (Rostamian et al. 2008). Abbaspour et al. (2007) modelled the water resources for the whole country using the SWAT model. Faramarzi et al. (2009) modelled blue and green water of Iran using the model. Gaffari et al. (2010) used the model to calibrate the streamflow and to understand the impacts of land use on the hydrological processes in the Zanjanrood Basin in northwest Iran. More recently, Ashraf et al. (2014) used the model to analyse the impact of climate change on water resources components, drought and wheat yield in semiarid regions, in the Karkheh River basin.

Other successful SWAT applications were made elsewhere: for example, Schilling et al. (2008) in Iowa; Githui et al. (2009) in Kenya; Fu et al. (2012) in Canada; Jang et al. (2012) in Korea; Güngör and Göncü (2013) in Turkey; Al-Mukhtar et al. (2014) in Germany; Bannwarth et al. (2014) in Thailand; and Raghavan et al. (2014) in Singapore.

3.2.2 Hydrological components of SWAT

The SWAT system is embedded within a GIS (ArcGIS interface), in which different spatial environmental data, including climate, soil, land cover and topographic characteristics, can be integrated. In the SWAT model, the watershed is divided into sub-basins based on the digital elevation model (DEM) (Figure 3.1). These are further disaggregated into Hydrologic Response Units (HRUs). HRUs are defined as packages of land that have unique distinguishable features identified by slope, soil and land use area within the borders of the sub-basin. The HRUs represent percentages of a sub-basin area and hence are not spatially defined in the model. There must be at least one HRU in each basin. HRUs enable the user to identify the differences in hydrologic conditions such as evapotranspiration for varied soils and land uses. Routing of water and pollutants are predicted from the HRUs to the sub-basin level, and then through the river system to the watershed outlet. A brief description of the SWAT hydrologic components is provided in this study. Further detailed descriptions for each component are found in the SWAT Theoretical Documentation (Neitsch et al. 2011), from which the following descriptions are adopted.

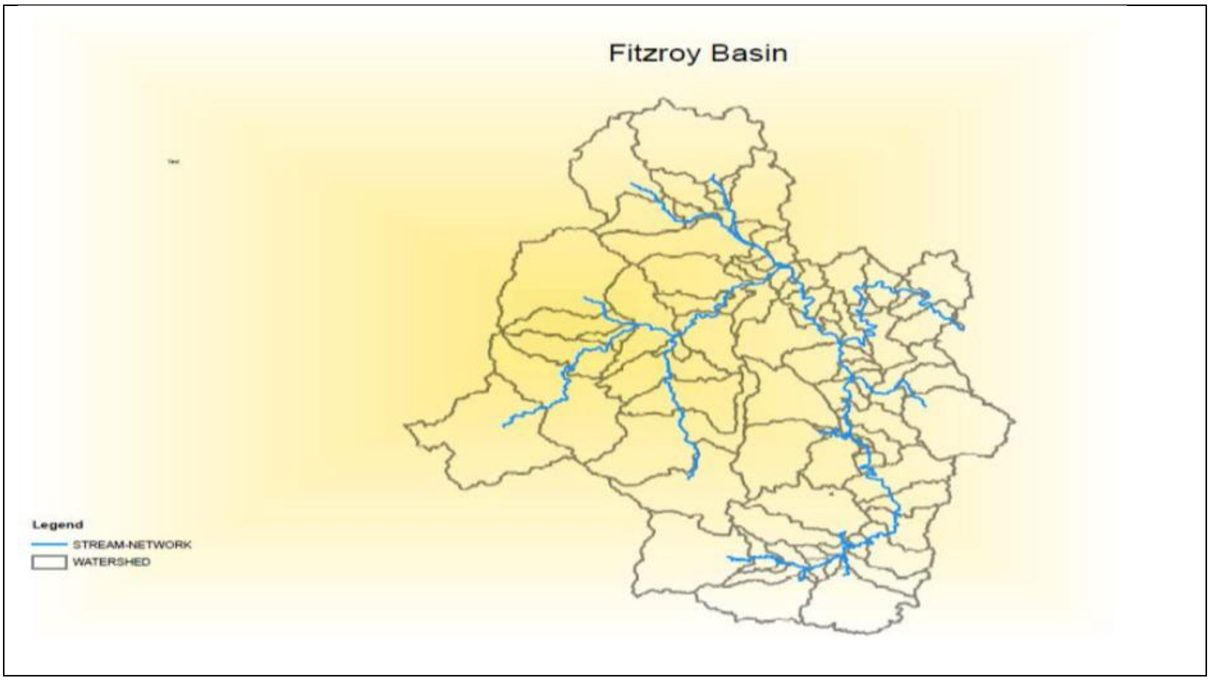

Figure 3.1 Sub-basin delineation of the Fitzroy River basin (Source: original work created for this thesis)

Two major divisions, land phase and routing phase, are enacted to simulate the hydrology of a watershed. The land phase of the hydrological cycle (Figure 3.2) predicts the hydrological components, including surface runoff, lateral flow, groundwater, evapotranspiration, ponds, tributary channels and return flow.

The routing phase of the hydrological cycles is "defined as the movement of water, sediments, nutrients and organic chemicals through the channel network of the watershed to the outlet" (Arnold et al. 1998). In the land phase of the hydrological cycle, the simulation of the hydrological cycle is based on the water balance equation:

$$SW_t = SW_0 + \sum_{i=1}^{n} \left(R_{day} - Q_{surf} - E_a - W_{seep} - Q_{gw}\right) \qquad (2)$$

where SW_t is the final soil water content (mm), SW_o is the initial soil water content on day i (mm), t is the time (days), R_{day} is the amount of precipitation on day i (mm), Q_{surf} is the amount of surface runoff on day i (mm), E_a is the amount of evapotranspiration on day i (mm), W_{seep} is the amount of water entering the vadose zone from the soil profile on day i(mm), and Q_{gw} is the amount of return flow on day i (mm).

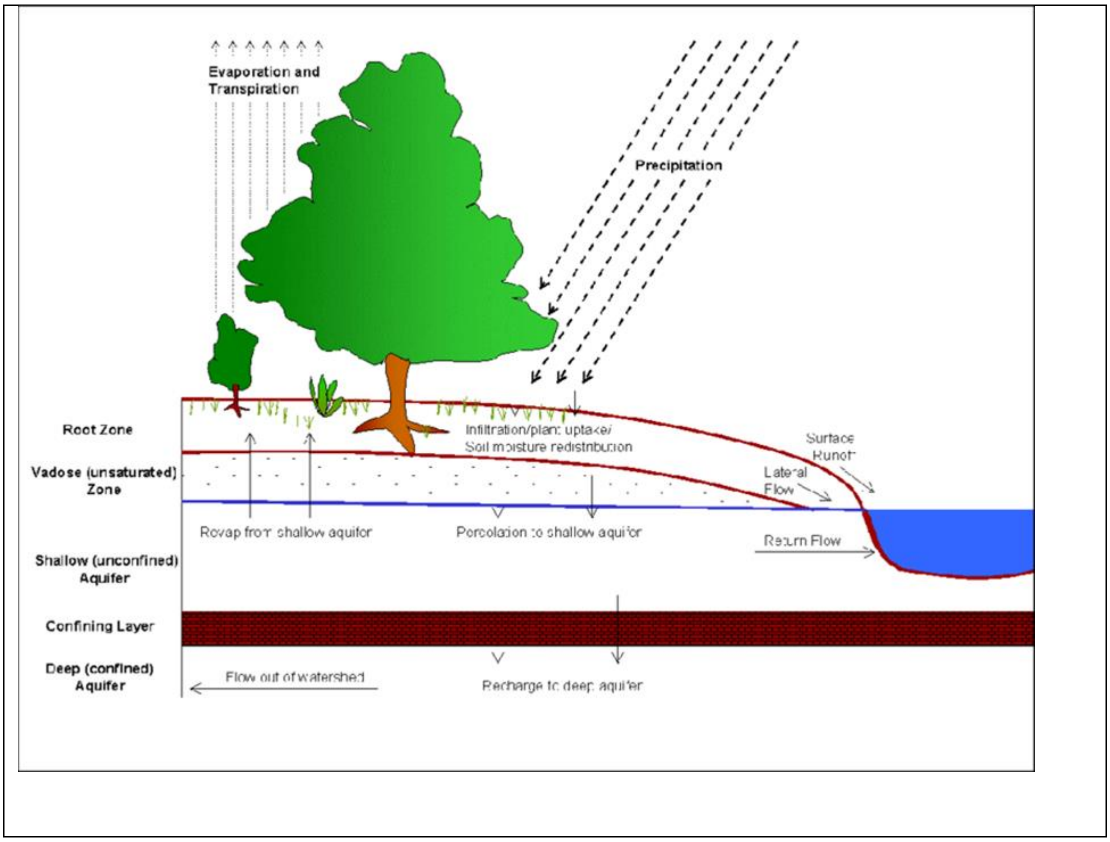

Figure 3.2: Schematic representation of the hydrological cycle (Source: original diagram created using data from Arnold et al. (1998).

The subdivision of basins allows the model to incorporate the differences in evapotranspiration for different crops and soils. Runoff is modelled individually for each HRU and then routed to obtain the total runoff for the basin (Arnold et al. 1998). This increases the accuracy of the physical description of water balance. A brief description of some of the main hydrological elements of the model is presented in this study; comprehensive descriptions can be obtained from Nietsch et al. (2011). Figure 3.3 captures the sequence of processes used by the model to simulate the land phase of the hydrological cycle.

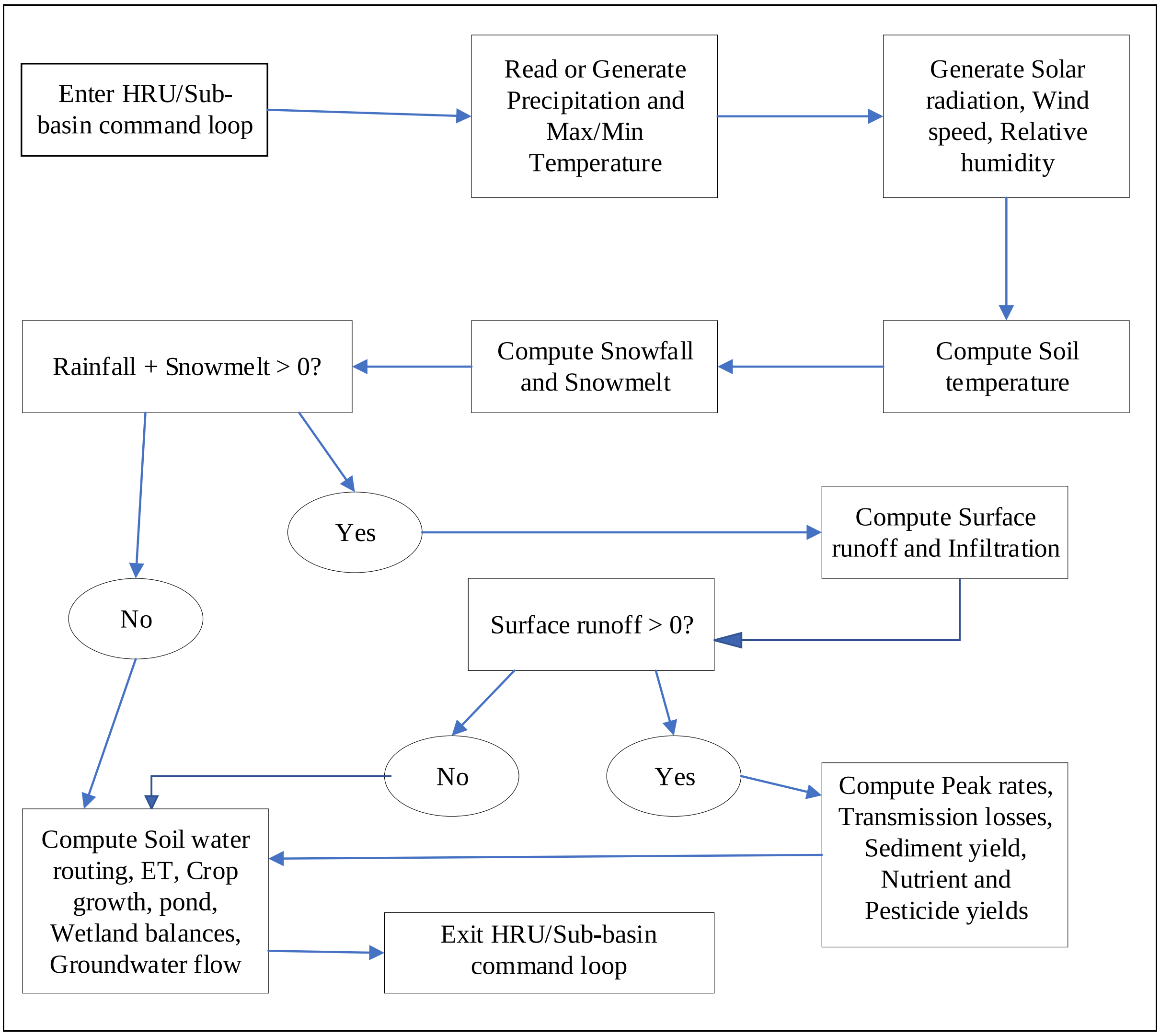

Figure 3.3: HRU/ Sub-basin loop command (Source: original diagram created using data from Arnold et al. (1998)

Surface runoff

Surface runoff occurs when the water application rate to the ground is higher than the infiltration rate. SWAT is capable of simulating runoff volumes and peak runoff rates for each HRU. It enables users to estimate surface runoff through two methods; the **soil conservation service** (SCS) curve number procedure (SCS 1972, in Arnold et al. 1998) and the Green and

Ampt infiltration method (Green and Ampt 1911). SCS can be defined as a sampling, widely used, and efficient method for determining the approximate amount of runoff from a rainfall even in a particular area. Although the method is designed for a single storm event, it can be scaled to find average annual runoff values. The SCS method is used in this study due to non-availability of sub-daily data that is required by the Green and Ampt infiltration method.

The SCS curve number equation is:

$$Q_{surf} = \frac{\left(R_{day} - 0.2\mathrm{S}\right)^{2}}{(R_{day} + 0.8\mathrm{S})} \tag{3}$$

where, Q_{surf} is the accumulated runoff or rainfall excess (mm), R_{day} is the rainfall depth for the day (mm), and S is the retention parameter (mm). The retention parameter differs spatially owing to various soils, land use, management, and slope within a catchment, and temporally because of changes in soil water content. The retention parameter is defined by the equation:

$$S = 25.4\left(\frac{1000}{CN} - 10\right) \tag{4}$$

where CN is the **curve number** for the day; it can be defined as an experiential factor used in hydrology for forecasting direct runoff or infiltration from rainfall excess.

SWAT offers two methods for estimating the retention parameter. The traditional method (soil moisture method) allows the retention parameter to be varied with soil profile water content. An alternative method added to SWAT 2012 is to allow the retention parameter to vary with accumulated plant evapotranspiration. The soil moisture method predicts too much runoff in shallow soils, but, adding the calculation of daily CN value as a function of plant evapotranspiration, the value becomes less dependent on soil storage and more dependent on antecedent climate.

When the retention parameter is to be varied with soil profile water content, the following equation will be used:

$$S = S_{max} * \left(1 - \frac{SW}{[SW + \exp(w_1 - w_2 * \mathrm{SW})]}\right) \quad (5)$$

where S is the retention parameter for a given day (mm), S_{max} is the maximum value that the retention parameter can be achieved on any given day (mm), SW is the soil water content of the entire profile excluding the amount of water held in the profile at wilting point (mm), and w_1 and w_2 are shape coefficients. The maximum retention parameter value, S_{max}, is calculated by solving equation (4), using CN_1 as shown below:

$$S_{max} = 25.4\left(\frac{1000}{CN_1} - 10\right) \quad (6)$$

When the retention parameter differs with plant evapotranspiration, the equation below is used to update the retention parameter at the end of every day:

$$S = S_{prev} + E_o \exp\left(\frac{-\mathrm{cncoef} - S_{prev}}{S_{max}}\right) - R_{day} - Q_{surf} \quad (7)$$

where S_{prev} is the retention parameter for the previous day (mm), E_o is the potential evapotranspiration for the day (mm/day), *cncoef* is the weighting coefficient used to calculate the retention coefficient for daily curve number calculations which depend on plant evapotranspiration, S_{max} is the maximum value the retention parameter that can be achieved on any given day (mm), the R_{day} is the rainfall depth for the day (mm), and Q_{surf} is the surface runoff (mm). The initial value of the retention parameter is defined as S = 0. $9S_{max}$.

Percolation

SWAT classifies soil into mutable layers and allows users to calculate percolation for each soil layer in profile. Water starts to percolate when the water content is higher than the field capacity for that layer and the layer below is not saturated. The percolation rate is zero at field capacity and increases to a maximum at saturation. When a soil layer is frozen, no percolation event occurs. Water that permeates from all soil layers accretes to groundwater and contributes as part of base flow to the stream.

Snow and Snowmelt

In SWAT, precipitation is classified as a rain or snow based on air temperature. Snowmelt is governed by the air and snowpack temperature (Nietsch et al. 2011).

Transmission loss

Transmission loss occurs when the water table is lower than the channel bottom. SWAT estimates such losses using Lane's method to calculate transmission loss as a function of channel width, length, and flow duration (Nietsch et al. 2011).

Groundwater

The groundwater model is separated into two aquifers: an unconfined and a confined aquifer in every catchment. The unconfined aquifer, which is called a shallow aquifer, is the main contributor to streamflow in the main channel of the sub-basin. Water that infiltrates into the confined aquifer apparently contributes to streamflow outside the watershed. The water balance equation for the shallow aquifer is:

$$aq_{sh,i} = aq_{sh,i-1} + w_{rchg.sh} - Q_{gw} - w_{revap-} - w_{pump.sh} \qquad (8)$$

where aq_{shi} is the amount of water stored in the shallow aquifer on day i (mm), $aq_{sh,i-1}$ is the amount of water stored in the shallow aquifer on day $i-1$ (mm), $w_{rchrg.sh}$ is the amount of recharge entering the aquifer on day i (mm), Q_{gw} is the groundwater flow, or base flow, into the main channel on day i (mm), w_{revap} is the amount of water moving into the soil zone in response to water deficiencies on day i (mm), and $w_{pump,sh}$ is the amount of water removed from the shallow aquifer by pumping on day i (mm).

The steady-state response of groundwater flow to recharge is calculated by the equation below (Hooghoudt 1940, in Arnold et al. 1998):

$$Q_{gw} = \frac{8000 * K_{sat}}{{L_{gw}}^2} * h_{wtbl} \tag{9}$$

where K_{sat} is the hydraulic conductivity of the aquifer (mm/day), L_{gw} is the distance from the ridge or sub-basin divide for the groundwater system to the main channel (m), and h_{wtbl} is the water table height (m).

Potential evapotranspiration

Three methods are provided by the SWAT model to estimate potential evapotranspiration (PET): the Penman-Monteith method (Monteith 1965), the Priestley-Taylor method (Priestley and Taylor 1972) and the Hargreaves method (Hargreaves et al. 1985). The Penman-Monteith method requires air temperature, wind-speed, solar radiation, and relative humidity; the Priestley-Taylor method needs air temperature and solar radiation, while the Hargreaves method needs only daily temperature as inputs.

Lateral subsurface flow

Lateral flow occurs below the surface when the water rates in a layer exceed the field capacity after percolation. A kinematic storage model is utilized to predict lateral flow through each soil layer. The model estimates the volume of lateral flow depending on the variation in conductivity, slope, and soil water content.

3.2.3 Sediment component

Total sediment yield that generates from watersheds is calculated by the Modified Universal Soil Loss Equation (MUSLE) as shown in the equation (Williams 1975) below:

$$Sed = 11.8\ \left(Q_{surf} * q_{peak} * area_{hru}\right)^{0.56} * K_{USLE} * P_{USLE} * C_{USLE} * LS_{USLE} * \mathrm{CFRG}\Big) \tag{10}$$

where *Sed* is the sediment yield on a given day (metric tons), 11.8 is a unit conversion constant, Q_{surf} is the surface runoff volume (mm /ha), q_{peak} is the peak runoff rate (m^3/s), $area_{hru}$ is the area of the hydrologic unit area (HRU) in hectares, K_{USLE} is the *USLE* soil erodibility factor (0.013 metric ton m^2 hr/(m^3-metric ton cm), C_{USLE} is the *USLE* cover and management factor, P_{USLE} is the support practice factor, LS_{USLE} is the topographic factor, and *CFRG* is the coarse fragment factor.

3.2.4 Routing phase of the hydrological cycle

In SWAT, water is routed through the channel network by applying either the variable storage routing or Muskingum river routing methods using the daily time step. The sediment routing model (Arnold et al. 1998) comprises two components running at the same time in the channel: deposition and degradation utilizing the same channel dimensions for the entire simulation. The details of the water and sediment routing methods can be found in Arnold et al. (1998).

3.2.5 Model input

The different inputs and processes involved in the phase of hydrological cycle are:

Weather

The SWAT model requires daily precipitation and 0.5 hourly precipitation, maximum and minimum air temperature, relative humidity, solar radiation, and wind speed. SWAT allows users to input observed weather data or work with generated data during the run. Australian weather data were collected from the Australian Bureau of Meteorology (http://www.bom.gov.au/climate/data/). The Iraqi weather data were obtained from Iraq's Bureau of Meteorology.

Digital Elevation Model (DEM)

DEM can be defined as a database that represents the topographical elevation of any point in a particular area at a particular spatial resolution (Arnold et al. 1998). A 25m by 25m resolution of Fitzroy River Basin was obtained from Queensland Government Data (https://data.qld.gov.au/dataset/digital-elevation-models-25metre-by-catchment-areas-series/resource/51189337-7cc3-4826-82c6-bdddf598dfd7) (Figure 3.4. Right). A 30 m by 30 m resolution DEM for Iraq was downloaded from ASTER Global Digital Elevation Model (ASTERGDM) (https://asterweb.jpl.nasa.gov/gdem.asp) (Figure 3.4, Left). The DEM was used for efficient delineation of watershed and for drainage pattern generation. DEM was used also for identifying sub-basin characteristics such as slope gradient, slope length of the land, and the stream network features such as length, width and slope of the channel.

Soil data

Soil properties such as soil texture, hydraulic conductivity, available water content, bulk density and organic carbon content for different layers of each soil type are essential to run the SWAT model. These soil data for Fitzroy River Basin were obtained from ASRIS Australian Soil Resource Information System (http://www.asris.csiro.au/themes/Atlas.html) (Figure 3.5, Right). The Iraqi soil data were extracted from Digital Soil Map of the World and Derived Soil Properties CD-ROM FAO (1995) (Figure 3.5, Left).

Land use

The land use map of the Fitzroy River Basin 2002 was collected from Australian Government's Department of Agriculture and Water Resources (http://www.agriculture.gov.au/abares/aclump/land-use/land-use-mapping) (Figure 3.6, Right). For the Iraqi land cover map, the land cover map was obtained from the European Environment Agency (http://www.eea.europa.eu/data-and-maps/data/global-land-cover-250m) with a 250-meter grid raster for the year 2000 (Figure 3.6, Left).

River discharge

Daily stream flow data for Fitzroy Basin were collected from the Queensland Department of Natural Resources and Mines' Water Monitoring Portal (https://www.dnrm.qld.gov.au/water/water-monitoring-and-data/portal). Daily stream flow data for Iraqi Basin were obtained from the Iraqi Ministry of Water Resources' National Water Centre.

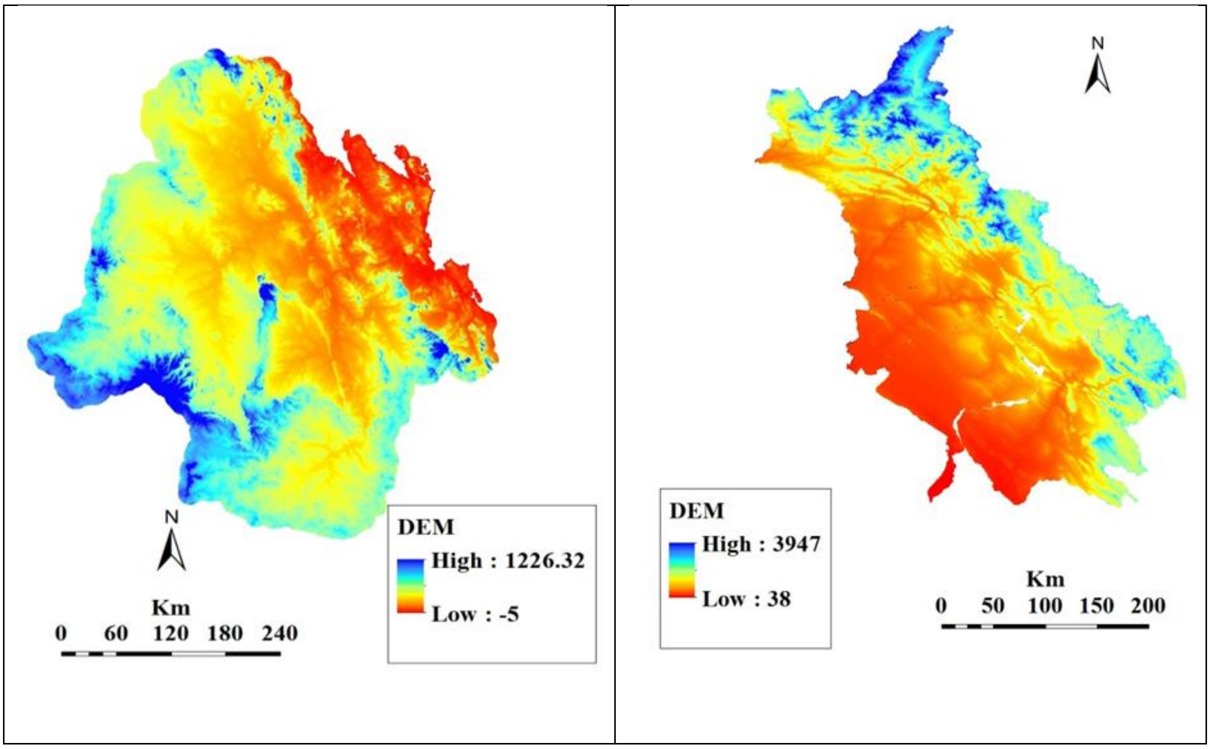

Figure 3.4: DEM of Fitzroy Basin (left) and Tigris Basin (right) (Source: original work created for this thesis)

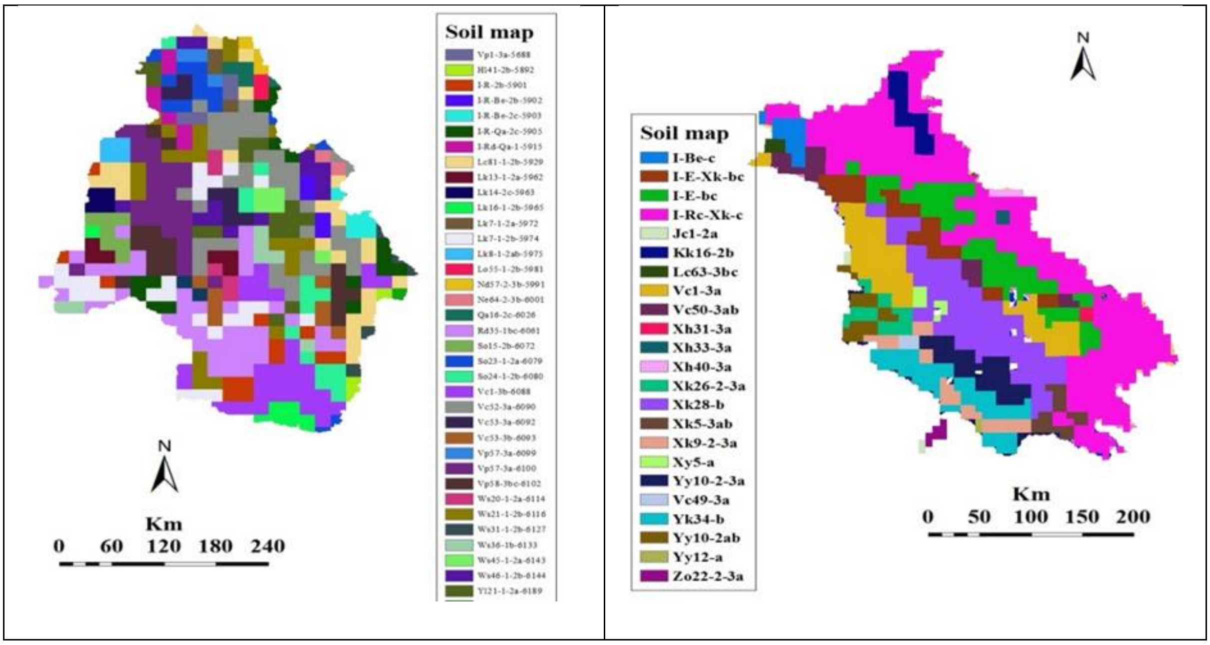

Figure 3.5: Soil map of Fitzroy basin (left) and Iraqi basin (right) (Source: original work created for this thesis)

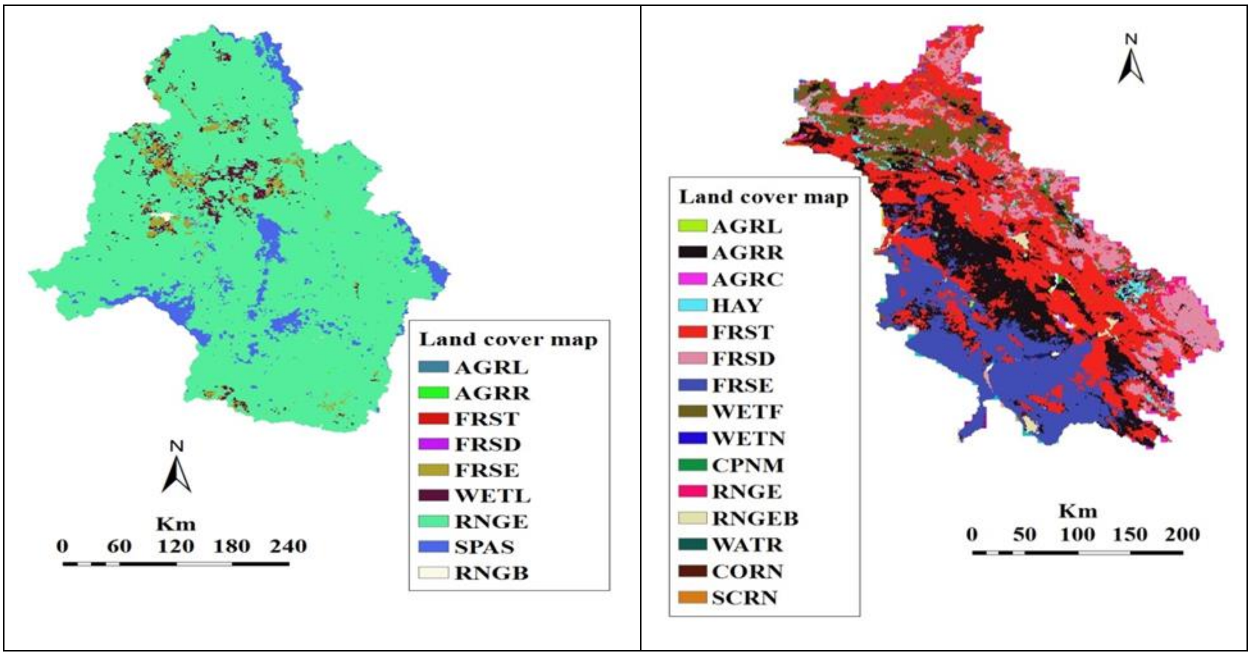

Figure 3.6: Land use map of Fitzroy basin (left) and Iraqi basin (right) (Source: original work created for this thesis)

3.2.6 Description of SUFI-2

To evaluate the performance of the SWAT model, the sequential uncertainty fitting algorithm application (SUFI-2), embedded in the SWAT-CUP package (Abbaspour et al. 2007), can be used. The advantages of SUFI-2 are that it combines optimisation and uncertainty analysis, can handle a large number of parameters through Latin hypercube sampling and is easy to apply (Abbaspour et al. 2004). Furthermore, compared to different techniques in connection to SWAT, such as generalized likelihood uncertainty estimation (GLU), parameter solution (parsol), and Markov Chain Monte Carlo (MCMC), the SUFI-2 algorithm was found to obtain good prediction uncertainty ranges with a low number of runs (Yang et al. 2008). This efficiency is of great significance when implementing complex and large-scale models (Abbaspour et al. 2004; Schuol et al. 2008).

SUFI-2 first identifies the range for each parameter. Then the Latin Hypercube Method is used to generate multiple combinations among the calibration parameters. Finally, the model runs with each combination and the obtained results are compared with observed data until the optimum objective function is achieved. Since the uncertainty in forcing inputs (e.g., temperature, rainfall), the conceptual model and measured data are not avoidable in hydrological models, the SUFI-2 algorithm computes the uncertainty of the measurements, the conceptual model and the parameters by two measures: P factor and R factor. P factor is the percentage of data covered by the 95% prediction uncertainty (PPU), which is quantified at 2.5% and 97.5% of the cumulative distribution of an output variable obtained through Latin Hypercube Sampling (Abbaspour et al. 2007). The R factor is the average width of the 95 PPU divided by the standard deviation of the corresponding measured variable. In an ideal situation, P-factor tends towards 1 and R-factor to zero (0) (Abbaspour et al. 2007). The objective of the algorithm is to increase P-factor and reduce R-factor in order to achieve the optimal parameter range. These factors together reflect the strength of the calibration-uncertainty analysis. Furthermore, SUFI-2 calculates the coefficient of determination (R^2) and the Nasch-Sutcliff efficiency (ENC) (Nash and Sutcliffe 1970) to assess the goodness of fit between the measured and simulated data. R^2 shows the strength of the relationship between the simulated and observed data. It ranges from 0 (zero) to 1 (Legates and McCabe 1999). The higher values of R^2 reflect less error variance, and values greater than 0.5 are satisfactory (Moriasi et al. 2007). R^2 has been widely used to provide an assessment of climate change detection, and hydrological and hydroclimatological applications (Santer et al. 1995, Hegerl et al. 1996, Legates and McCabe 1999). R^2 is given by

$$R^2 = \left[\frac{\sum_{i=1}^{n}(O_i - \bar{O})(P_i - \bar{P})}{[\sum_{i=1}^{n}(O_i - \bar{O})^2]^{0.5}[\sum_{i=1}^{n}(P_i - \bar{P})^2]^{0.5}}\right]^2 \quad (11)$$

where O_i is the observed stream flow, Pi is the simulated stream flow and $\bar{O}$ is the mean observed stream flow during the evaluation period, and $\bar{p}$ is the mean simulated streamflow.

The ENC value is an indication of how well the plot of the observed against the simulated values fits the 1:1 line. It can range from negative infinity (-∞) to 1. The closer the value to 1, the better the prediction is. A value of less than 0.5 indicates unsatisfactory model performance (Moriasi et al. 2007). ENC is calculated as shown below:

$$ENC = 1 - \left[\frac{\sum_{i=1}^{n}(O_i - P_i)^2}{\sum_{i=1}^{n}(O_i - \bar{O})^2}\right] \quad (12)$$

where Oi is the observed stream flow, Pi is the simulated stream flow, and $\bar{O}$ is the mean observed stream flow during the evaluation period.

ENC is recommended to be used for calibration, since it has been approved by ASCE (1993). It has been recommended by Legates and McCabe (1999) because of its direct physical interpretation (Raghavan et al. 2014). Moreover, it has seen widespread applications, offering extensive information on reported values (Moriasi et al. 2007).

SUFI-2 enables users to conduct global sensitivity analysis, which is computed "by plotting the Latin Hypercube generated parameters against the values of the objective function using multiple linear regression analysis. Then a *t*-test which indicates parameter sensitivity is used to determine the relative significance for each parameter" (Al-Mukhtar et al. 2014) – the more sensitive the parameter, the greater is the *t*-test value (Abbaspour et al. 2007). In this study, global sensitivity analysis, R^2, ENC, P-factor and R-factor have been evaluated to assess the SWAT model performance.

3.2.7 Water availability indicators

There is no agreed universal indicator to define water availability, especially when one considers the accessibility issues. Though Sullivan (2002) introduced accessibility in his concept of the Water Poverty Index (WPI), which includes spatial and temporal water availability, the population with access to safe water, and time and effort to collect water, the deficiencies of the WPI have been identified by others (Angulo et al. 2016). Thus, for simplicity in this paper, we limit the definition of water availability or lack of it (water scarcity) as aggregated water availability per person.

Blue water availability can be used for water scarcity analysis. Among many available water scarcity indicators, a widely used indicator is the water stress threshold, which is defined as 1700 $m^3.capita^{-1}.year^{-1}$ by Falkenmark (1989). This value is estimated based on household water needs, agricultural usage, industrial and energy sector consumptions, and demand for the environment (Rijsberman 2006). A value equivalent to or higher than 1700 $m^3.capita^{-1}.year^{-1}$

is generally accepted as sufficient to meet water demand. Once water supply declines below 1000 $m^3.capita^{-1}.year^{-1}$, it is considered water scarcity, and below 500 $m^3.capita^{-1}. year^{-1}$ is considered as extreme scarcity. The water accessibility per capita and water stress indicators were assessed for each of the 320 HRUs via the 2.5 arcmin population map available from the Center for International Earth Science (CIESIN) Gridded Population of the World (GPW, version 3, http://sedac.ciesin.columbia.edu/gpw) for 2005.

3.3 General Circulation Models (GCMs)

General Circulation Models (GCMs) are numerical models that reflect procedures in the atmosphere, cryosphere, ocean and land surface. Currently, GCMs are the main tools obtainable for modelling changes in climate in response to changes in greenhouse gas concentrations (Abbaspour et al. 2007). GCMs describe the climate through a three-dimensional grid of points on the globe, a horizontal resolution of between 250 and 600 km, 10 to 20 vertical layers in the atmosphere and 30 layers in the oceans (IPCC 2014). Therefore, their resolution is rather coarse compared to the amount of exposure units in most impact assessments (IPCC 2014). Thus, they produce a high degree of uncertainty on modelling parameters.

3.3.1 *Coupled Model Intercomparison Project (CMIP)*

The Intergovernmental Panel on Climate Change (IPCC) collects and evaluates global climate models as part of the International Climate Change Assessment Reports; the ensemble of the models is called the Coupled Model Intercomparison Project (CMIP) (IPCC 2014). It is a collaborative effort of climate scientists initiated by the US Department of Energy. The CMIP "is a framework and the analog of the Atmospheric Model Intercomparison Project (AMIP) for global coupled ocean-atmosphere general circulation models (GCMs)". The Working Group on Coupled Modelling (WGCM) introduced the CMIP as a typical experimental procedure to study the output of coupled atmosphere-ocean general circulation models (AOGCMs). The main objective of the CMIP is to provide a better understanding of past, present and future climate changes due to changes in radiative forcing in a multi-model concept. The CMIP began in 1995 and the first set of common experiments documented was achieved using a CO_2 increase of 1% per year compounded. Since then a number of CMIP experiments has been developed. In this study, we used CMIP3 and CMIP5.

CMIP3 is the model ensemble for the IPCC's Fourth Assessment Report (AR4) and was released in 2010. The CMIP3 simulations of the 21th century represent the emissions scenarios from the Special Report on Emissions Scenarios. The emission scenarios of CMIP3 are SRES A1F1, A2, A1B and B1, listed in order of high to low emissions (Figure 3.7). Only three emissions scenarios were used in the CMIP3 climate change simulation runs for the IPCC Fourth Assessment report: SRES-B1, SRES-A1B and SRES-A2. These scenarios represent the estimate of future emissions based on different combinations of global population growth, and policies associated with alternative energy systems and conservative fossil fuel sources (Figure 3.8):

- SRES A2 (A2 family) describes a very heterogeneous world with a rapid population growth, slow economic development, and technological change.
- SRES A1B (A1 family) describes a future of a very high economic growth with a greater introduction to more efficient technologies with population growth that increases in mid-century and decreases thereafter.
- SRES B1 describes (B1 family) describes a cooperating world with rapid introduction of clean and resource-efficient technologies but the same global population as in the A1 SRES.

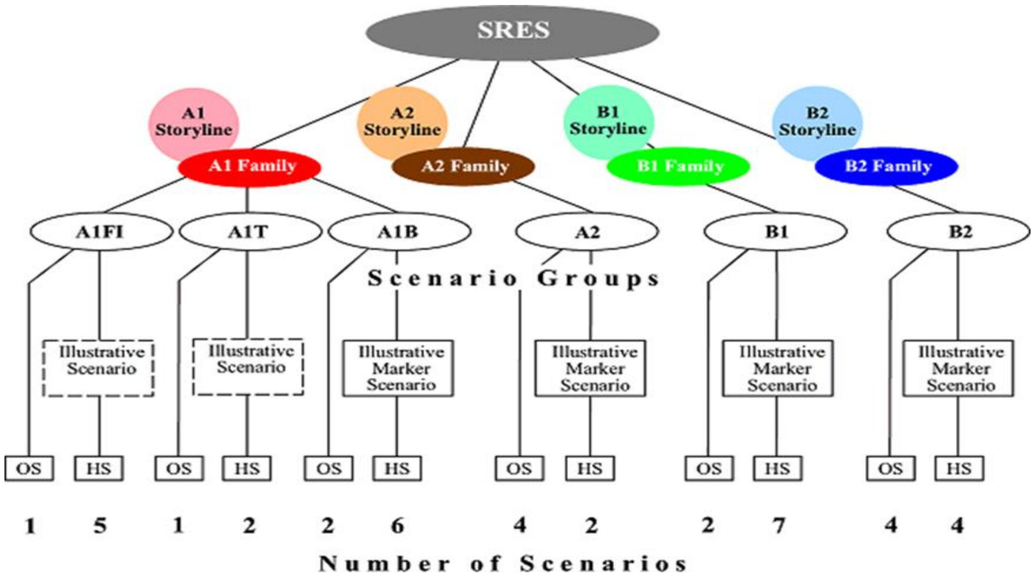

Figure 3.7: Schematic illustration of SRES scenarios. Four qualitative storylines yield four sets of scenarios called families: A1, A2, B1, and B2 (Source: original diagram created using data from IPCC, 2007)

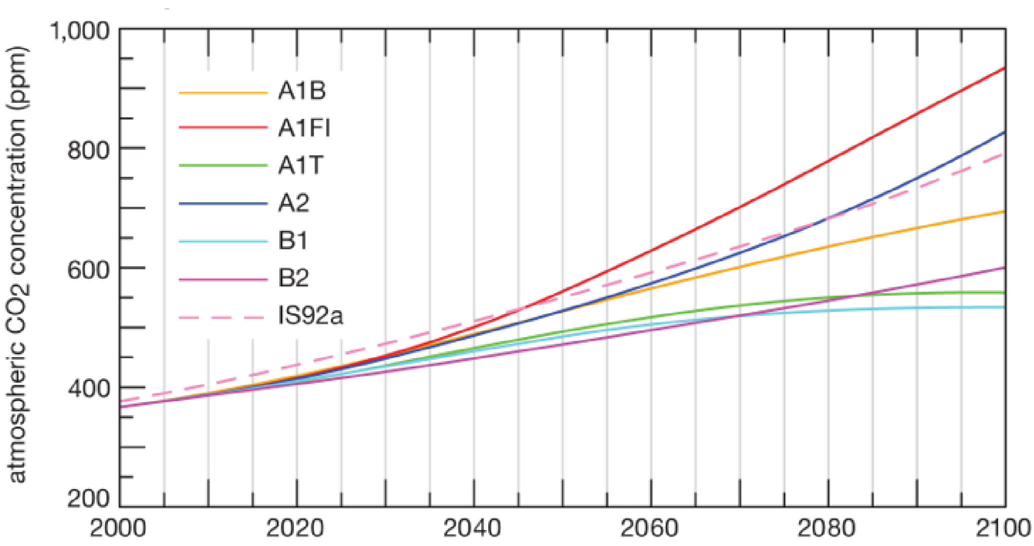

Figure 3.8: Timeline of expected changes for different scenarios of CO_2 in air (Source: original diagram created using data from IPCC, 2007)

GCM outputs were downloaded from the World Climate Research Programme's (WCRP's) Coupled Model Inter-comparison Project phase 3 (CMIP3) multi-model dataset. Daily precipitation and maximum and minimum air temperatures were extracted from six models:

CGCM3.1/T47, CNRM-CM3, GFDL-CM2.1, IPSLCM4, MIROC3.2 (medres) and MRI CGCM2.3.2. These data were used to alter the historical data sets for the baseline period of 1980 to 2010. The output was then applied to the SWAT model to simulate water resources of two future periods, 2046-2064 and 2080-2100, and then the results were compared with the baseline period data.

CMIP5 is the model ensemble for the Fifth Assessment Report of IPCC (AR5) and was introduced in 2013. The CMIP5 simulations of the 21st century reflect the representative concentration pathways (RCPs). The RCPs do not describe emissions but describe the concentrations of greenhouse gases and aerosols. RCPs characterize and cover the range of current estimates of the concentrations of greenhouse gases regarding the evolution of radiative forcing. The total amount of additional energy enters the climate system over the 21st century. RCPs do not adopt particular climate policy actions. However, scientists are free to develop mitigation scenarios leading to one of the RCPs (RCP 8.5, RCP 6.5, RCP 4.5, RCP 2.6). The CMIP5 climate scenarios used in this research are RCP 8.5, RCP 4.5 and RCP 2.6, which represent increases in radiative forcing to roughly 8.5 W/m^2 and 4.5 W/m^2 and 2.6 W/m^2 above preindustrial levels by the year 2100 (IPCC 2014).

These models were chosen because they offered acceptable daily precipitation, and minimum and maximum temperature outputs to CMIP3 and 5. In addition, these GCMs simulated the current climate most faithfully, which gives confidence that these GCMs would also produce the most reliable representation of future climate. Also, they provide acceptable spatial precision for each of the study areas.

In summary this chapter, presents the methodology used in this research. For hydrologic modelling SWAT was chosen because of its wide popularity and its prior successful applications in similar catchments throughout the world. In addition, SWATCUP, which is used for statistical analysis, was embedded in that SWAT model, which made the calibrations and validations highly accurate. To capture the effects of climate change, GCM outputs were used because, hitherto, GCMs have provided the most reliable forecasts.

CHAPTER 4

CLIMATE CHANGES IN THE STUDY AREAS

4.1 Introduction

The primary controlling factors of a climatic regime are atmospheric temperature and precipitation. If these two factors change, other factors such as humidity will be affected. It is therefore imperative to study thoroughly changes in atmospheric temperature and precipitation to investigate possible climate change. This section describes the observed and projected changes in climate as they relate to water in both regions.

4.2 Observed climate and its trends in Central Queensland

4.2.1 Air temperature

Increase in air temperature over land is one of the clearest signs of a rapidly changing climate system in Australia (Lough and Hobday 2011). Australia's continental average temperature has risen by about 0.9°C over the last century, higher than the global average of 0.7°C for the same period (Hughes 2003). Most of this increase occurred after the 1950s (Karoly and Braganza 2005). For example, since the 1950s, the average temperature has increased by around 0.7°C with 0.1°C to 0.2°C per decade, and every decade has become warmer than previously (Clarke et al. 2013). The decade ending in 2010 has been the warmest decade since 1910 (Keenan and Cleugh 2011). Clarke et al. (2013) also point out that the 2013 year was Australia's warmest year on record, being 0.17°C above of the previous warmest year in 2005. These trends are consistent with those measured globally (Hughes 2003). In Queensland, the mean air temperature has risen by about 1^0C since early last century with the highest rate of warming occurring since the 1950s (Clarke et al. 2013) (Figure 4.1). The historical temperature records show that the Central Queensland region has experienced the highest average temperature since the late 1950s (Government of Queensland 2014) (Figure 4.2).

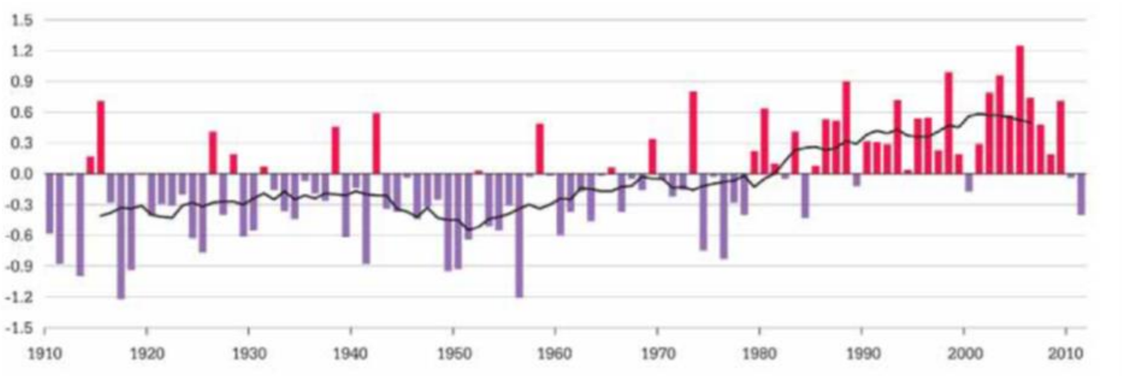

Figure 4.1: Annual average temperature for Queensland. The black line shows the 11-year average (Source: original diagram created using data from Government of Queensland, 2014)

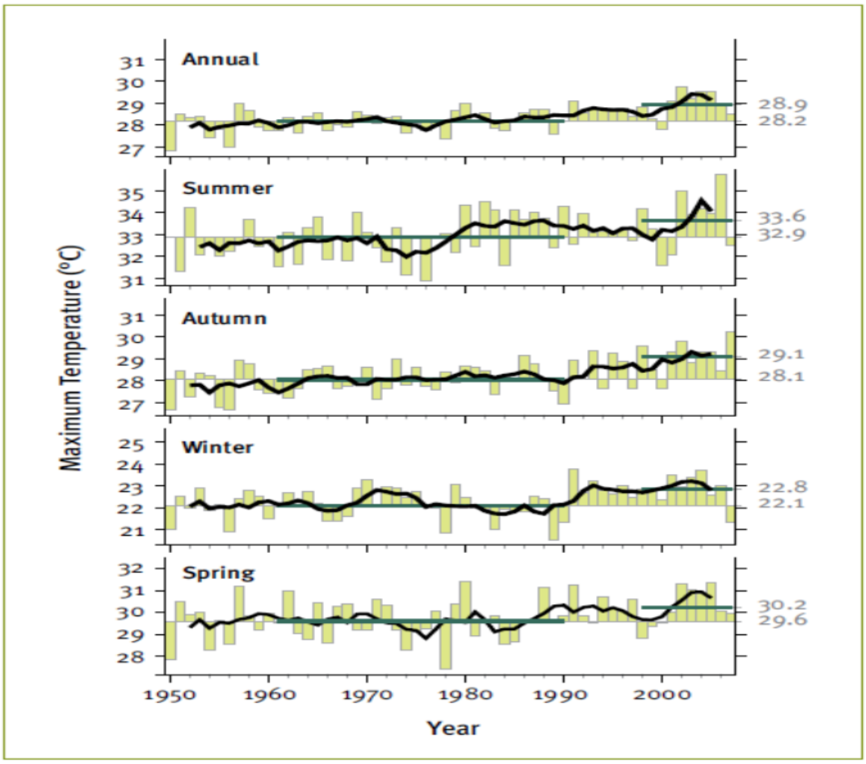

Figure 4.2: Annual and seasonal maximum temperatures for the Central Queensland region for the period 1950–2007, recent averages compared to the baseline period 1961–1990
(Source: original diagram created using data from Government of Queensland, 2014)

In Figure 4.2, the black line is a five-year running average and the green lines indicates the average temperature for the baseline of 1961–1990 and the last decade 1998–2007, which is indicated numerically at the right of the graph.

Along with increased average temperatures, there have been decreases in extreme cold events, and increases in numbers of extremely warm events in the last 50 years (Alexander and Arblaster 2009; Lough and Hobday 2011). For instance, in Rockhampton, since the 1980s the number of days where the maximum temperature has exceeded 35^{0}C is given year-wise in Figure 4.3.

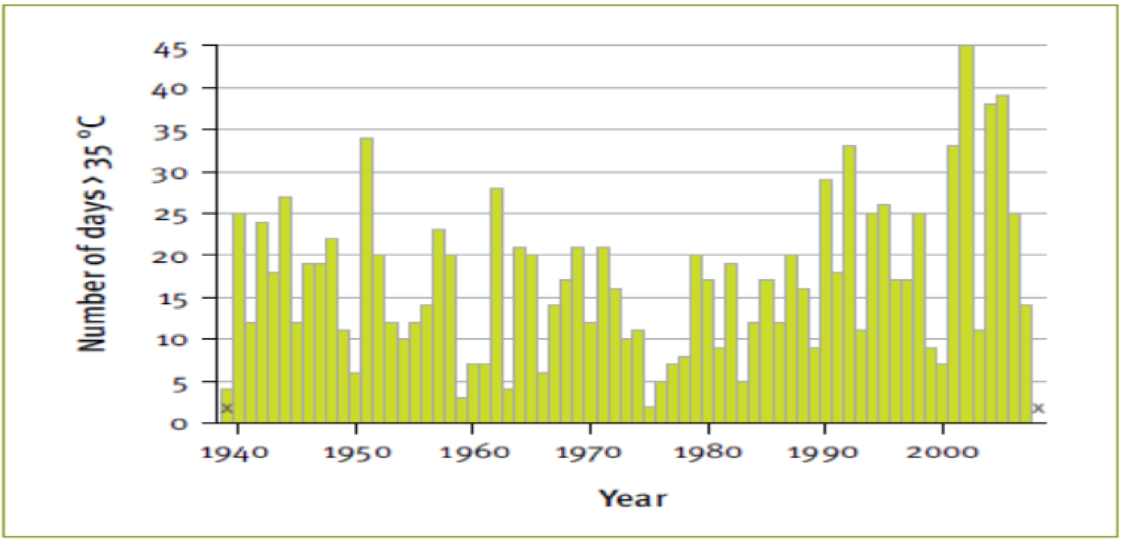

Figure 4.3: Number of days in a year where the temperature has been higher than 35°C for Rockhampton (Source: original diagram created using data from Government of Queensland, 2014)

4.2.2 Rainfall

Australian mean annual rainfall distribution is captured in Figure 4.4. The interior of the continent is dry, with less than 100 mm rainfall because of its location beneath the downward branch of the subtropical ridge, as is characteristic of the planet's deserts (Risbey 2011). Australian rainfall variability is much higher than elsewhere in the world, with climates seemingly similar to the Sahara or Gobi deserts (Nicholls et al. 1997).

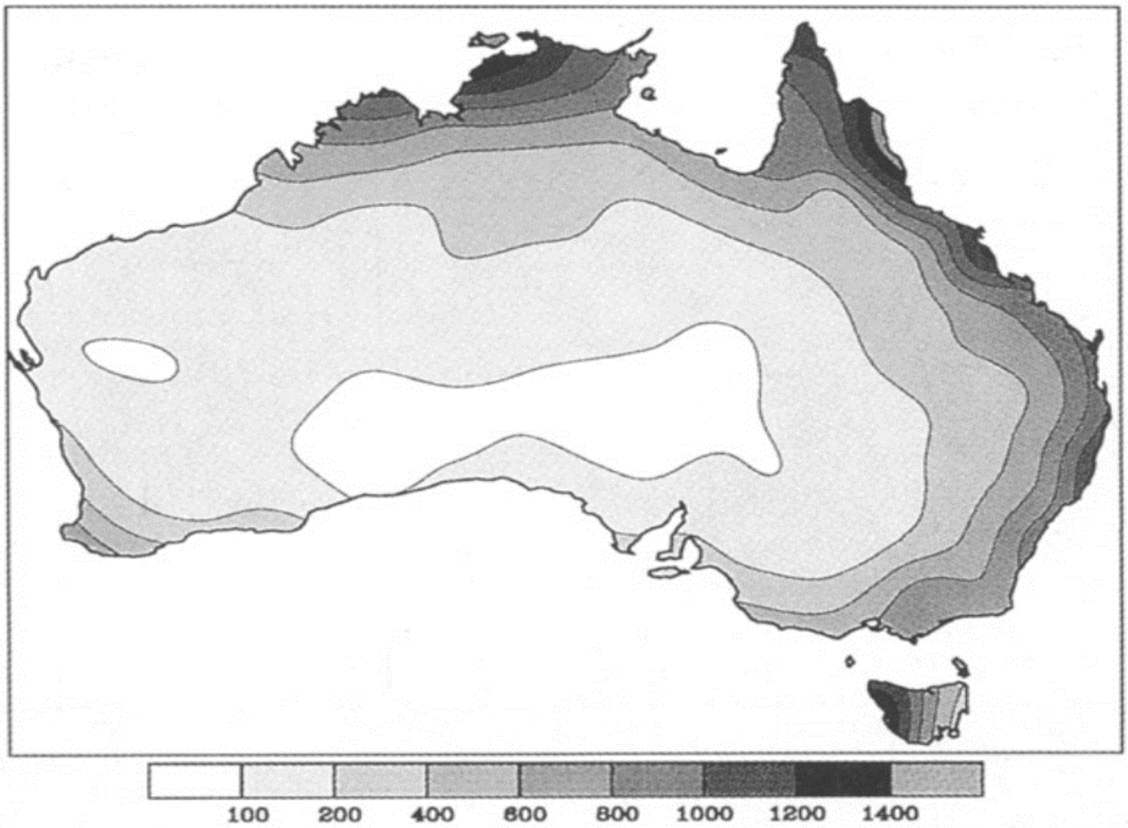

Figure 4.4: Mean annual rain (mm) in Australia using the data from 1910 to 1992 (Source: original diagram created using data from Nicholls et al., 1997)

This variability is driven by a number of factors, including the El Niño Southern Oscillation (ENSO), the Pacific and Indian Ocean sea surface temperatures (SSTs), the Indian Ocean Dipole (IOD), the Southern Annular Mode (SAM), and the Madden-Julian Oscillation (MJO) (Risbey et al. 2009; Lough and Hobday 2011). El Niño is recognised as the primary source of inter-annual variability across much of Australia, particularly in Queensland, although its effects vary across seasons and regions (Lough 2008). Over the last century, rainfall patterns in Queensland have changed: some areas have become wetter and others have become drier. For example, Queensland has experienced more rainfall, apart from the coastal regions, including Central Queensland, which has become drier between 1970 and 2011 (Figure 4.5) (Clarke et al. 2013).

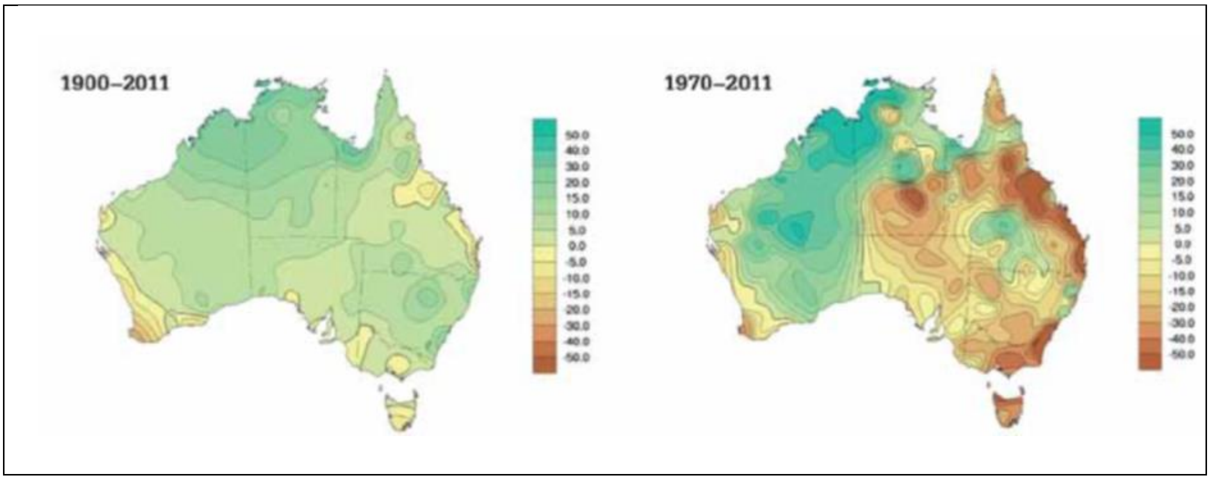

Figure 4.5: Spatial distribution of annual rainfall trends (mm/10 yrs) for the periods 1900–2011 and 1970–2011 (Source: original diagram created using data from Clarke et al., 2013)

Figure 4.6 captures the variability of seasonal and annual rainfall over the last five decades in Central Queensland: over the last decade autumn rainfall has declined by 38% compared to the 1960-2000 mean rainfall.

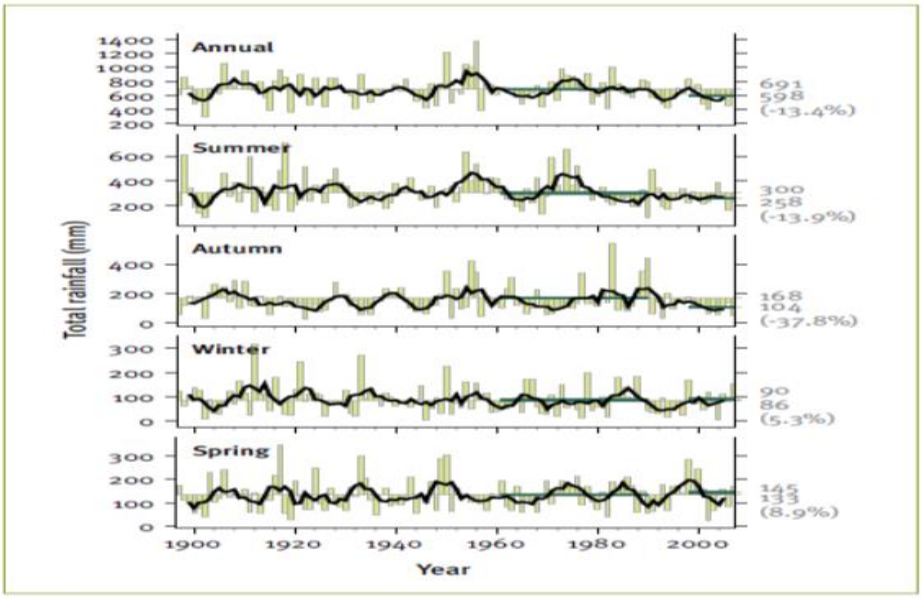

Figure 4.6: Historical annual and seasonal total rainfall for the Central Queensland region for the period 1897–2007 (Source: original diagram created using data from Government of Queensland, 2014)

In Figure 4.6, the black line indicates a five-year running average rainfall and the green lines show the average for the baseline 1961–1990 and the last decade 1998–2007. The difference in rainfall between the baseline period and the last decade is shown in percent at the right of the graph.

The high Australian rainfall variability has a number of implications. It makes it more difficult to detect the long-term trends due to the higher inter-annual noise resulting from this variability; it also affects Australian vegetation and agriculture (Nicholls et al. 1997). Furthermore, it makes Australia highly susceptible to climate change (Head et al. 2014).

4.2.3 Sea surface temperature (SST)

Remarkable warming is already apparent in Australia’s surrounding oceans (Lough and Hobday 2011) (Figure 4.7). Sea surface temperatures (SSTs) in many tropical regions such as the Queensland region have increased by about 1°C over the past 100 years, higher than the global average of 0.7°C, and are currently increasing at 1-2°C per century (Hoegh-Guldberg 1999; Hughes 2003). Temperatures measured show that 2016 was the warmest year on record for the Great Barrier Reef in the century (Greater Barrier Reef Marine Park Authority 2017). These changes are attributed to the enhanced greenhouse effect and natural climate variability influences such as the El Niño-Southern Oscillation (Lough 2008). Changes in SSTs were associated with significant coral bleaching that occurred in the Great Barrier Reef in both 1998 and 2002 (Hoegh-Guldberg 1999), due to the inability of the Reef to adapt to such changes in SSTs (Lough 2008). Lough (2008) also observes that coral reef ecosystems are highly prone to further bleaching due to thermal stress increase.

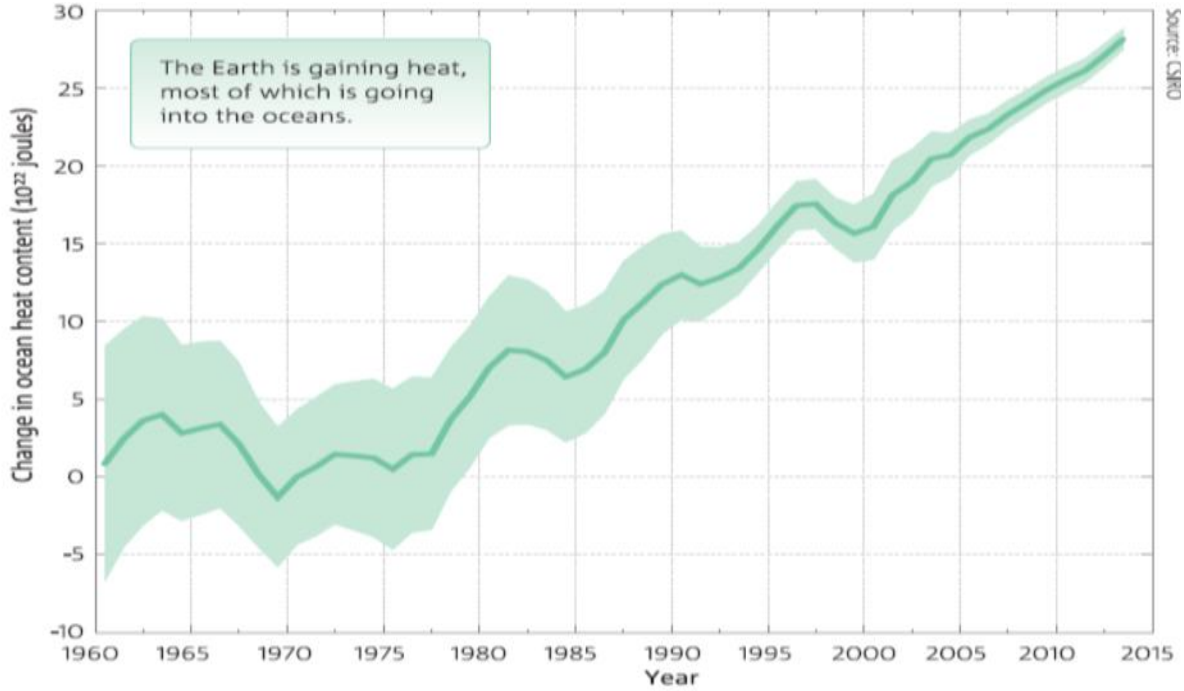

Figure 4.7 Changes in ocean heat content for the period of 1960 to 2015, shading indicates the confidence range of the estimate (Source: Keenan and Cleugh, 2011)

4.2.4 Sea levels

Globally, mean sea level has increased by 200 mm since the late 19th century at a rate of 2.8 mm/year (Figure 4.8). Rising sea levels have accelerated to 3.2 mm/year over the last three decades (Lough and Hobday 2011) at a rate near to the upper end of the Intergovernmental Panel on Climate Change projections (Keenan and Cleugh 2011). This is mostly due to thermal expansion of the oceans, with a small contribution from the loss of mass from land ice (Church et al. 2006; Gregory and Huybrechts 2006). Although monitoring sea levels around the Australian coastline was initiated in the early 1990s, which makes it difficult to infer significant trends due to the short period of monitoring, sea levels have increased around Australian region, consistent with global trends (Hoegh-Guldberg 1999; Church and White 2006). Sea-level rising rates are variable regionally, as has been detected along Queensland's coasts. Sea-level rise has been the highest along Queensland's coasts (Chambers et al. 2005). The variations in sea level rise are associated with inter-annual climate variations (e.g., owing to ENSO), changes in the strength of the east Australia current (EAC), and atmospheric circulation dynamics (Lough and Hobday 2011). Rising sea levels have enhanced the frequency and intensity of extreme sea-wave events in Australia and overseas (Keenan and Cleugh 2011). The rate of extreme sea-wave events has become three times more frequent in the latter half of the 20th century compared to the former half (Church et al. 2006). Most experts suggest that by 2100 a rise of sea level within the range of 500 mm to 1000 mm is highly likely. However, this depends on the constancy of the great ice sheets in Greenland and the Antarctic – a sea-level rise of over 1000 mm is a real possibility (Steffen et al. 2012).

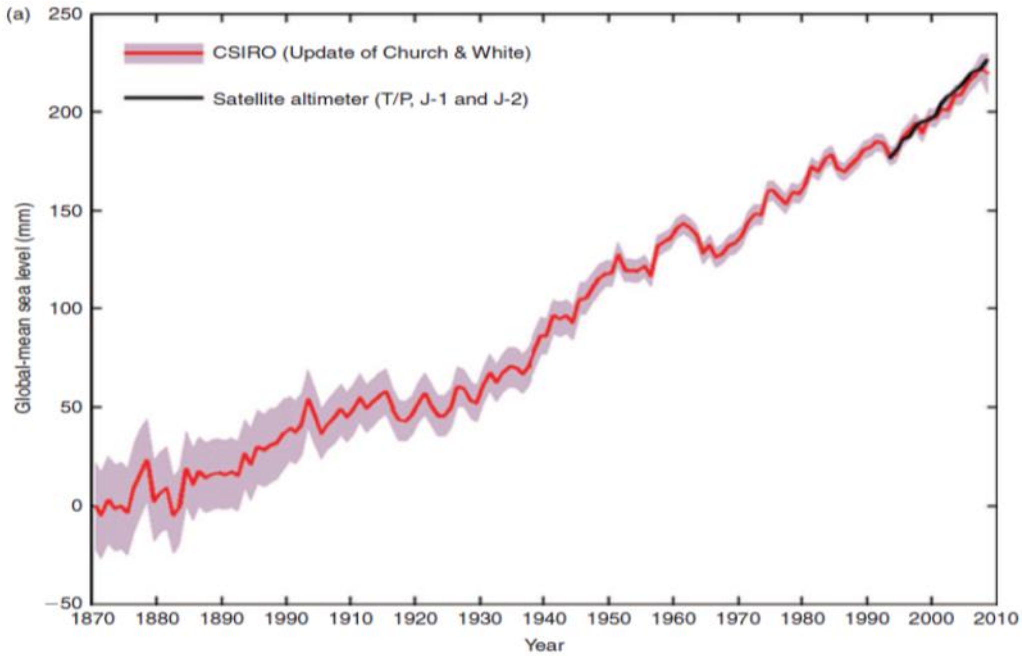

Figure 4.8: Global Mean Sea Level (GMSL), 1870- 2008 (Source: original diagram created using data from Church and White, 2006)

4.2.5 Ocean acidification

Since the 1970s, the oceans have absorbed about a third of anthropogenic CO_2 emissions into the atmosphere (Lough and Hobday 2011). Ocean absorption of CO_2 has decreased near the surface; ocean pH has decreased by about 0.1 and is projected to decrease further by 0.2-0.3

by 2100 (Keenan and Cleugh 2011). Changes in water chemistry would have significant impacts on corals and plankton, and other marine organisms that cover the entire marine food chain (Lough and Hobday 2011).

4.2.6 Ocean salinity

Increased rainfall or decreased evaporation in some parts of the oceans have led to water dilution, making these parts fresher, whereas other parts have become noticeably saltier owing to increased evaporation or decreased rainfall or both (Keenan and Cleugh 2011).

4.3 Observed climate and trends in Northeast Iraq

The climate of Iraq can be described as mostly a hot desert with arid and semi-arid climate. Thus, the days can be very hot and the nights cold, with scanty rainfall, gusty winds and plenty of sunshine.

4.3.1 Air temperature

Zakaria et al. (2013) point out that the average annual temperatures reached 21.62 ^{o}C, 21.73 ^{o}C, 21.58 ^{o}C and 21.61 ^{o}C in four historical periods of 1900-1930, 1930-1960, 1960-1990 and 1990-2009, respectively. For the future sub-periods of 2020-2039, 2040-2059, 2060-2079 and 2080-2099, they will reach 18.94 ^{o}C , 20.24 ^{o}C, 21.39 ^{o}C and 22.85 ^{o}C, respectively. A comparison between these values shows that the increase of annual temperature was limited during the historical period 1900-2009, but it was relatively more significant during the future period 2020-2099 (Figure 4.9).

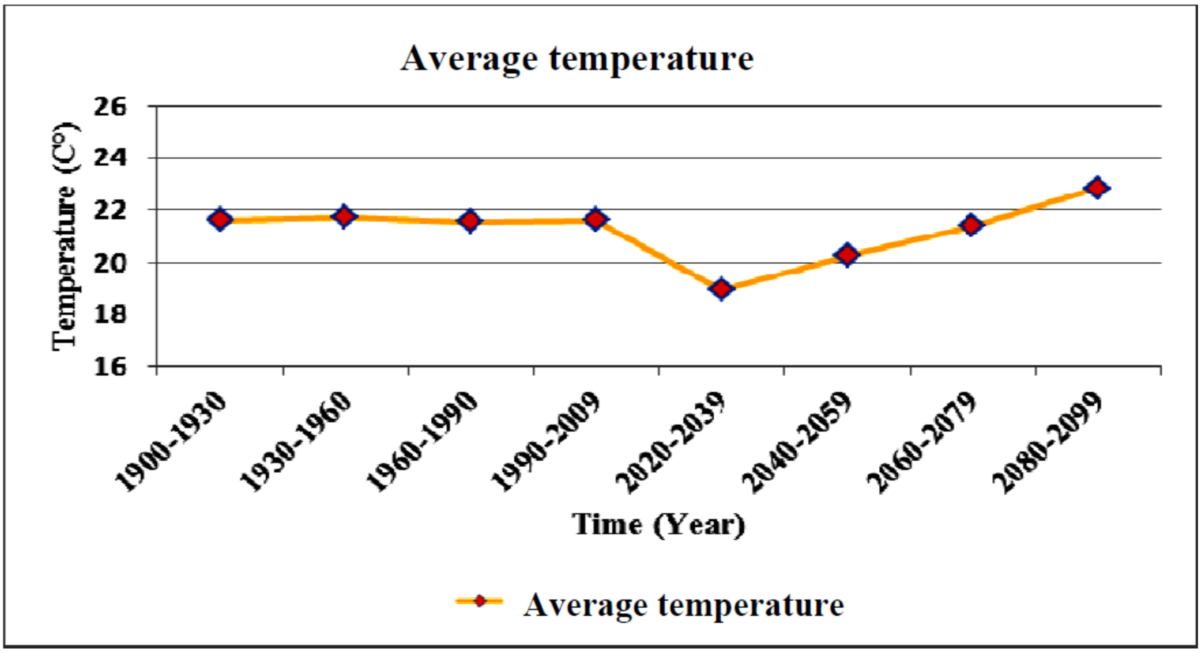

Figure 4-9: Average annual temperature over the historical and future periods (Source: original diagram created using data from Zakaria et al., 2013)

However, the IPCC (2014) points out that the Iraqi surface air temperature increased unevenly from 1970 to 2003, ranging from 0.2°C to 2°C, and it is expected to increase by about 5°C by the end of the 21st century. These changes will give rise to a higher level of climate variability, potentially resulting in a higher frequency of extreme weather events.

4.3.2 Rainfall

Zakaria et al. (2013) show that an increase and decrease of average annual rainfall occurred over both the historical and future periods 1900-1930, 1930-1960, 1960-1990 and 1990-2009. The average annual rainfall for the four historical sub-periods was 182.5, 194.7, 168.9 and 162.6mm, respectively. Comparing the first and the second sub-periods, the total rainfall value showed a percentage increase of 6.68%. However, from the second to the third sub-periods the total rainfall showed a percentage decrease of 13.25%. From the third to the fourth sub-periods the total rainfall fell again by 6.3 mm with a percentage decrease of 3.73%. The average annual of the rainfall was falling from 194.7 mm during the period of 1930 -1960 to reach its lowest value of 162.6 mm during 1990-2009 (Figure 4-10). Zakaria et al. (2013) also point out that the decline trend is expected to continue into the future.

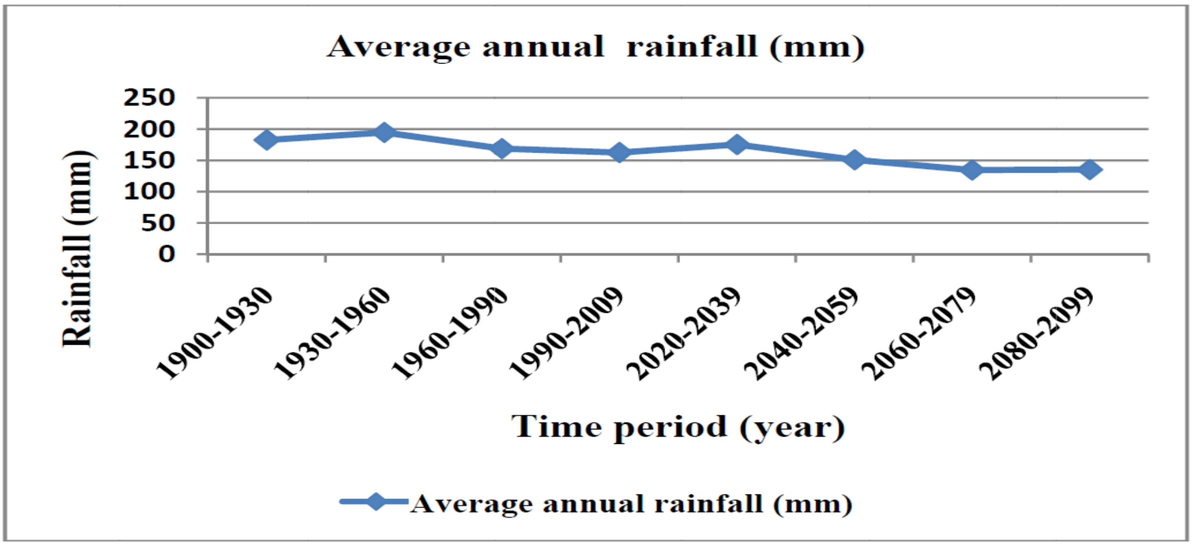

Figure 4-10: Average annual rainfall (mm) over the historical and future periods (Source: original diagram created using data from Zakaria et al., 2013)

4.3.3 Weather pattern changes

A number of profound issues that can be attributed to climate change have been apparent in the Iraqi climate. The desertification processes, frequent and intense dust storms, rising air temperatures above 50°C, prolonged drought conditions and sudden heavy rainfall and storms have become increasingly frequent in the Iraqi climate (Janabi 2013). For example, extreme drought that occurred between 2005 and 2007 was followed by several months of sudden heavy rainfall and storms during which vast parts of central and southern Iraq received 200% of normal rainfall (United Nations Country Team Iraq 2012). The effects of significant changes in weather patterns are exacerbated by inability to store water during rainfall events, abandonment of agricultural land during drought, reduction in flow rates in the Tigris and Euphrates Rivers, shrinking of the marshlands, soil erosion and an increased salinity in the Shatt al-Arab estuary as well as in groundwater in the south.

4.4 Impacts of climate change on water resources and hydrology

On a global scale, significant trends in streamflow were observed in many regions: some were increases and others were decreases (IPCC 2014). However, these trends cannot be confidently attributed to climate change, as it is difficult to differentiate the impacts of variations in temperatures and precipitation from the effects of human involvement in the catchment, such as land use change and reservoir construction (Nicholls et al. 1997). In addition, variation in streamflow from year to year is strongly associated with the atmospheric circulation patterns such as ENSO, which could be aggravated by global warming (IPCC 2014).

4.4.1 Observed changes in streamflow in Queensland

In Queensland, flows are extremely variable during and between years: higher than 90% of flow takes place in the wet season in summer and autumn from December to May (Lough 2007). In December of 2010 Queensland experienced the wettest year on record, leading to a devastating flood in Rockhampton, Bundaberg areas and then in Brisbane. The wettest places along the east coast documented higher than 1200 millimetres of precipitation above the long-term average of 623.34 millimetres, taken from 1961-1990 (Nancarrow 2011). This flood was mainly attributable to climate change and has led to severe damage to infrastructure, crop and livestock loss and eventually severe damage to communities (Government of Queensland 2014). The Fitzroy River at Rockhampton was well above its moderate flood level. The Central Queensland University established an evacuation centre. Nearly 4000 properties were damaged. Approximately 1000 households had yard flooding, while 200 were inundated (Queensland Floods Commission 2011). Three years after this devastating flood, Queensland faced a severe drought: in March 2014, 50 local governments in the state announced that 80% of the state was in drought, the largest area to be ever officially declared in drought. In February

2015, the number of local governments who declared drought reduced slightly to 44 and thus a considerable percentage of the state remained in drought. Mandatory water restrictions were applied that showed that average water usage in some suburbs dropped to 129 litres per person per day, compared to a regional urban use of 375 litres under normal operating conditions.

4.4.2 Observed changes in streamflow in Northeast Iraq

Iraq was considered rich in its water resources until 1970 owing to the existence of the Tigris and Euphrates Rivers (Al-Ansari et al. 2014). The historical name "Mesopotamia" means the land between two rivers. However, storage projects that Turkey and Syria have commenced to build on the upper parts of the rivers have led to a significant reduction in their flows. Climate change in Iraq is exacerbating water scarcity. The Tigris discharges have decreased to less than a third of their regular capacity and are predicted to fall further in coming decades and be completely dry by 2040 due to water-related activities of upper riparian countries and climate change (Al-Ansari et al. 2014), if the current trends continue unabated. The sharp decreases in water flow have led to severe problems, such as a rapid development of the desertification process, progressively frequent and severe dust storms, and continued drought conditions (Janabi 2013). These in turn have led to severe decline in agricultural production: for example, Iraq's wheat production in 2009 decreased to 45 percent below that of a typical harvest (Holthaus 2014).

To summarise, this chapter has presented observed and projected changes in the climate of study areas and the neighbourhood, as they are related to water. In both regions, it is evident that there have been significant changes in recent times in weather such as air temperatures and precipitation. In both regions, air temperatures have increased in the last three decades. The precipitation in the Fitzroy River catchment has been very variable and there has been no clear trend in the last three decades. However, in the Tigris River catchment, precipitation has noticeably decreased over time. In general, weather in both the regions is projected to get hotter in the future while precipitation is projected to increase in the Fitzroy Basin and decrease in the Tigris River basin.

CHAPTER 5

MODEL DEVELOPMENT, CALIBRATION, AND VALIDATION

5.1 Introduction

Given that SWAT has been chosen as the model to simulate hydrologic processes for this study, it is required to develop the model selecting appropriate parameters and calibrate and validate the values of those. Sensitivity analysis of model parameters is capable of identifying the relevant parameters from the myriad of possible parameters. Calibration and validation of the model parameters are usually done using R^2 and the ENC index to assess the model performance, as is evident from published literature.

5.2 Sensitivity analysis of model parameters

Sensitivity analysis was conducted for the 25 parameters related to streamflow in the SWAT model (Table 5.1), from which the 12 most sensitive parameters have been considered for implementing the model calibration for both the Tigris and Fitzroy Basins. The 12 model parameters were grouped into three categories which govern basin, surface and sub-surface responses:

- **Basin response parameters**

Three basin response parameters (SURLAG, CH-K2, SFTMP) were calibrated in the SWAT model for both the regions. SURLAG (Surface runoff lag time) governs the portion of the total water that is permitted to enter the reach in one day (Cibin et al. 2010). CH-K2 (effective hydraulic conductivity of channel) directs the movement of water from the channel-bed to the subsurface for transient streams (Ghaffari et al. 2010). SFTMP is the mean air temperature at which precipitation is equally likely to be rain or snow (Sanadhya et al. 2014).

- **Surface response parameters**

Parameters that control the surface water response to be calibrated in SWAT comprise the runoff curve number (CN2), available soil water capacity (SOL-AWC), the soil evaporation compensation factor (ESCO), average slope length (SLSUBBSN) and slope steepness (HRU-SLOP). The CN2 is used to estimate the amount of runoff from the total rainfall event. It is a function of basin properties, including land use, soil type and antecedent moisture condition (Arnold et al. 1998). The greater the CN2, the greater is the generated surface runoff (Sanadhya et al. 2010). The SOL-AWC is the amount of water that is available to plant for uptake when the soil is at field capacity. It is assessed by subtracting the amount of water existing at permanent wilting point from that existing at field capacity (Arnold et al. 1998). The ESCO governs the soil evaporative demand that is to be met from different soil depths (Cibin et al. 2010). The SLSUBBSN is measured to the point that flow starts to concentrate (Arnold et al. 1998). The HRU-SLOP is average slope steepness.

Table 5.1: Description of input parameters of SWAT related to streamflow (Source: Arnold et al. 1998).

Group	Parameter	Description	Unit
Soil	SOL_ALB	Moist soil albedo	-
	SOL_AWC	Available water capacity	mm mm^{-1}
	SOL_K	Saturated hydraulic conductivity	mmh^{-1}
	SOL_Z	Depth to bottom of second soil layer	mm
Groundwater	ALPHA_BF	Base flow Alpha factor	days
	GW_DELAY	Groundwater delay	days

	GW_REVAP	Groundwater 'revap' coefficient	-
	GWQMN	Threshold depth of water in the shallow aquifer for return flow to occur	mm H_2O
	REVAPMN	Threshold depth of water in the shallow aquifer for 'revap' to occur	mm H_2O
Sub-basin	TLAPS	Temperature laps rate	°C km^{-1}
HRU	EPCO	Soil evaporation compensation factor	-
	ESCO	Plant uptake compensation factor	-
	CANMX	Maximum canopy storage	mm H_2O
	SLSUBBSN	Average slope length	m
Routing	CH_N2	Manning's n value for the main channel	-
	CH_K2	Effective hydraulic conductivity in main channel alluvium	mm h^{-1}
Management	BIOMIX	Biological mixing efficiency	-
	CN2	Initial SCS runoff curve number for moisture condition II	-
General data basin	SFTMP	Snowfall temperature	°C
	SMFMN	Minimum melt rate for snow during year	mm H_2O $°C^{-1}$ day^{-1}
	SMFMX	Maximum melt rate for snow during year	mm H_2O $°C^{-1}$ day^{-1}
	TEMP	Snowpack temperature lag factor	-
	SURLAG	Surface runoff lag time	days

Group	Parameter	Description	Unit
	BLAI	Maximum potential leaf area index for land cover/plant	-
	SLOPE	Slope	-

- **Sub-surface response parameters**

Four calibration parameters contribute to the sub-surface water response in SWAT: ALPHA_BF, GWQMN, GW_REVAP, and GW_DELAY. ALPHA_BF is a direct index of groundwater flow response to changes in recharge (Arnold et al. 1998). GWQMN is the threshold depth of water in the shallow aquifer required for return flow to occur (Winchell et al. 2007). GW_REVAP governs the volume of water that transfers from the shallow aquifer to the root zone due to soil moisture depletion (Sanadhya et al. 2014). GW_DELAY is the time required for water departing the bottom of the root zone to reach the shallow aquifer (Winchell et al. 2007).

5.2.1 Sensitivity Analysis for the Tigris Basin

The ranking of the 12 highest sensitive parameters for each watershed is presented in Table 5.2. For the Khbour, Greater Zab and Diyala, SFTMP was the most sensitive parameter, but it ranked eighth for Al-Adhaim and Lesser Zab. These results appear reasonable, since Khbour, Greater Zab and the upper part of Diyala Rivers are snow-dominated mountainous terrains. The CN2 was the dominant SWAT calibration parameter for Al-Adhaim and Lesser Zab. However, it was ranked the second, third and fourth for the Khbour, Diyala and Greater Zab, respectively. In most SWAT applications in other watersheds, the CN2 has been found to be the most sensitive parameter (Cibin et al. 2010). The CN2 has a major impact on the amount of runoff generated from the HRU; thus a relatively high sensitivity index can be expected for most of the basins (Veith et al. 2010). SOL_AWC came third for Al-Adhaim, Greater Zab and Lesser Zab, while it was fifth and sixth for Diyala and Khbour, respectively. Al-Adhaim River showed much higher sensitivity to ESCO compared to the rest of the watersheds, mainly due to the higher mean air temperature and solar radiation, which result in higher evapotranspiration losses. The identification by SWAT for the arid Al-Adhaim catchment that the greatest sensitive parameters were CN2, SOL_AWC and ESCO is consistent with the report of Veith et al. (2010), who found that the SWAT model is highly sensitive to surface runoff parameters (CN2, ESCO, SOL_AWC) when the watershed is categorized as an arid basin.

Among the four groundwater parameters, ALPHA-BE was observed to be the most sensitive parameter overall for all watersheds. ALPHA-BE was ranked the second for Diyala, Greater Zab and Lesser Zab, whereas it was ranked third and fourth for Khbour and Al-Adhaim catchments, respectively. This result is consistent with the findings of Li et al. (2009), who found that ALPHA-BE is a highly sensitive groundwater parameter in SWAT calibrations. SWAT was observed to be relatively sensitive to GW-DELY for Diyala, Khbour and Lesser Zab.

Table 5.2: Ranks of 12 highest sensitive parameters related to streamflow in the five basins in Tigris Basin.

Parameter	Al-Adhaim	Diyala	Khbour	Greater Zab	Lesser Zab
CN2	1	3	2	4	1
ALPHA_BF	4	2	3	2	2
SFTMP	8	1	1	1	8
SOL_AWC	3	5	6	3	3
GW_DELAY	6	4	4	12	4
ESCO	2	8	11	8	11
HRU_SLP	7	11	12	5	7
SURLAG	5	12	10	7	5
GW_REVAP	12	7	9	11	6
GWQMN	9	6	8	9	9
SLSUBBSN	10	9	5	6	12
CH_K2	11	10	7	10	10

5.2.2 Sensitivity analysis for the Fitzroy River basin

The ranking of the 12 uppermost sensitive parameters for the Fitzroy Basin is shown in Table 5.3. The CN2 was observed to be the most sensitive. ALPHA-BE was ranked the second highest sensitive parameter. Among groundwater parameters ALPHA-BE was the top sensitive parameter; GW_DELAY was the third. It can be noticed clearly that CN2 and ALPHA_BF are the most sensitive parameters in either the Tigris or Fitzroy Basins. The reasons were given in the previous section.

Table 5.3: Ranking of 12 most sensitive parameters related to streamflow in the Fitzroy River basin.

Parameter	*Rank*	*Initial values*	*Fitted values*
CN2	1	-0.2 – 0.2	-0.12
ALPHA_BF	2	0 – 1	0.95
GW_DELAY	3	30 – 450	401
CH_K2	4	5 – 130	27.9
OV-N	5	-0.2 – 0	-0.19
HRU_SLP	6	0 – 0.2	0.01
ESCO.hru	7	0.8 – 1	0.85
REVAPMN	8	0 – 10	2.5
GW_REVAP	9	0 – 0.2	0.023
SLSUBBSN	10	0 – 0.2	0.13
SOL_AWC	11	-0.2 – 0.4	-0.03
GWQMN	12	0 – 2	1.83

5.3 Calibration and Validation

5.3.1 Tigris Basin

The SWAT model was calibrated for nine discharge stations distributed in the five sub-basins of the Tigris River. Three of these stations are located in Greater Zab: the Bekhme Dam Station, Bakrman Dam Station and Eski Kelek Station. Alunkubri and Dokan Stations are located in Lesser Zab. In Diyala Basin, there are two stations: Derbendi-Khan and Discharge Site Station. Zakho and Injana Stations are located in Khbour Basin and Al-Adhaim Basin, respectively. Table 5.4 shows the period of calibration and validation in each station. The period of validation in Zakho, Alunkubri and Discharge Site Station was set short due to the short discharge data period. The first three years in all stations was set as a warmup period.

Table 5.4: The period of calibration and validation for each station

Discharge Station	Calibration period	From- To	Validation period	From-To
Zakho	10	1977-1986	4	1987-1990
Bekhme	18	1979-1996	8	1997-2004
Bakrman	18	1979-1996	8	1997-2004
Eski Kelek	18	1979-1996	8	1997-2004
Alunkubri	8	1977-1984	3	1985-1987
Dokan	16	1977 - 1995	9	1996-2004
Injana	13	1979-1991	6	1992-1997
Derbendi-Khan	18	1979-1996	8	1997-2004
Discharge Site Station	10	1979-1988	3	1989-1991

Khbour sub-basin

SWAT calibration and validation was conducted at Zakho Discharge Station, which is the solo station within this basin. It is located at latitude 37.14^0N and longitude 42.69^0 E, at the outlet of the basin. For Zakho Station, in the calibration period, R^2 and ENC were 0.89 and 0.89, respectively. The observed data being covered by P-factor was 0.88 with R-factor of 1.16. In the validation period, R^2 and P-factor remained nearly consistent, ENC declined to 0.61, and R-factor increased to 1.41, as shown in Figure 5.1.

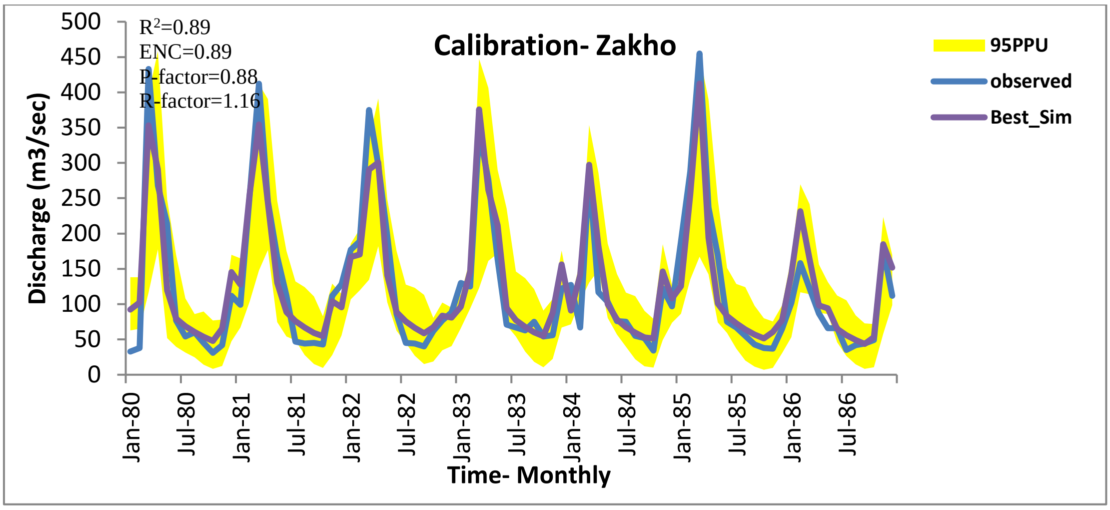

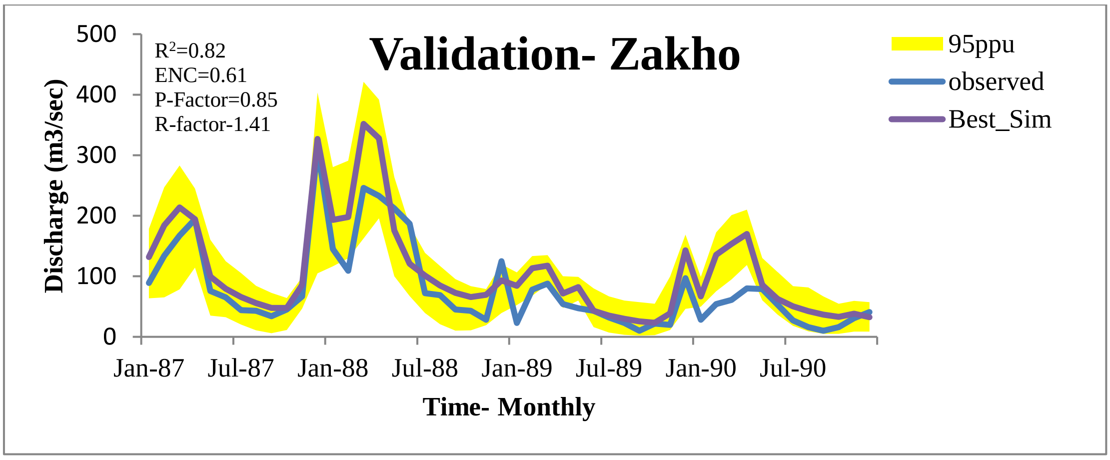

Figure 5.1: Calibration and Validation of the SWAT model (monthly scale) at Zakho Station within Khbour sub-basin (Source: original work created for this thesis)

Greater Zab sub-basin

SWAT was calibrated and validated for Greater Zab Basin at three discharge stations on a monthly scale (Bekhme Station, Bakrman Station and Eski Kelek Station). Bekhme Station lies at latitude 36.63^{0}N and longitude 44.48^{0}E, northeast of the basin. Bakrman Station is located near the Greater Zab outlet, at latitude 36.33^0 N and longitude 43.55^{0}E on the Khazir River, one of the Greater Zab's tributaries. Eski Kelek Station is situated in the lower part of the basin, at the basin outlet, at latitude 36^{0}N and longitude 43.35^{0}E.

The results of monthly discharge calibration and validation for the Bekhme Station are shown in Figure 5.2. For calibration, R^2 value was 0.69 and ENC index was 0.66. Seventy-seven percent of the observed data was bracketed by 95 PPU (P-factor) with R-factor of 1.08. During the validation, R^2 increased to 0.89, but ENC decreased to 0.60. P-factor decreased to 0.51 and R-factor increased to 1.34.

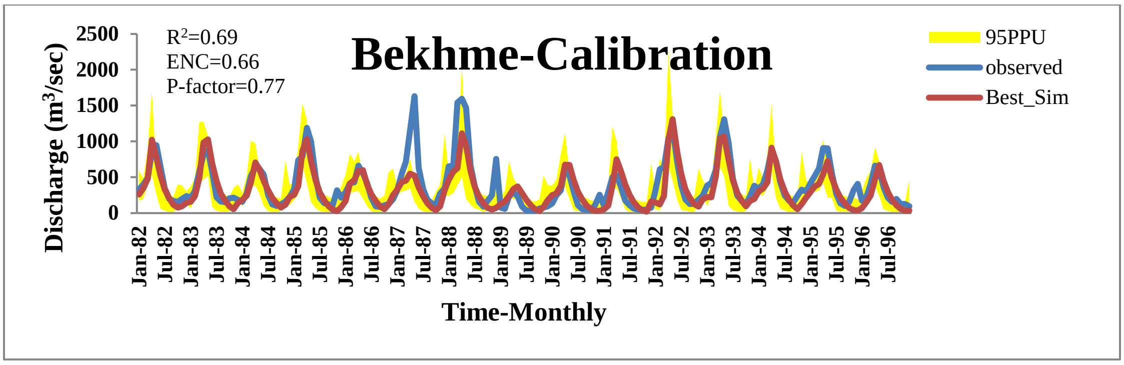

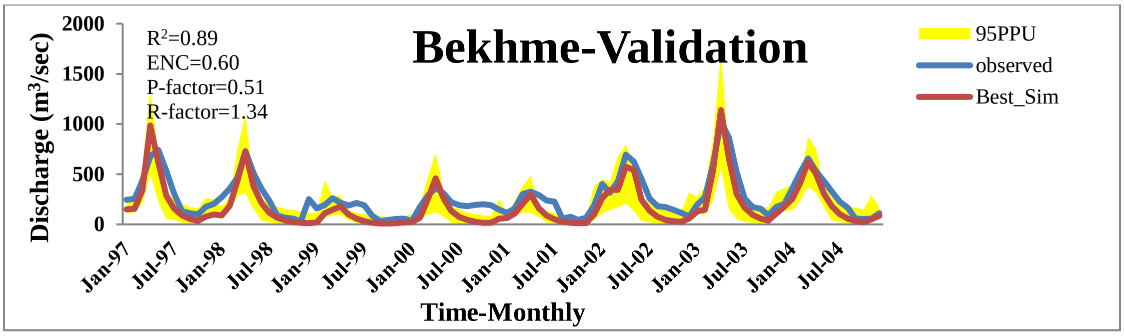

Figure 5.2: Calibration and Validation of the SWAT model at monthly scale at Bekhme Station within Greater Zab sub-basin (Source: original work created for this thesis)

At Bakrman Dam Station, the results of monthly discharge calibration and validation are presented in Figure 5.3. R^2 and ENC were 0.53 and 0.55, respectively. Fifty-eight percent of the observed data was bracketed by P-factor with R- factor of 0.88. In the validation period, R^2 increased to 0.66 and ENC remained approximately consistent. P-factor and R-factor increased to 0.89 and 1.76, respectively.

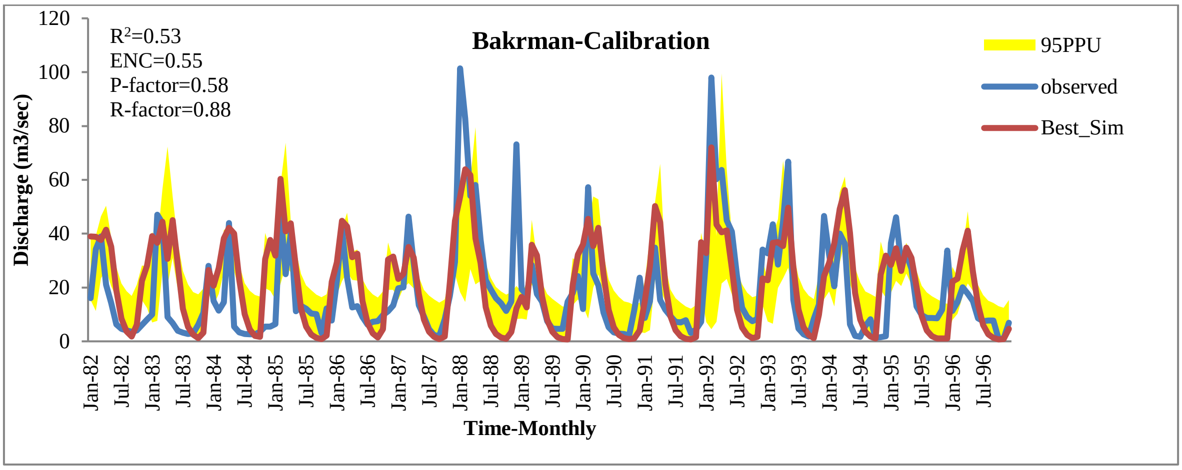

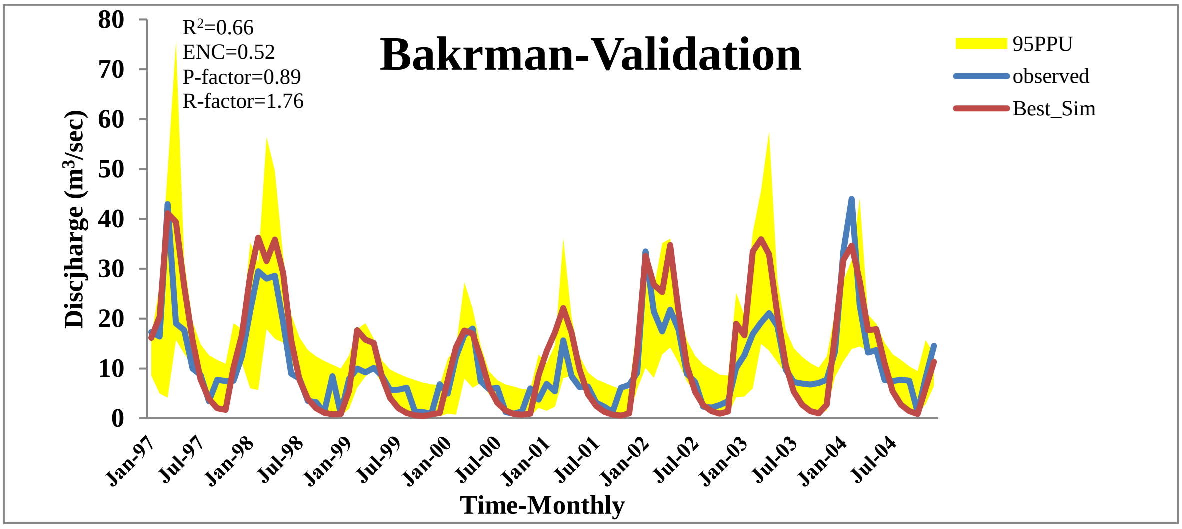

Figure 5.3: Calibration and Validation of the SWAT model at monthly scale at Bakrman Station within Greater Zab sub-basin (Source: original work created for this thesis)

The calibration and validation results for the Eski Kelek Station are shown in Figure 5.4. In the calibration process, R^2 was 0.58 and ENC was 0.56. Observed data was bracketed by P-factor with 0.76. For the validation, R^2 remained consistent; ENC, P-factor and R-factor decreased to 0.51, 0.55 and 0.38, respectively.

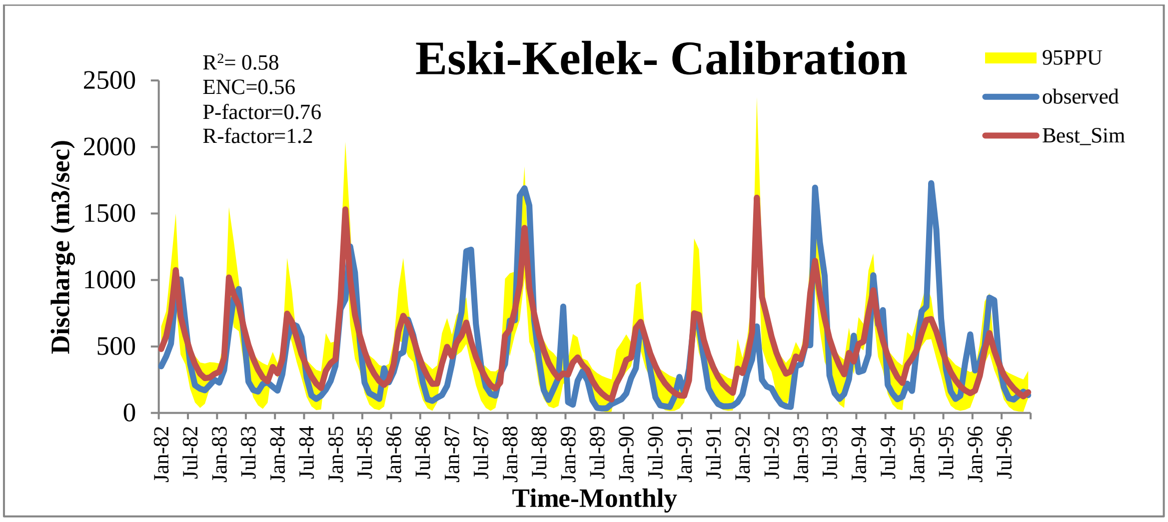

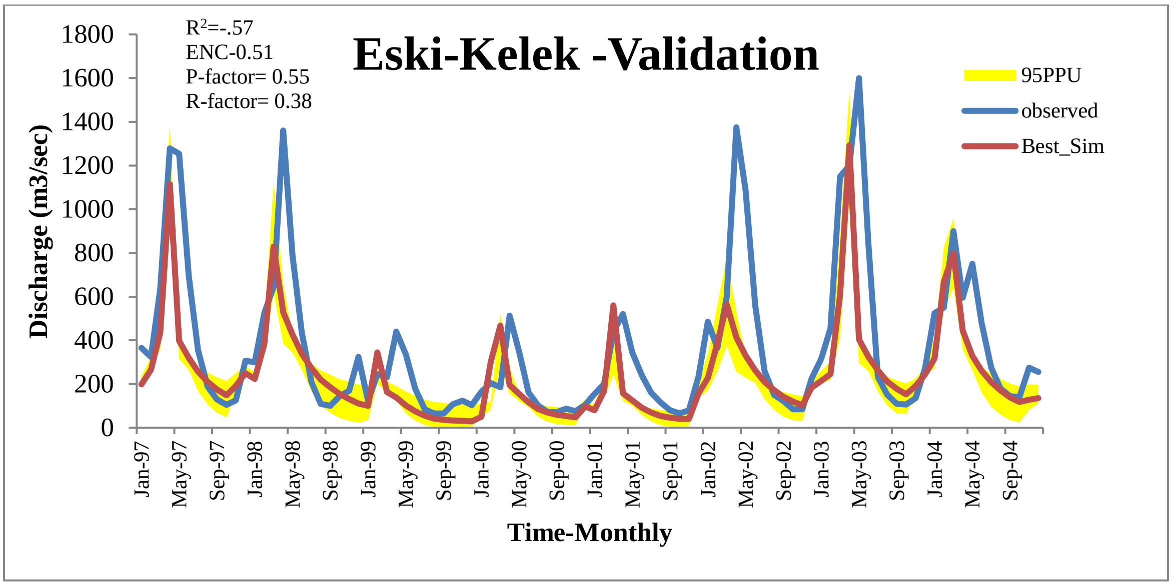

Figure 5.4: Calibration and validation of the SWAT model at monthly scale at Eski Kelek Station within Greater Zab Basin (Source: original work created for this thesis)

Lesser Zab sub-basin

The model was calibrated and validated at two discharge stations: Alunkubri and Dokan Stations. Alunkubri Station is located at latitude 35.75^0 N and longitude 44.13^0 E, in the upper part of the basin. Dokan Station lies at latitude 35.88^0 N and longitude 44.96^0 E, in the lower part of the basin.

The results of SWAT calibration and validation at Alunkubri Station are shown in Figure 5.5. In calibration period, R^2, ENC and P-factor were 0.77, 0.76 and 0.88, respectively. For the validation period, R^2 increased to 0.87; ENC and P-factor remained nearly constant.

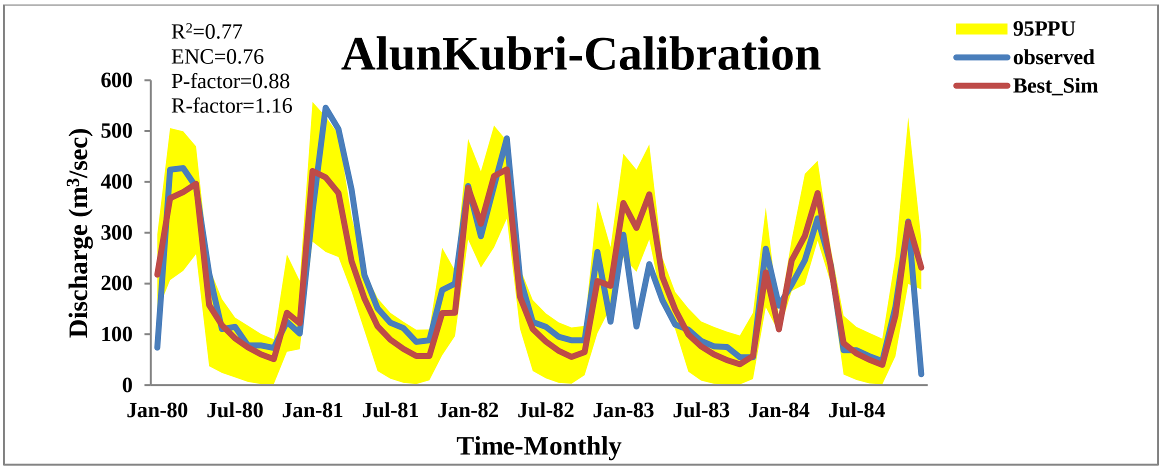

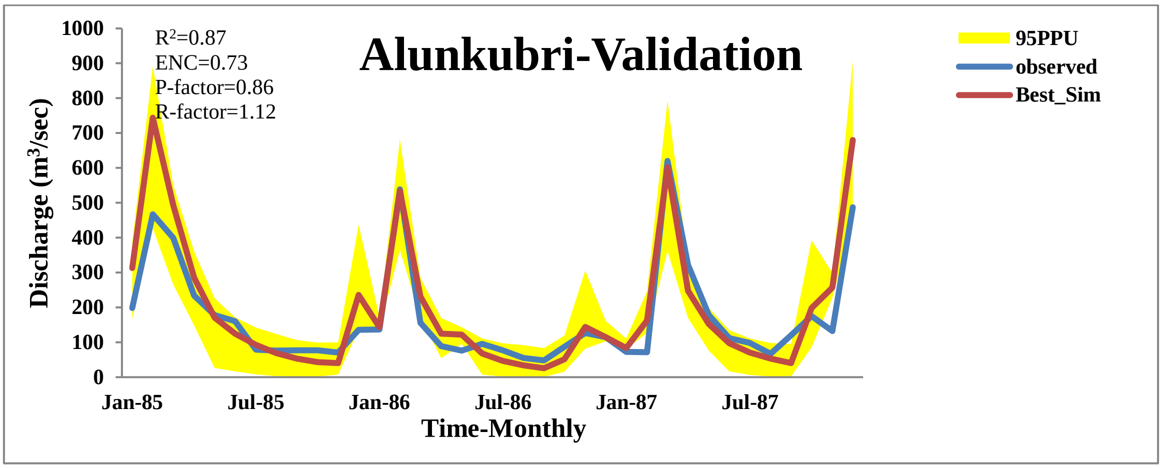

Figure 5.5: Calibration and validation of the SWAT model at monthly scale at AlunKubri Station within Lesser Zab(Source: original work created for this thesis)

At Dokan Station, for the calibration process, R^2, ENC and P-factor were 0.58, 0.54 and 0.72, respectively (Figure 5.6). During the validation period, R^2, ENC and P-factor increased to 0.76, 0.71 and 0.77, respectively.

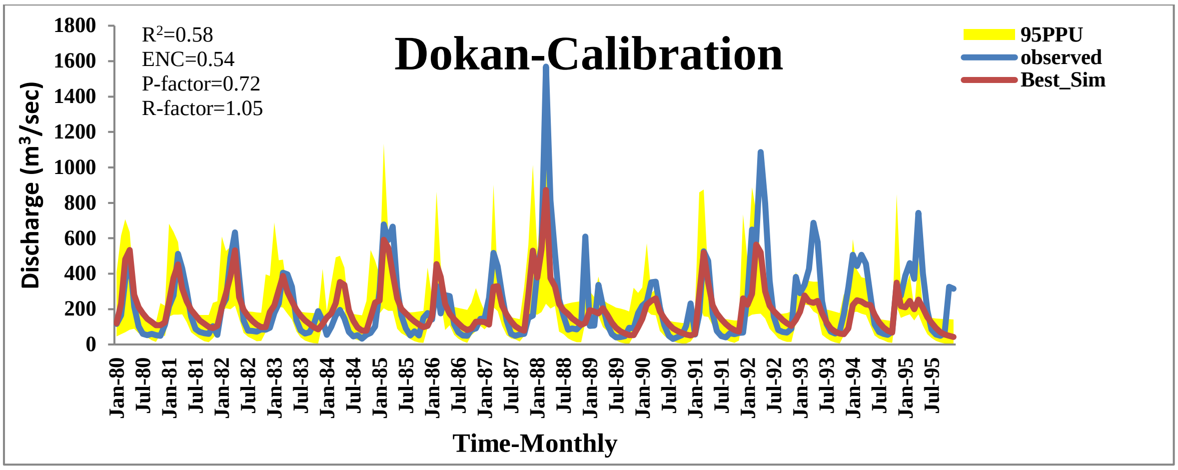

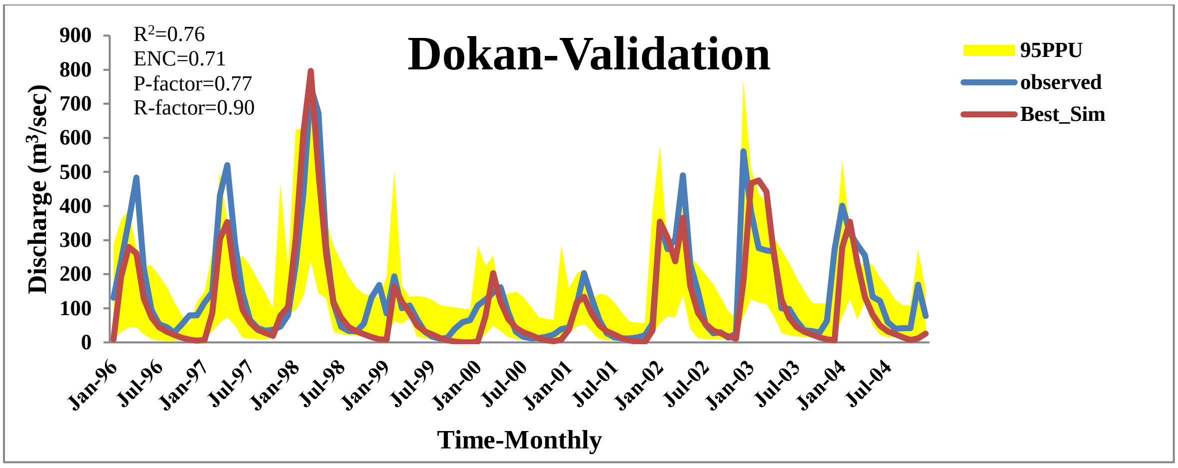

Figure 5.6: Calibration and validation of the SWAT model at monthly scale at Dokan Station within Lesser Zab sub-basin (Source: original work created for this thesis)

Al-Adhaim sub-basin

The Injana Station is the only station located at the Al-Adhaim River, which lies at latitude 34.5^{0}N and longitude 44.5^{0}E, in the lower part of the basin. The station was used to calibrate and validate the model. The results of the calibration and validation processes are shown in Figure 5.7. R^2, ENC and P-factor were 0.69, 0.67 and 0.54, respectively, during calibration. During the validation period, R^2 and ENC increased to 0.8 and 0.76, respectively, but P-factor decreased to 0.45.

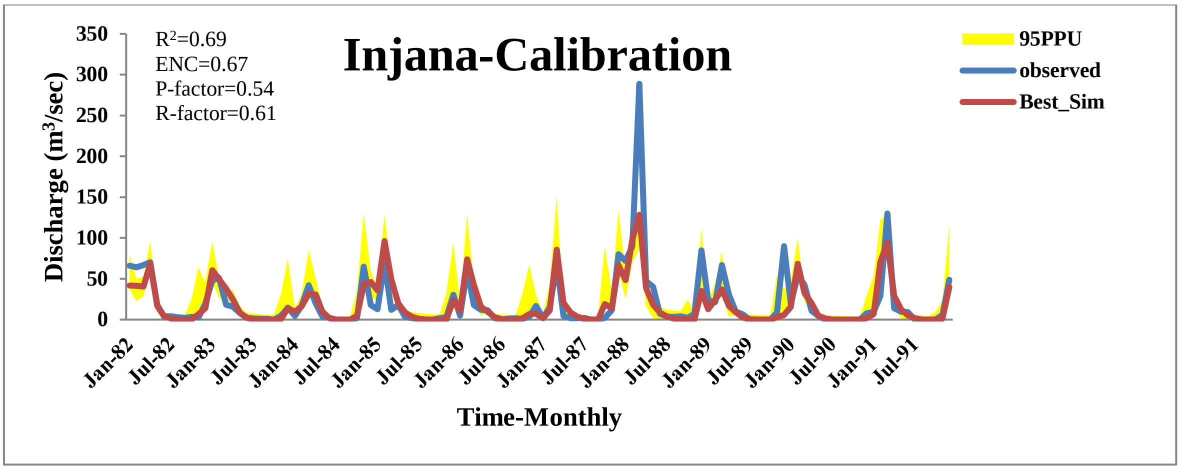

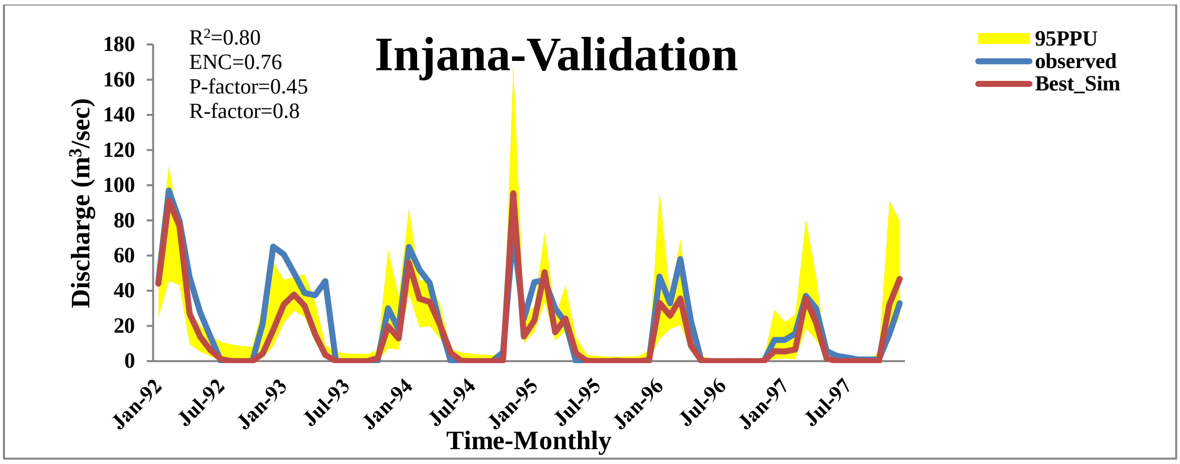

Figure 5.7: Calibration and validation of the SWAT model at monthly scale at Injana Station within Al-Adhaim (Source: original work created for this thesis)

Diyala sub-basin

In Diyala Basin, SWAT was calibrated and validated at two stations: Derbendi-Khan and Discharge Site Station. Derbendi-Khan Station lies at latitude 35.13^0 N and longitude 45.75^{0}E and Discharge Site Station lies at latitude 35.1^0 N and longitude 45.75^0 E; both stations are located in the upper part of the basin. The calibration and validation results at Derbendi-Khan are shown in Figure 5.8. During the calibration period, R^2, ENC and P-factor were 0.73, 0.67 and 0.73, respectively. In the validation period, both R^2 and ENC increased to 0.87 and P-factor increased to 0.86.

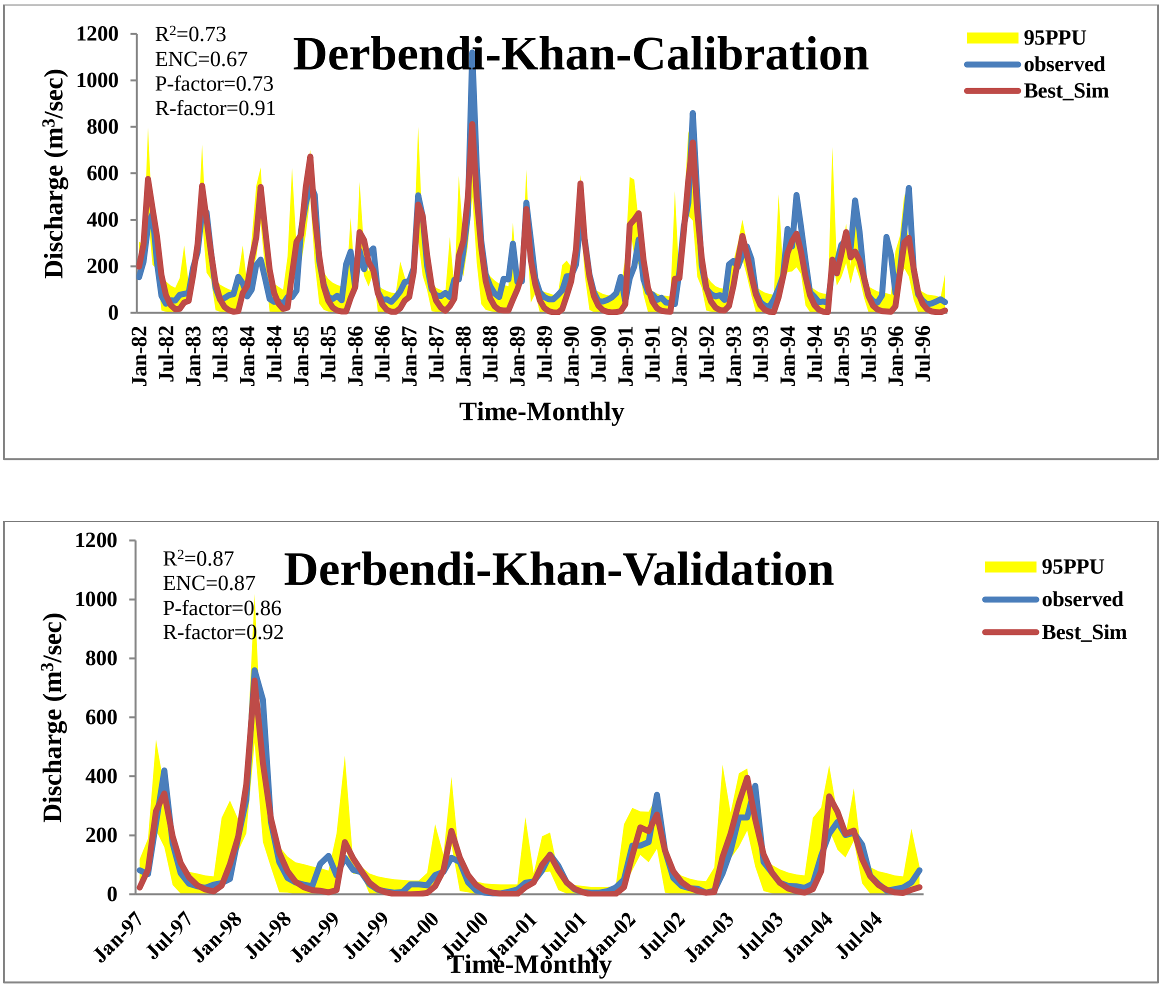

Figure 5.8: Calibration and validation of the SWAT model at monthly scale at Derbendi-Kan Station within Diyala Basin (Source: original work created for this thesis)

At Discharge Site Station, during the calibration period, R^2, ENC and P-factor were 0.68, 0.54 and 0.63, respectively. For the validation period, R^2, ENC and P-factor increased to 0.88, 0.71 and 0.92, respectively (Figure 5.9).

The statistical indices for assessing the model performance at the nine discharge stations are summarised in Table 5.5. The values of R^2 ranged from 0.53 to 0.89 in the calibration process, while they were between 0.66 and 0.89 in the validation process. This means that the model is able to explain at least 0.53 of temporal variability related to streamflow at any of the nine stations. The values of the ENC index were higher than 0.50 for both calibration and validation. Based on the R^2 and ENC values, the model performance can be judged as satisfactory (Moriasi et al. 2007; Legates and McCabe 1999). In the five watersheds, the model showed the best performance in the Khbour basin at Zakho Station, followed by the Lesser Zab Basin at Alunkubri Station and Diyala Basin at Derbendi-Khan Station. Generally, the SWAT model was unable to capture high-flow events. It is typical of mathematical models to under-capture extreme events if not specifically focussed on extreme events. SWAT is not designed to simulate extreme hydrological conditions (Tolson and Shoemaker 2007). These results are consistent with those of Rostamian et al. (2008), Al-Mukhtar et al. (2014), Santhi et al. (2001), Ndomba et al. (2008), Güngör and Göncü (2013), and Zhang et al. (2014).

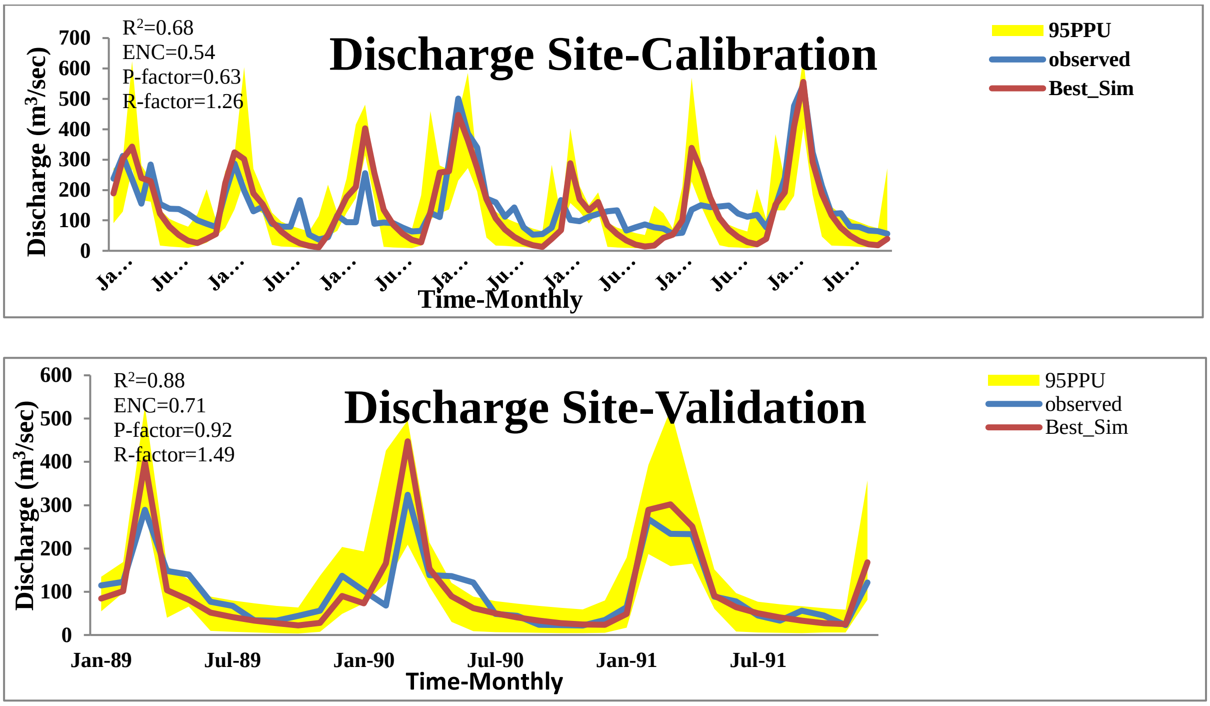

Figure 5.9: Calibration and validation of the SWAT model at monthly scale at Discharge Site Station within Diyala sub-basin (Source: original work created for this thesis)

Table 5.5: The statistical indices values (R^2, ENC, R. factor, P. factor) at the nine discharge stations within the five basins in the North East Iraq Region.

Watershed	Station	Calibration				Validation			
		R^2	ENC	R. factor	P. factor	R^2	ENC	R. factor	P. factor
Khbour	Zakho	0.89	089	1.16	0.88	0.82	0.61	1.41	0.85
Greater-Zab	Bekhme	0.69	0.66	1.08	0.77	0.89	0.53	1.34	0.51
Greatr-Zab	Bakrman	0.53	0.50	0.88	0.58	0.66	0.52	1.76	0.89
Greater-Zab	Eski Kelek	0.58	0.56	1.2	0.76	0.57	0.51	0.38	0.55
Lesser-Zab	Alulnkubri	0.77	0.76	1.16	0.88	0.87	0.73	1.12	0.86
Lesser-Zab	Dokan	0.58	0.54	1.05	0.72	0.76	0.71	0.90	0.77
Al-Adhaim	Injana	0.69	0.67	0.61	0.54	0.8	0.76	0.8	0.45
Diyala	Derbendi-Khan	0.73	0.67	0.91	0.73	0.87	0.87	0.92	0.86
Diyala	Discharge Site	0.68	0.54	1.26	0.63	0.88	0.71	1.49	0.92

5.3.2 Fitzroy Basin

The model was calibrated on a monthly scale for 22 years (1979-2000) and validated for 10 years (2001-2010); the first three years were used as a warm-up at eight different discharge stations located within the Fitzroy catchment (Table 5.6). Measured and simulated monthly flows at all discharge stations in the basin matched well in both calibration and validation processes as shown in Table 5.6.

Dawson sub-basin

The results of the calibration and validation processes of the Riverslea Monitoring Station, located near the Dawson Watershed outlet, have shown good agreement between observed and simulated values (Figure 5.10). R^2 value was 0.70 and the ENC index was 0.58. In addition, 64% of observed data was bracketed by 95 PPU (P-factor) with R-factor of 0.93. During the validation, R^2 and P-factor remained nearly consistent, ENC increased to 0.68 and R-factor decreased to 0.62 (Figure 5.10).

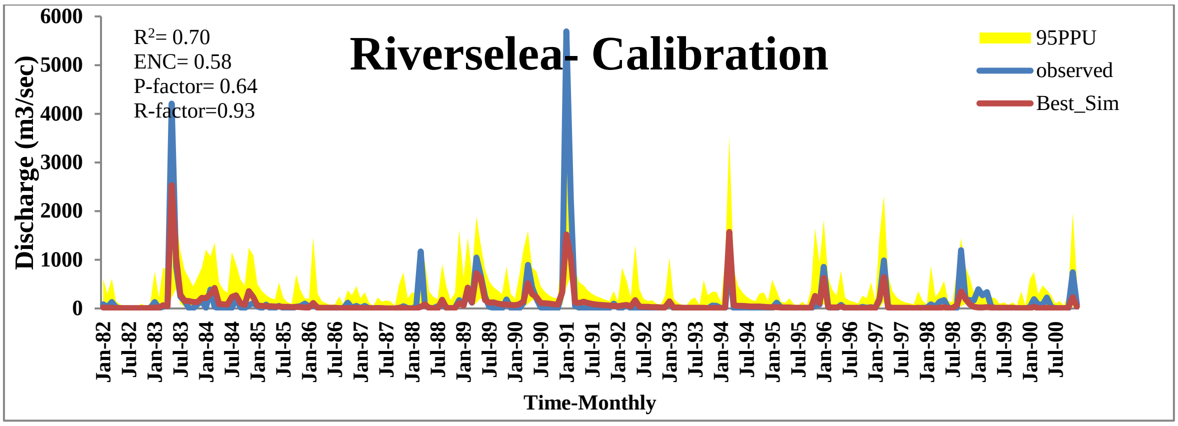

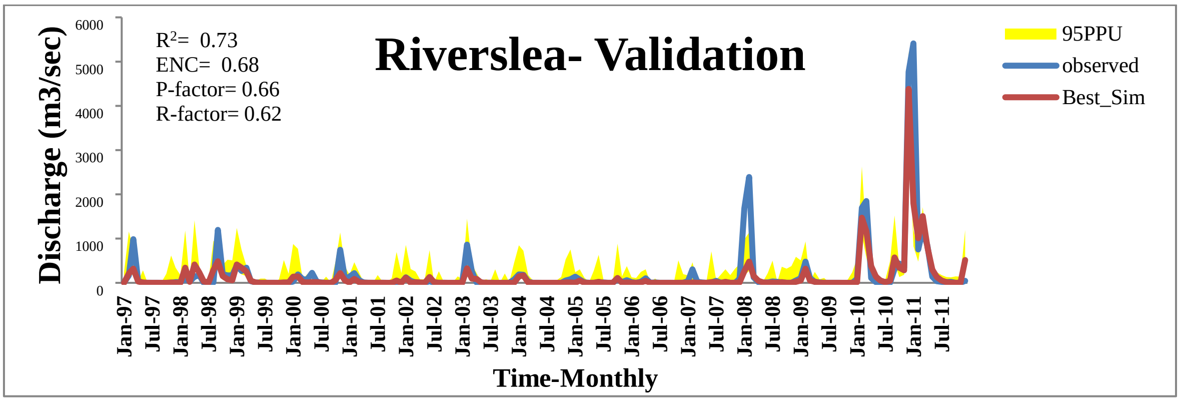

Figure 5.10: Calibration and validation of the SWAT model at monthly scale at Riverslea Station within Dawson (Source: original work created for this thesis)

The results of monthly discharge calibration and validation for the Redcliffe Station, located in the lower part of the Dawson Watershed, are shown in Figure 5.11. During the calibration, R^2 and ENC were 0.68 and 0.53, respectively. Twenty-nine percent of the observed data was bracketed by P-factor, and R-factor was 0.79. In the validation period, R^2 increased to 0.79, while ENC and P-factor remained consistent and R-factor decreased to 0.55.

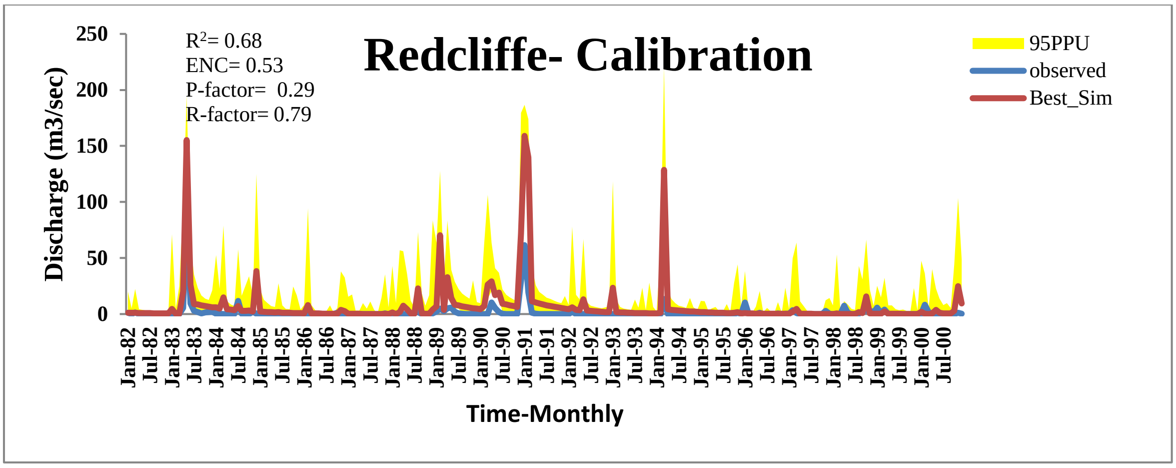

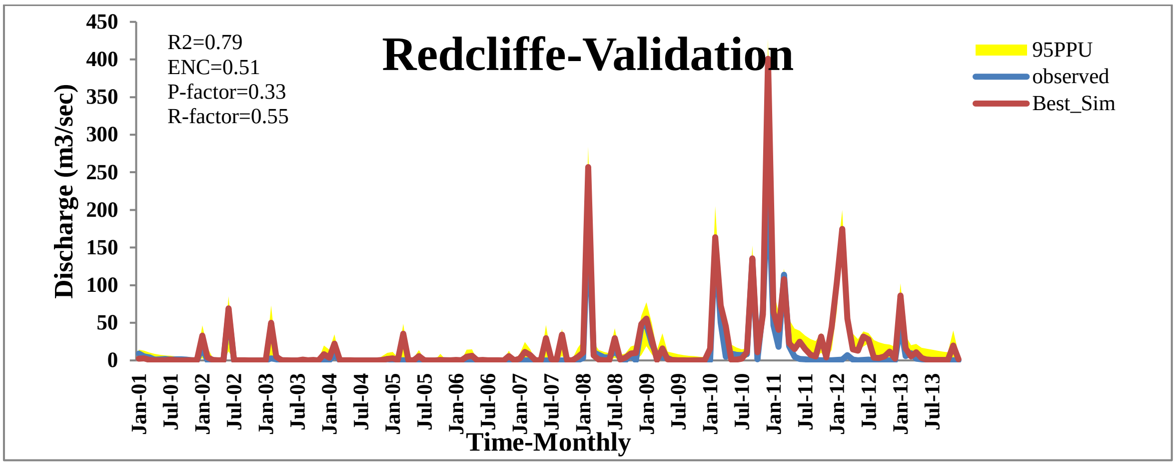

Figure 5.11: Calibration and validation of the SWAT model at monthly scale at Redcliffe Station within Dawson Watershed (Source: original work created for this thesis)

The calibration and validation results for Taroom Discharge Station, located in the upper part of Dawson Basin, are shown in Figure 5.12. In the calibration process, R^2 and ENC were 0.70 and 0.53, respectively. Observed data was bracketed by P-factor with 0.37. For the validation, R, ENC and P-factor increased to 0.84, 0.76 and 0.60, respectively.

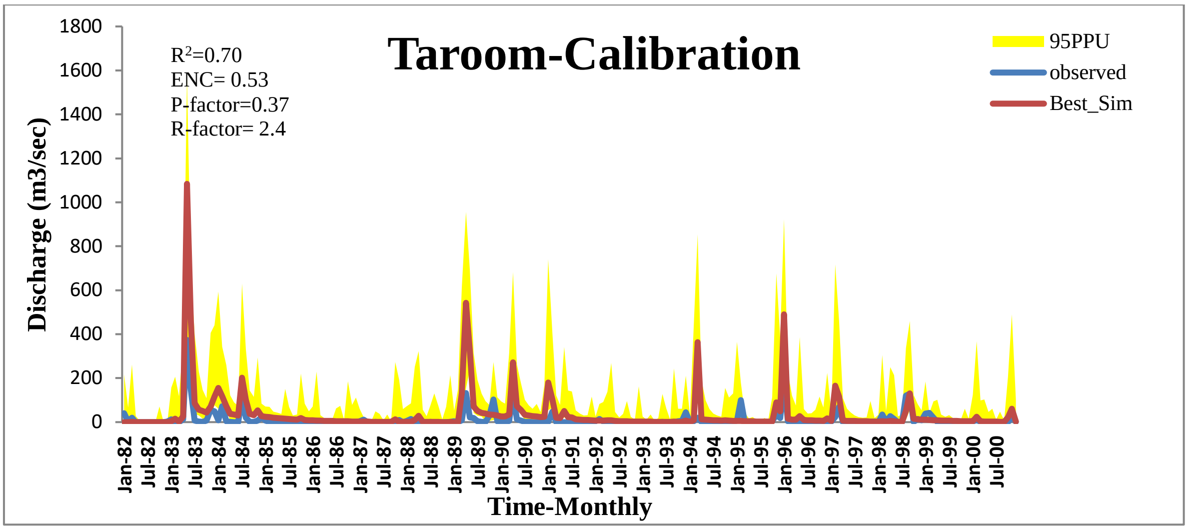

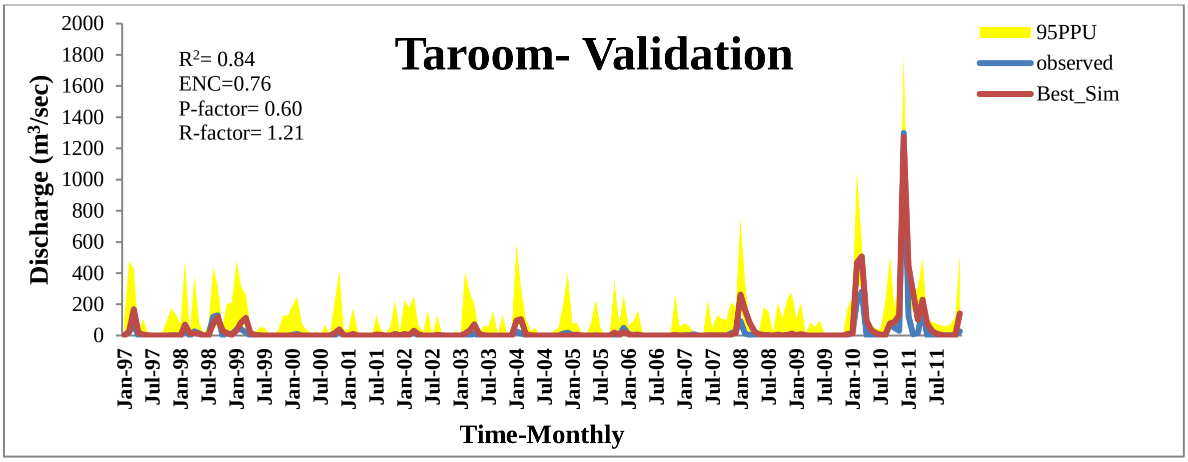

Figure 5.12: Calibration and validation of the SWAT model at monthly scale at Taroom Station within Dawson Basin (Source: original work created for this thesis)

Isaac sub-basin

The calibration and validation results for the Nebo Discharge Station, located in the outlet of the Isaac Basin, are shown in Figure 5.13. In the calibration process, R^2 and ENC were 0.74 and 0.73, respectively. Observed data was bracketed by P-factor with 0.42. For the validation, R^2 and ENC decreased to 0.63 and 0.62, respectively.

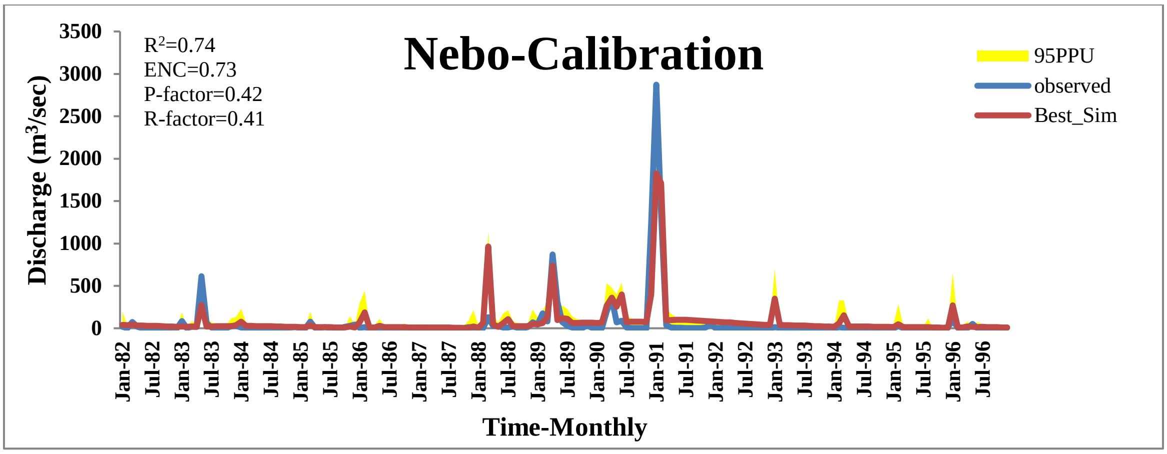

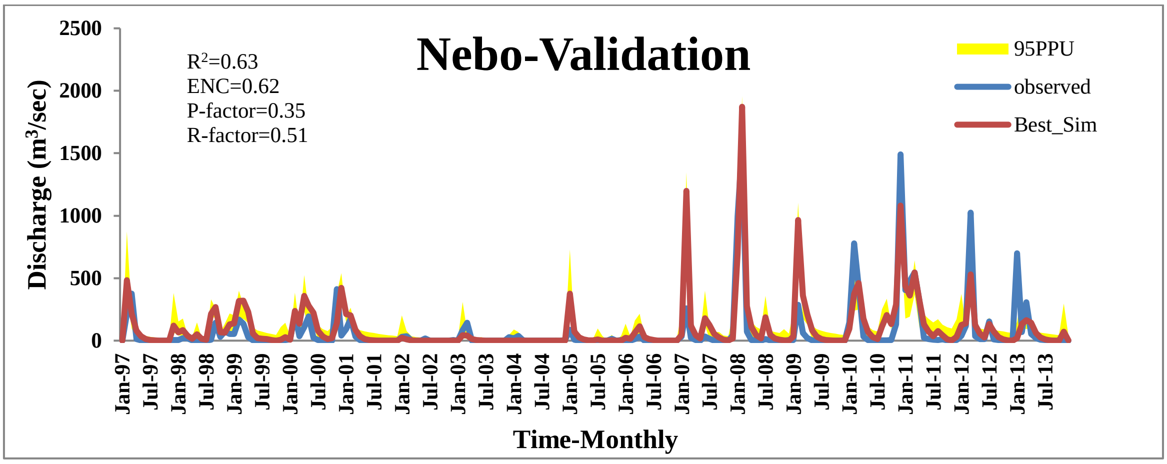

Figure 5.13: Calibration and validation of the SWAT model at monthly scale at Nebo Station within Isaac Watershed(Source: original work created for this thesis)

Comet sub-basin

The results of discharge calibration and validation for the Lake Station, located in the lower part of the Comet Watershed, are shown in Figure 5.14. During the calibration, R^2 and ENC were 0.86 and 0.83, respectively. Twenty-five percent of the observed data was bracketed by P-factor. R^2, ENC and P-factor increased to 0.89, 0.86 and 0.34, respectively.

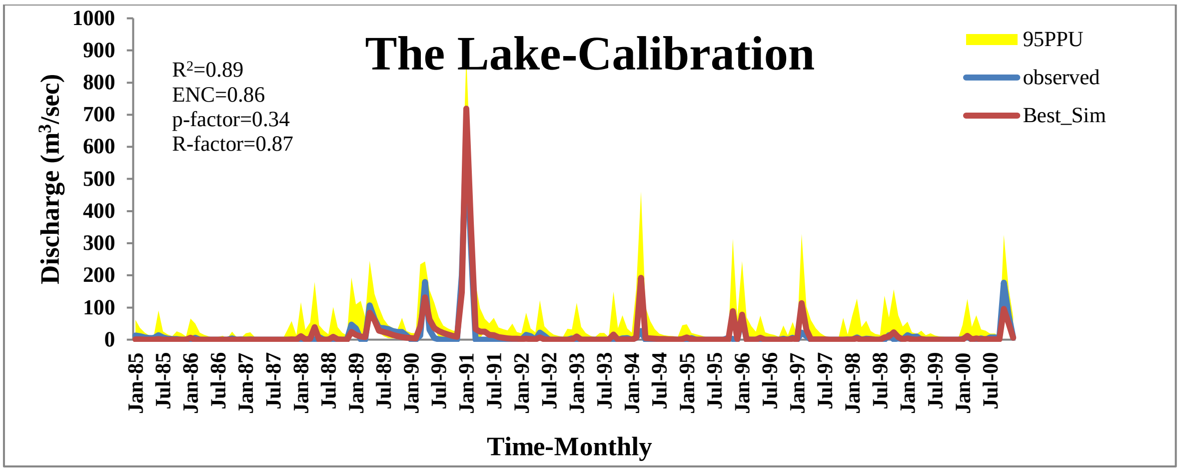

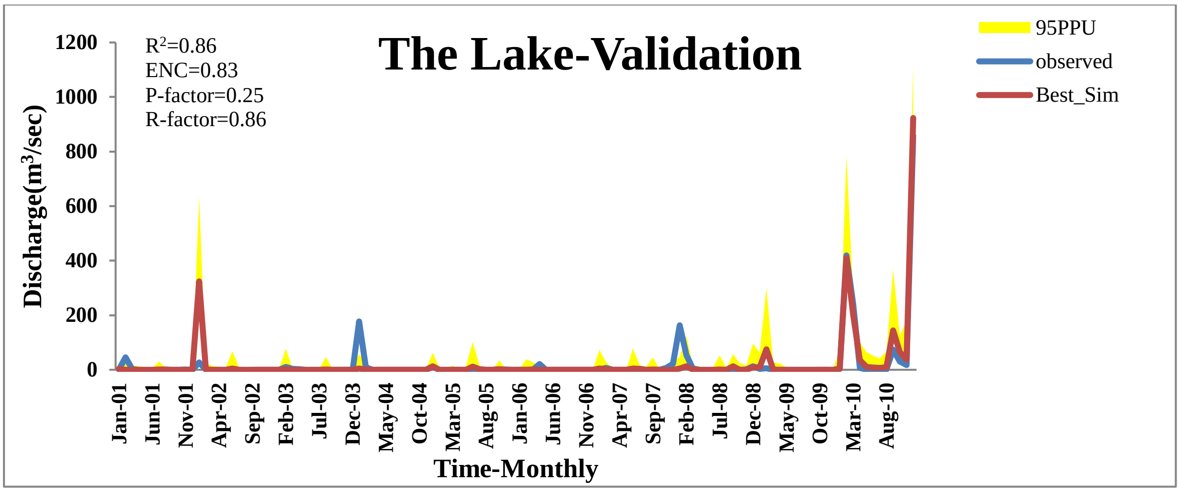

Figure 5.14: Calibration and validation of the SWAT model at monthly scale at the Lake Station within Comet Watershed (Source: original work created for this thesis)

Mackenzie sub-basin

The results of the calibration of the Coolmaringa Monitoring Station, located at Mackenzie River, are shown in Figure 5.15. R^2, ENC and P-factor were 0.62, 0.51 and 0.26, respectively. During the validation R^2 decreased to 0.58, ENC remained consistent and P-factor increased to 0.49.

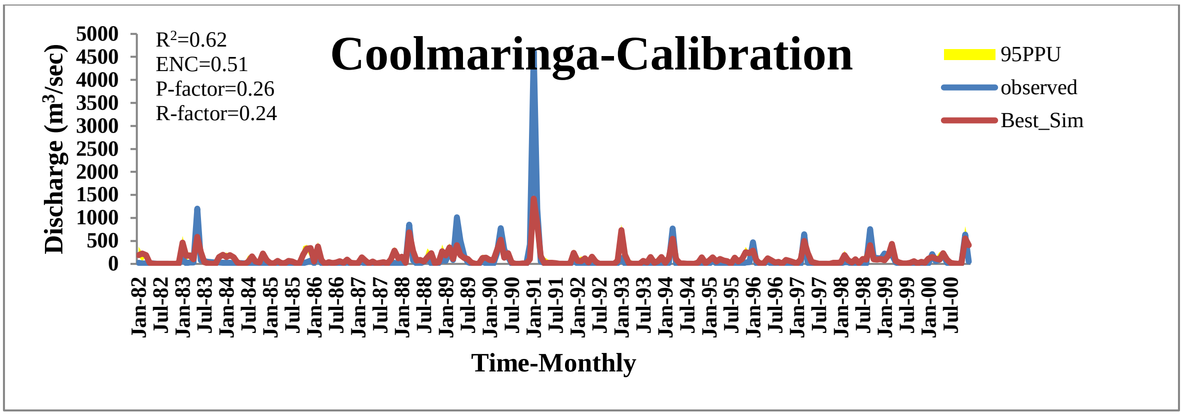

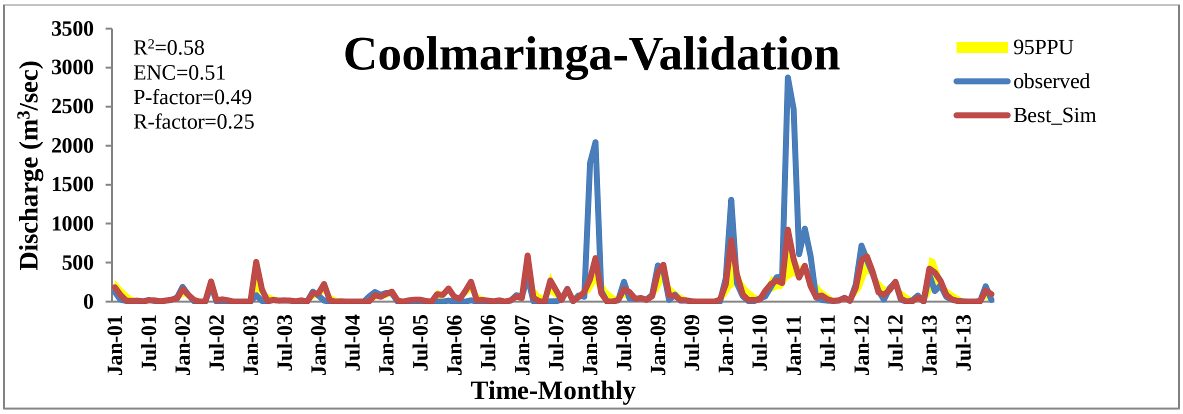

Figure 5.15: Calibration and validation of the SWAT model at monthly scale at Coolmaringa Monitoring Station, within Mackenzie Watershed (Source: original work created for this thesis)

Nogoa sub-basin

The results of the discharge calibration of the Gregory Highway Monitoring Station, located at Theresa Creek within the Nogoa Watershed, are shown in Figure 5.16. R^2, ENC index and P-factor were 0.69, 0.53 and 0.69, respectively. During the validation, R^2 and P-factor increased to 0.89 and 0.75, respectively. ENC decreased to 0.55.

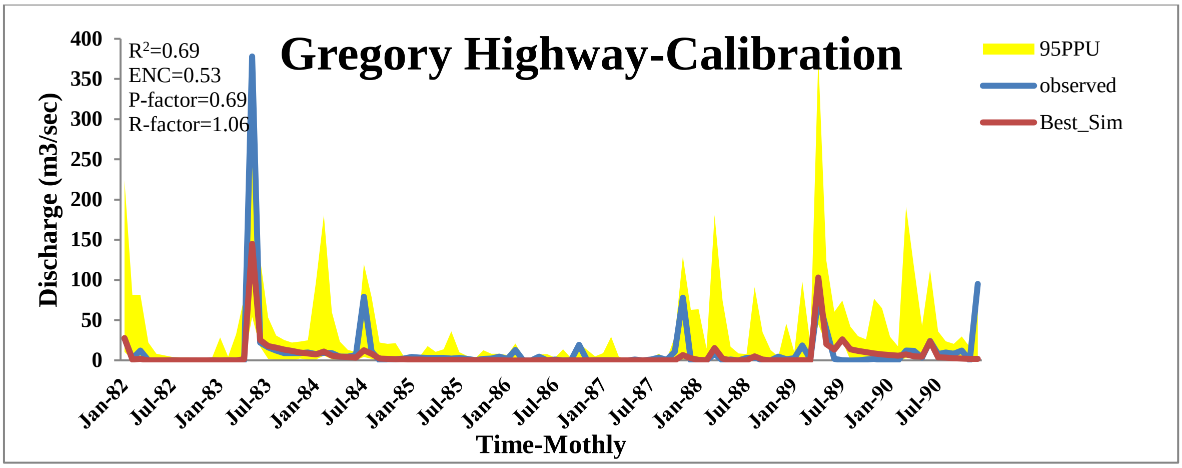

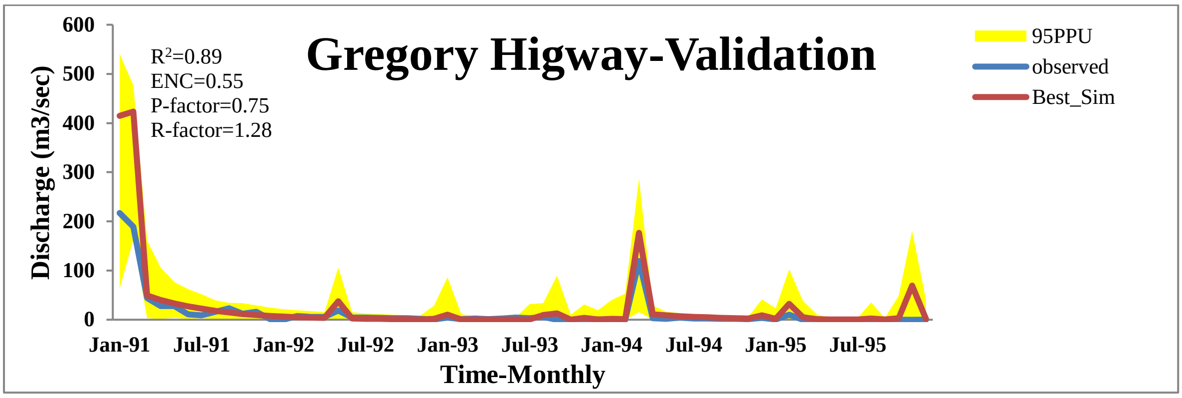

Figure 5.16: Calibration and validation of the SWAT model at monthly scale at Gregory Highway Monitoring Station, within Nogoa Watershed (Source: original work created for this thesis)

Table 5.6: The statistical indices values (R^2, ENC, R. factor, P. factor) at the seven discharge stations in the Fitzroy Basin.

Watershed	Station	Calibration				Validation			
		R^2	ENC	R. factor	P. factor	R^2	ENC	R. factor	P. factor
Dawson	Riverslea	0.70	0.58	0.93	0.64	0.63	0.68	0.62	0.66
Dawson	Redcliffe	0.68	0.53	0.79	0.29	0.79	0.51	0.55	0.33
Dawson	Taroom	0.70	0.53	2.4	0.37	0.84	0.76	1.21	0.60
Isaac	Nebo	0.74	0.73	0.41	0.42	0.63	0.62	0.51	0.35
Comet	The Lake	0.86	0.83	0.87	0.34	0.89	0.86	0.86	0.25
Mackenzie	Coolmaringa	0.62	0.51	0.24	0.26	0.58	0.51	0.25	0.49
Nogoa	Gregory	0.69	0.53	1.06	0.69	0.89	0.55	1.28	0.75

To summarise, the SWAT model performed well for both the Tigris and Fitzroy Basins, as evidenced from calibrations and validations, despite under-predictions and over-predictions during too-wet and too-dry months, yet well within the bands of acceptability criteria used in published literature. The underestimation and overestimation during some months is typical of simulation models, which cannot often capture shocks (extreme high or low values) in the system, such as the extreme rainfall events of July 1983 and January 1991 in calibration and validation processes, respectively, at Gregory Station, as shown Figure 5.16, albeit those also could be due to errors in measuring flow, unevenly distributed rainfall stations and spatial variability in soil and land use (Santhi et al. 2001, Ndomba et al. 2008). Within the norms of reliability and validity of acceptable model performance, the model has established itself as quite capable of simulating the streamflow of the two regions.

CHAPTER 6

RESULTS

6.1 Introduction

Historically, availability of water resources from observations and anecdotal evidences dates back to many years for both the Tigris and Fitzroy Basins. However, this chapter only presents results of the analysis of recorded data. Water availability is separated into two components: blue water and green water. Their availability is captured both in terms of changes that occurred during the period of recorded data and in future projections for about a half-century ahead (2046-2064) and a century ahead (2080-2100).

6.1.1 Water resources availability in Tigris river basin

Blue Water Availability

Figure 6.1 shows the spatial distribution of water resources per capita per year during the period of 1980-2010. High spatial variability in the region can be attributed to two main factors, geographic and social. Due to the geographic factor, blue water availability decreases from upstream mountainous areas to downstream flat areas, since annual precipitation decreases from upstream to downstream. The social factor is that upstream areas are sparsely populated, whereas downstream areas are densely populated with some large metropolitan areas, resulting in decreased water purity. In general, a major part of the region is experiencing severe water scarcity.

Green Water Storage Availability

Although green water is often ignored in water resources management, it plays a fundamental role in rain-fed crop production and for other environmental purposes (Zang et al. 2012). Green water availability was assessed by the average of months per year for the period 1980-2010 when green water storage is available (defined as >1 mm.m-1) and is shown in the left of Figure 6.2. The standard deviations (SDs) of the months per year without depleted soil water are presented for the 1980–2010 period to the right of Figure 6.2. The areas with high SDs can often experience reduced crop yield. These areas require irrigation systems which can adjust to high demands or adoption of alternative cropping practices that require less water.

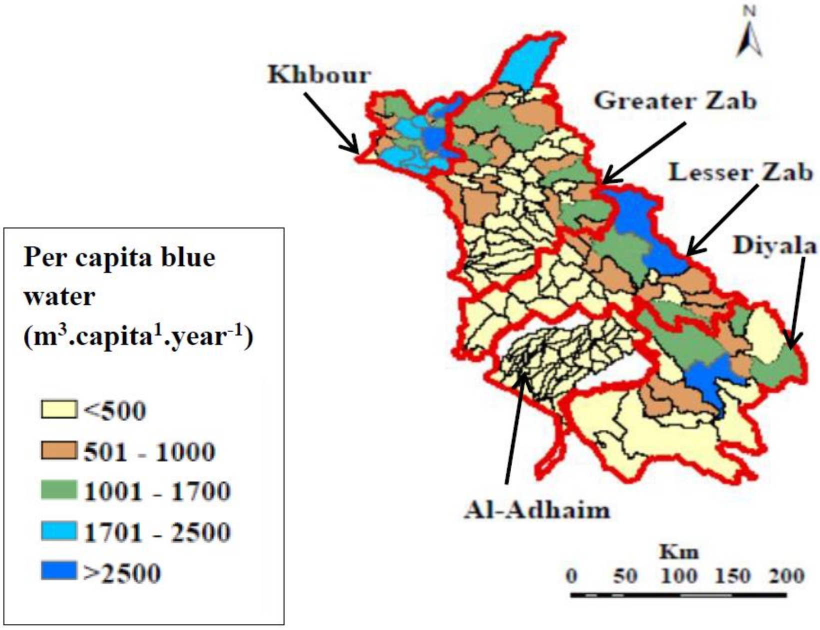

Figure 6.1: Water scarcity in northeast Iraq from 1980-2010 average annual blue water flow availability per capita per year using population of 2005 (Source: original work created for this thesis)

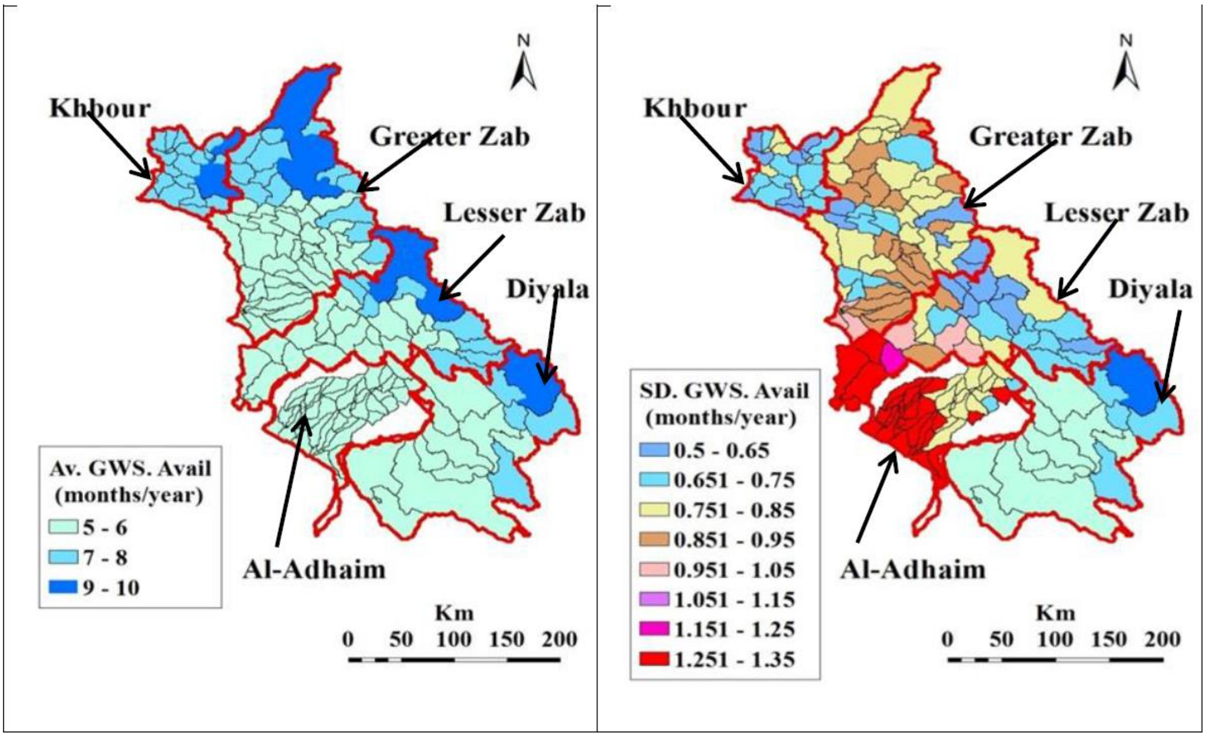

Figure 6.2: (Left) The 1980–2010 average green water storage (Av. GWS) and (Right) standard deviation calculated for the number of months per year where the green water storage is available (SD. GWS Avail) (Source: original work created for this thesis)

Water resources availability at city scale

To gain an appreciation of what is going on at local levels, where transportation of water mostly seems infeasible due to lack of infrastructure, the researcher looked at four townships: Dihok, Al-Sulaimaniyah, Erbil and Al-Tamim (Kirkuk governorate). These range from high- to low-precipitation townships. The results of the analysis are presented in Figure 6.3a. The location of the townships is shown in Figure 6.3b. The green water storage at Al-Tamim is not as poor as it may appear from the precipitation values only.

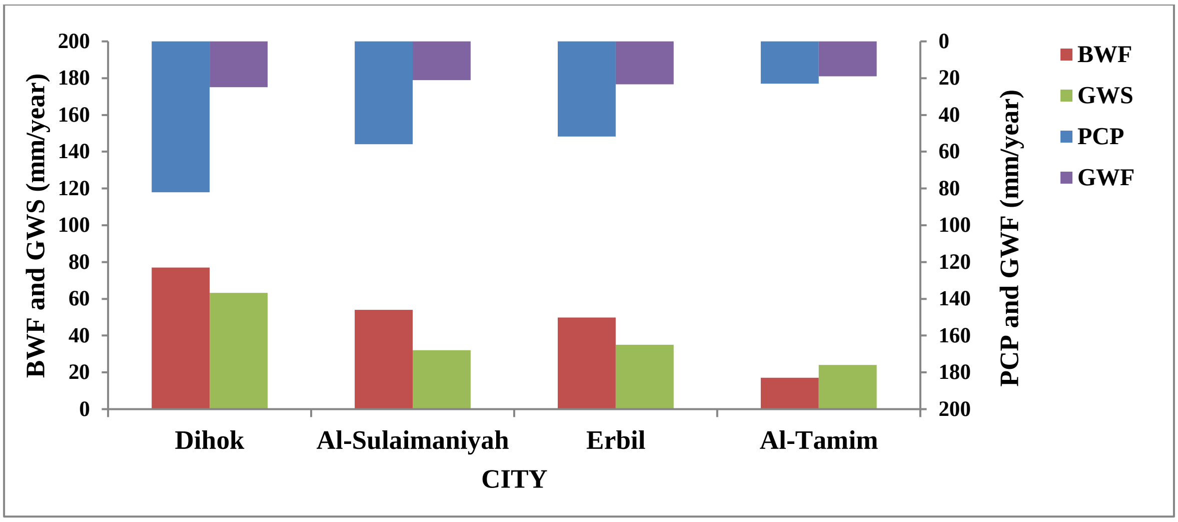

Figure 6.3a: Simulated average (1980–2010) annual city precipitation (PCP), blue water flow (BWF), green water flow (GWF) and green water storage (GWS) for four major cities in northeast Iraq (Source: original work created for this thesis)

Figure 6.3b The map of the location of townships where water resources availability was looked at at township level (Source: original diagram edited using data from (Iraqi Ministry of Water Resources 2015)

Water resources availability at river catchment scale

Mean monthly precipitation and water availability for various HRUs were combined to calculate water availability at the river watershed scale for the period 1980-2010. The highest precipitation occurs in Khbour, followed by Greater Zab, and the lowest precipitation occurs in Al-Adhiam (Figure 6.4). Blue water flow in the five river catchments demonstrates high uncertainties during the wet season (December–April). In almost all catchments (except Al-Adhaim) the blue water flow touches the peak in March, instead of February, when the highest precipitation occurs. This is because the Khbour, Greater Zab, Lesser Zab and upper Diayla catchments are snow-dominated, mountainous basins, and snow melt starts to occur from March to May. However, in the arid Al-Adhiam Basin, the peak of blue water flow follows the precipitation peak. The green water storage tends to be similar to blue water flow in all catchments. Green water flows are rather stable in the different catchments, but this could be attributed partly to the rather stable land cover in the study areas.

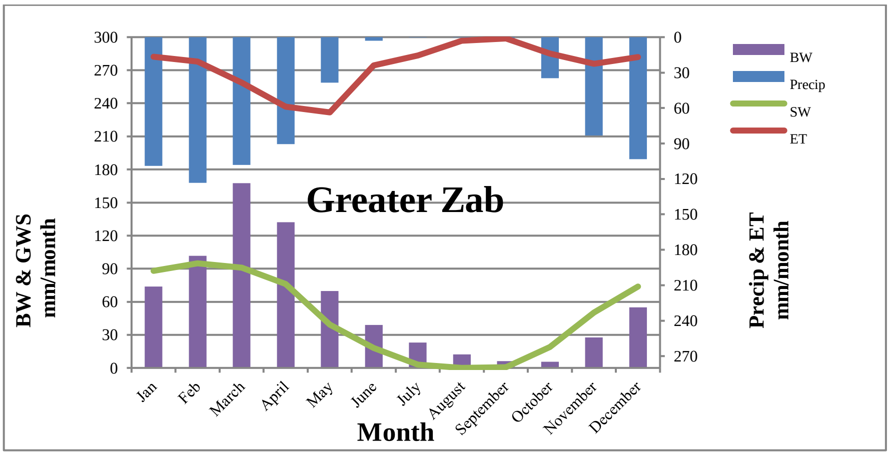

(Figure 6.4 continues over to next page.)

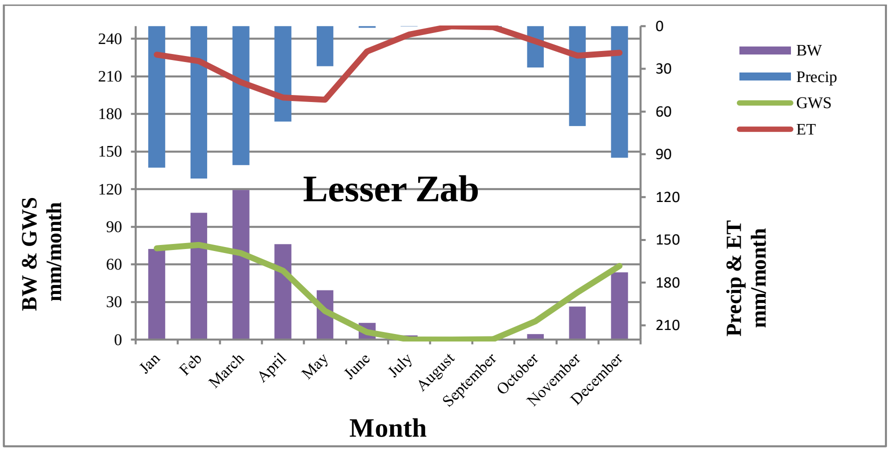

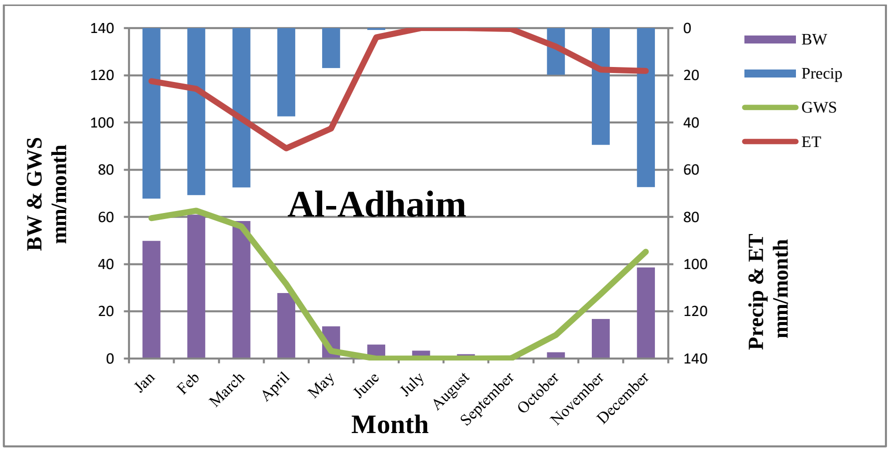

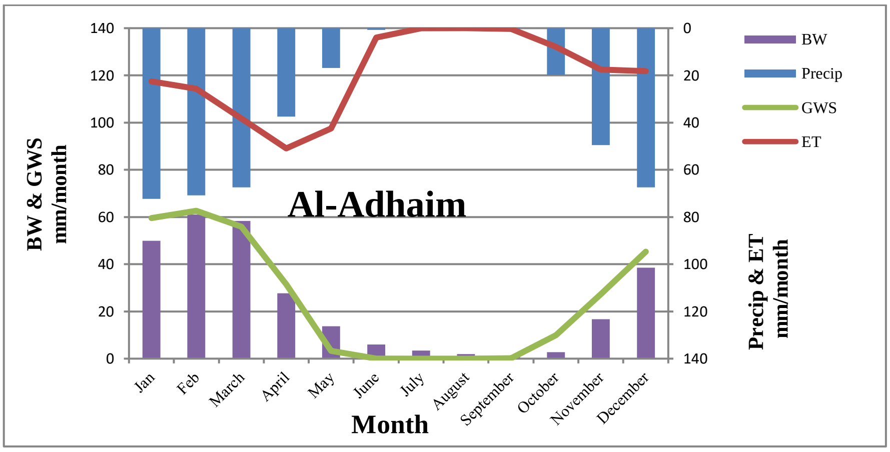

Figure 6.4: Average (1980–2010) monthly ranges of the blue water flow, green water storage, precipitation and ET in the Khbour, Greater Zab, Lesser Zab, Al-adhaim and Diayla Rivers. (Source: original work created for this thesis).

Trends in Precipitation, Blue Water and Green Water

Using the calibrated model, annual and monthly precipitation, blue water and green water storage were assessed for the entire region during the last three decades to identify the recent trends in the water cycle components. Figure 6.5a captures the pictorial distribution of the decadal states and trends. In general, spatially there is a decreasing trend of precipitation from north to south and from east to west, which roughly fits the description that the more mountainous the terrain, the higher the precipitation amount. Blue water tends to be high where the runoff from the precipitation tends to accumulate (Figure 6.5b). Green water tracks blue water (Figure 6.5c). However, land cover contributes to the shaping of the spatial distribution of blue and green waters.

Looking at the temporal scale, there is a declining trend of precipitation over the last three decades. These trends are quantified in Table 6.1, and are fairly large numbers, except for green water flows. However, green water flow estimates could be the best-case scenario, since land cover was assumed to be static.

Table 6.1: Relative changes in precipitation, blue water, and green water in Iraqi northeast region over three decades.

Water component	Rate of relative change in the last three decades		
	1990s *vs* 1980s	2000s *vs* 1990s	2000s *vs* 1980s
Precipitation	-0.21	-0.21	-0.35
Blue water	-0.27	-0.37	-0.57
Green water availability	-0.15	-0.12	-0.28
Green water flow	-0.08	-0.09	-0.10

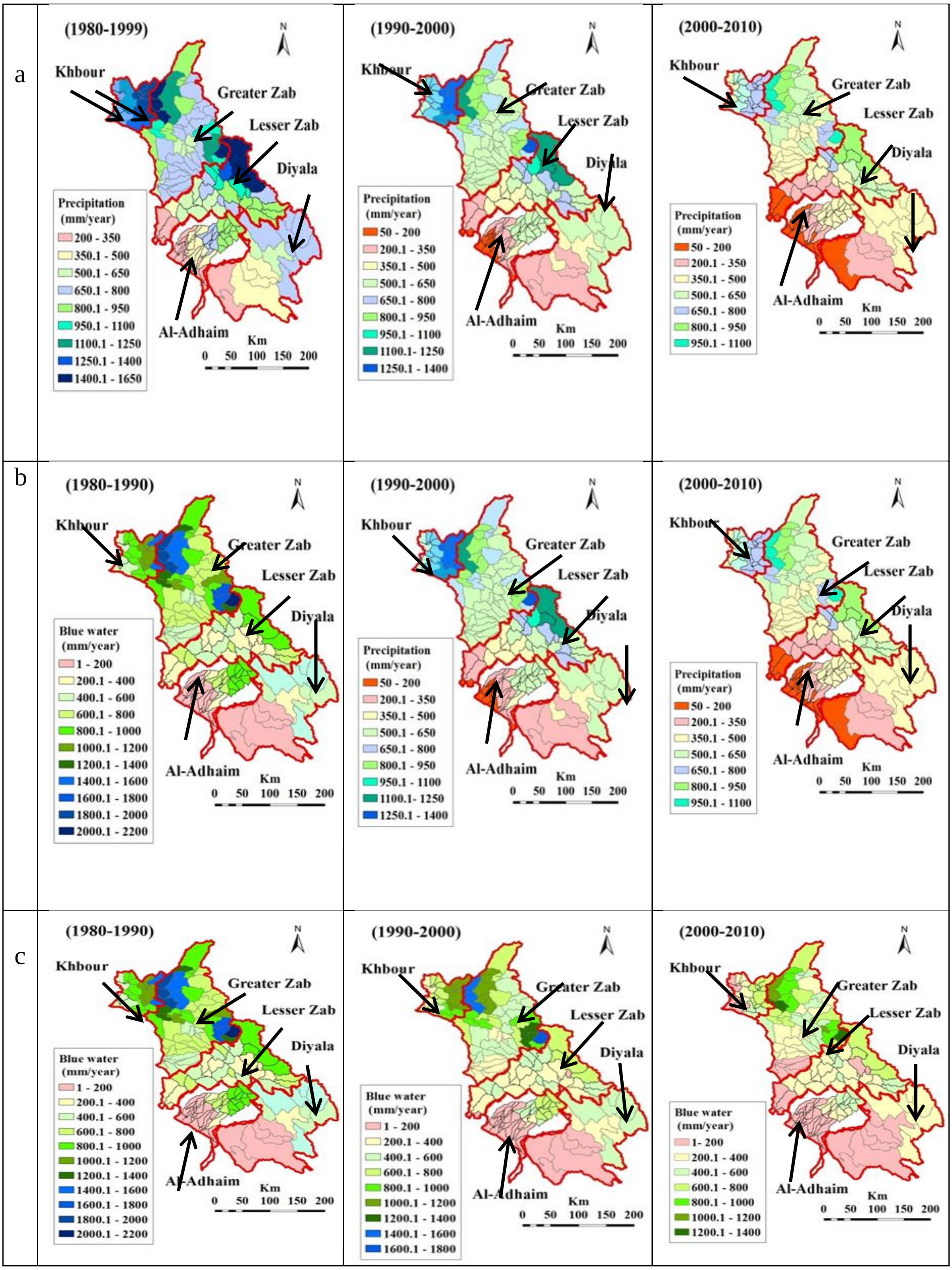

Figure 6.5: (a) Spatial distribution of precipitation, (b) Spatial distribution of blue water and (c) Spatial distribution of green water for the baseline period of 1980-2010 for northeast Iraq (Source: original work created for this thesis)

6.1.2 Water resources availability in Fitzroy River Basin

Blue water availability

The water availability per capita and water stress indicators were estimated for the Fitzroy River basin for each of the 42 HRUs of the five basins, using Australian Bureau of Statistics data to obtain population density per hectare. Figure 6.6 provides the spatial distribution of water resources per capita per year during the period 1980-2010 based on the population estimates for the year 2009. The entire region can be characterised as having sufficient water.

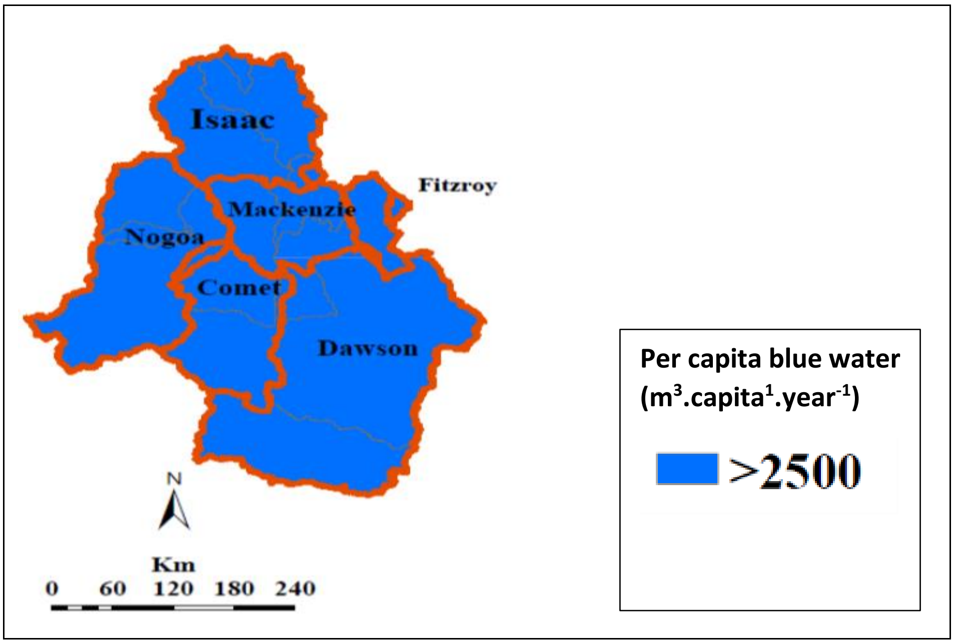

Figure 6.6: Water availability in Fitzroy basin from 1980-2010 average annual blue water flow availability per capita per year using population of 2009 (Source: original work created for this thesis)

Green water storage availability

The average of months per year for the period 1980 to 2010 where green water storage is available is shown in the left of Figure 6.7. Most of the basin experienced eight to nine months per year when groundwater was available, except for the Fitzroy sub-basin and a small part of Isaac and Dawson, which experienced 10-11 months per year availability. The standard deviations (SDs) of the months per year without depleted soil water are presented for the 1980–

2010 period to the right of Figure 6.7. The areas with high SDs such as Isaac and part of Nogoa and Dawson indicate high variability of green water storage availability.

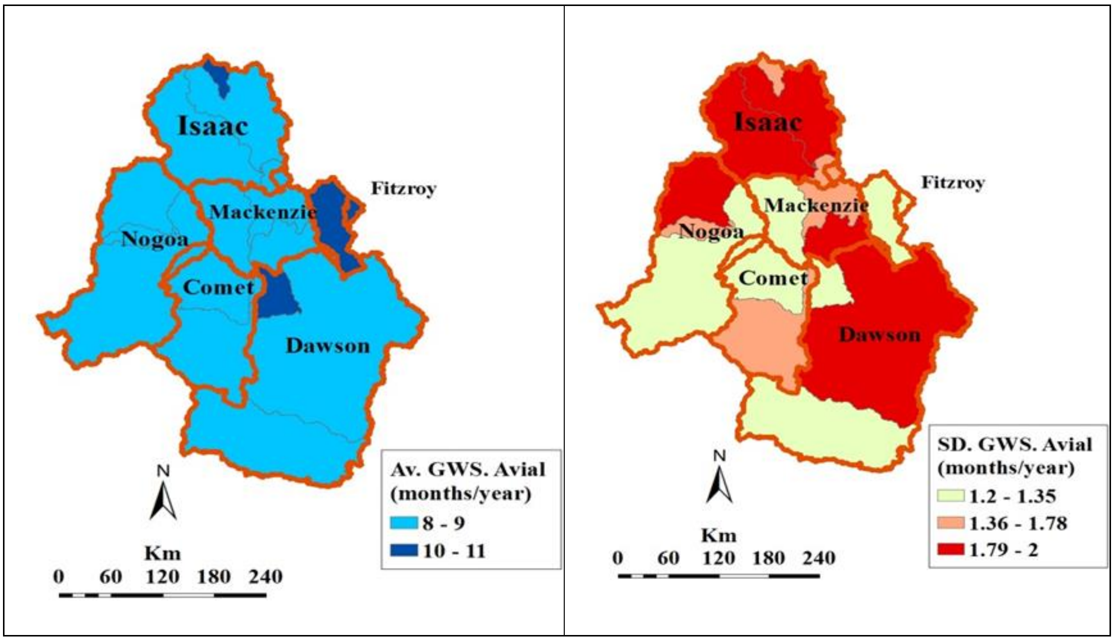

Figure 6.7: (Left) The 1980–2010 average green water storage (Av. GWS) and (Right) standard deviation calculated for the number of months per year where the green water storage is available (SD. GWS Avail). (Source: original work created for this thesis)

Water resources availability at river catchment scale

Mean monthly precipitation and water resources for different HRUs were combined to compute water resources availability at the river catchment scale (Figure 6.8). The highest precipitation occurs in Isaac (140 mm/month) followed by Fitzroy (120 mm/month). The highest precipitation over the rest of the basins (Nogoa, Dawson, Comet, Mackenzie) ranges between 100 and 110 mm/month. Blue water flow in the six river catchments reveals high uncertainties during the wet season (January–April). In almost all catchments, blue water flow reaches a peak in February when the highest precipitation occurs. Green water storage tends to be similar to blue water flow in all catchments. Green water flows are rather stable in different catchments, which could be attributed partly to the relative stable land cover in the study areas.

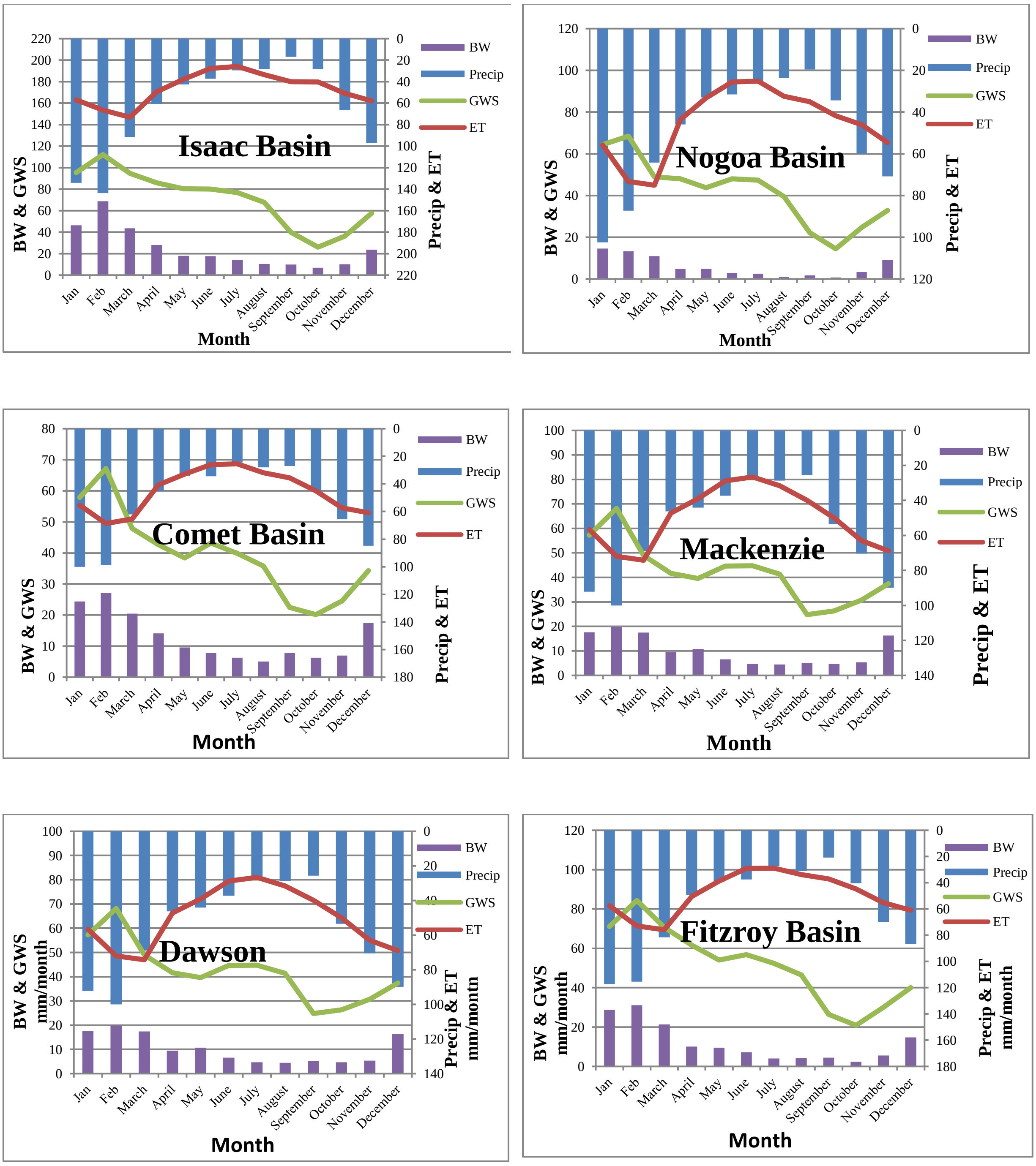

Figure 6.8: Average (1980–2010) monthly 95PPU ranges of the blue water flow, green water storage, precipitation and ET in the Isaac, Nogoa, Comet, Mackenzie, Dawson and Fitzroy Basins (Source: original work created for this thesis)

Trends in Precipitation, Blue Water and Green Water

Annual and monthly precipitation and blue water and green water storage were estimated for the entire region (42 HRUs) during the last three decades to identify recent trends in the water-cycle components. Figure 6.9a captures the spatial distribution of the decadal states and trends of precipitation. In general, spatially there is a variable trend of precipitation in the basin. Blue water follows precipitation distribution (Figure 6.9b). As shown in Figure 6.9c, green water tracks blue water. As mentioned previously, land cover has contributed to forming the spatial distribution of blue and green waters. The temporal scale revealed that there has been a highly variable trend in precipitation over the last three decades. These results are in line with the results of Nicholls (1997), who reported that Australian rainfall has higher variability with time. These trends are quantified in Table 6.2. Green water flow was nearly stable, because the land cover was assumed to be static.

Table 6.2: Relative changes in precipitation, blue water, and green water in Fitzroy region over three decades

Water component	Rate of relative change in the last three decades		
	1990s vs 1980s	2000s vs 1990s	2000s vs 1980s
Precipitation	-0.16	0.19	-0.04
Blue water	-0.45	0.79	0.015
Green water storage	-0.31	0.48	-0.02
Green water flow	-0.06	-0.09	-0.07

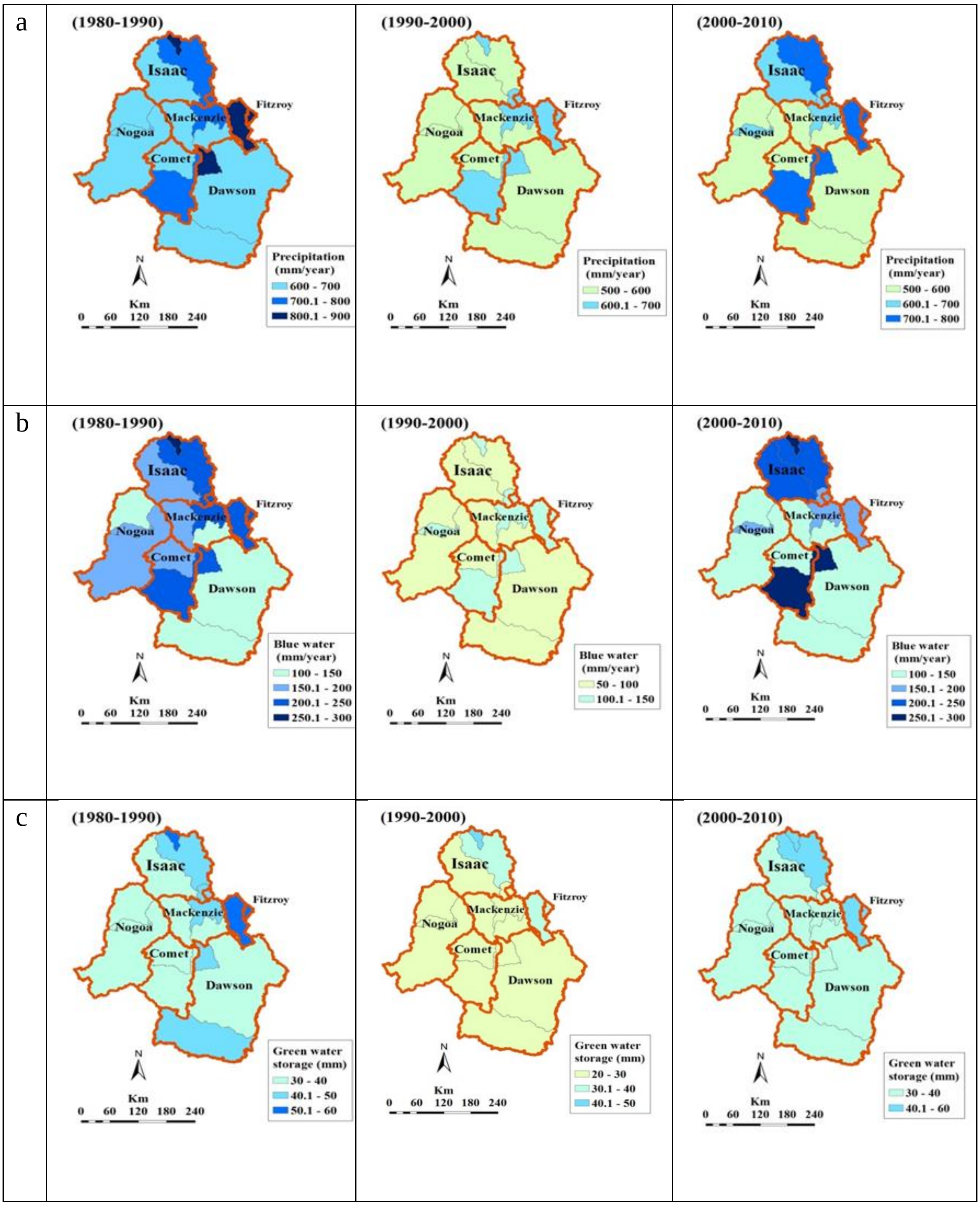

Figure 6.9: (a) Spatial distribution of precipitation, (b) Spatial distribution of blue water and (c) Spatial distribution of green water for the baseline period of 1980-2010 for Fitzroy basin (Source: original work created for this thesis)

6.2 Impacts of climate change on the Tigris Basin using CMIP3

6.2.1 Temperature forecasts

Mean annual temperature and precipitation outputs from the six GCMs identified earlier were processed for the whole basin under three scenarios (A2, A1B, B1). Table 6.3 captures the projected changes in mean annual temperature for the two future periods (2046-2064) and (2080-2100) relative to the base period (1980-2010). Changes in mean temperature tend to be steadier than precipitation. It can be seen clearly that there are consistent trends in increasing temperature in all models. Changes in mean temperature modify evapotranspiration and precipitation, and hence blue water and green water flows.

Table 6.3: GCM predicted changes in the mean annual temperature of the future under A2, A1B and B1

Periods	Annual change in max temperature (^{0}C)					
	CGCM3.1/T47	CNRM-CM3	GFDL-CM2.1	PSLCM4	MIROC3.2	MRI CGCM2.3.2
A2						
2046-2064	2.53	2	2.4	3	1.8	1.6
2080-2100	5.95	5.5	5.6	6	5.2	4.3
A1B						
2046-2064	2.16	2.6	3	32	2.7	1.8
2080-2100	4.29	4.6	5	5	5	3.4
B1						
2046-2064	1.5	1.5	1.2	1.6	1.5	1.5
2080-2100	1.7	1.7	0.9	1.7	1.7	1.3

6.2.2 Precipitation forcasts

Overall, all selected GCMs predicted a decrease in the mean annual precipitation for about a half-century lead time (2046-2064) and about a one-century lead time (2080-2100) for the five basins. Figure 6.10 shows the anomaly maps of precipitation distribution (maps of percent deviation from historic data, 1980-2010) for A2, A1B and B1 scenarios for the periods 2046-2064 and 2080-2100 for the average change from the multi-GCM ensemble. The A2 emission scenario produced the highest decreases, while the B1 emission scenario gave the lowest reductions for both periods for the entire region. The Diyala Basin is expected to experience the highest reduction in precipitation under the A2 (32%), A1B (21%) and B1(17%) scenarios for the 2046-2064 period, followed by Al-Adhiam under A2 (27%), A1B (23%), B1 (12%). This is an anticipated result, as Al-Adhiam and Diyala experience higher air temperatures and lower precipitation amounts compared to those of the Khbour, Greater Zab and Lesser Zab Basins. These reductions will likely increase further if the lead time is increased to 2080-2100. The Diyala Basin may experience further decreases by about 10%, 13% and 10% under A2, A1B and B1 scenarios, respectively. Al-Adhiam similarly may experience decreases by about 8%, 3% and 5% under A2, A1B, and B1 scenarios, respectively. The Khbour, Greater Zab and Lesser Zab Basins may experience nearly the same reductions under the three scenarios for both periods, as given in Table 6.4. Lesser Zab may experience increases of about 2% under B1 (2046-2064).

Table 6.4: The projected relative changes in precipitation (in percent) for the five basins under A2, A1B, and B1 scenarios for the periods 2046-2064 and 2080-2100.

	Scenarios					
	A2	A2	A1B	A1B	B1	B1
Basin	(2046-64)	(2080-00)	(2046-64)	(2080-00)	(2046-64)	(2080-00)
Khbour	-11	-24	-12	-23	-4	-10
Greater Zab	-12	-22	-16	-16	-5	-10
Lesser Zab	-13	-17	-12	-17	2	-6
Al-Adhiam	-27	-35	-23	-26	-12	-17
Diyala	-32	-41	-21	-34	-17	-27

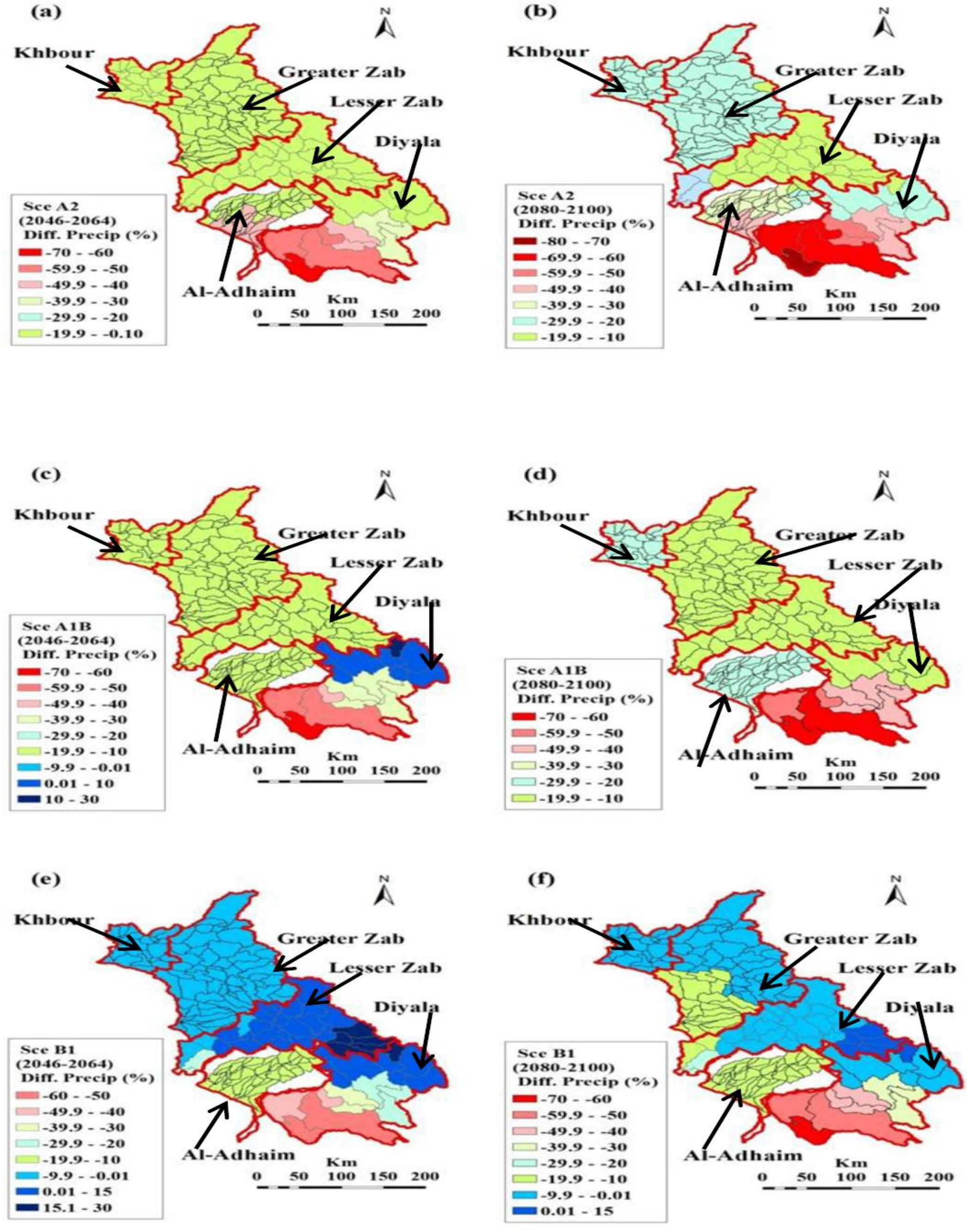

Figure 6.10: Projected impacts of climate change on the precipitation of the five basins (a) Anomaly based on scenario A2 for the period 2046-2064, (b) Anomaly based on A2 for 2080-2100, (c) Anomaly based on A1B for 2046-2064, (d) Anomaly based on A1B for 2080–2100, (e) Anomaly based on B1 for 2046-264, and (f) Anomaly based on B1 for 2080–2100 (Source: original work created for this thesis)

6.2.3 Blue water forecasts

Figure 6.11 captures the anomaly maps of blue water distribution (maps of percent deviation from historical data, 1980-2010) for the A2, A1B, and B1 scenarios for the periods 2046-2064 and 2080-2100 from the average change of the multi-GCM ensemble. The half-century projection (2046-2064) shows a decrease in blue water under all emission scenarios for the whole region. The Al-Adhiam Basin is likely to experience the highest reductions under the three scenarios in both periods, followed by Diyala. Khbour and Greater Zab will experience approximately the same reductions under the three scenarios for both periods, except for the A1B scenario to 2080-2100 when Khbour will experience a reduction of 38%, whereas the reduction in Greater Zab will reach up to 28%. Lesser Zab may experience lower decrease than Khbour and Greater Zab except for A2 scenario to 2046-2064. Table 6.5 provides the estimated values.

Table 6.5: Projected relative changes (in percent) in blue water for the five basins under A2, A1B, and B1 scenarios for the periods 2046-2064 and 2080-2100.

	Scenarios					
Basin	A2 (2046-64)	A2 (2080-00)	A1B (2046-64)	A1B (2080-00)	B1 (2046-64)	B1 (2080-00)
Khbour	-19	-39	-22	-38	-10	-17
Greater Zab	-21	-38	-22	-28	-12	-19
Lesser Zab	-23	-30	-14	-20	-3	-15
Al-Adhiam	-62	-66	-27	-49	-23	-34
Diyala	-35	-42	-22	-35	-11	-18

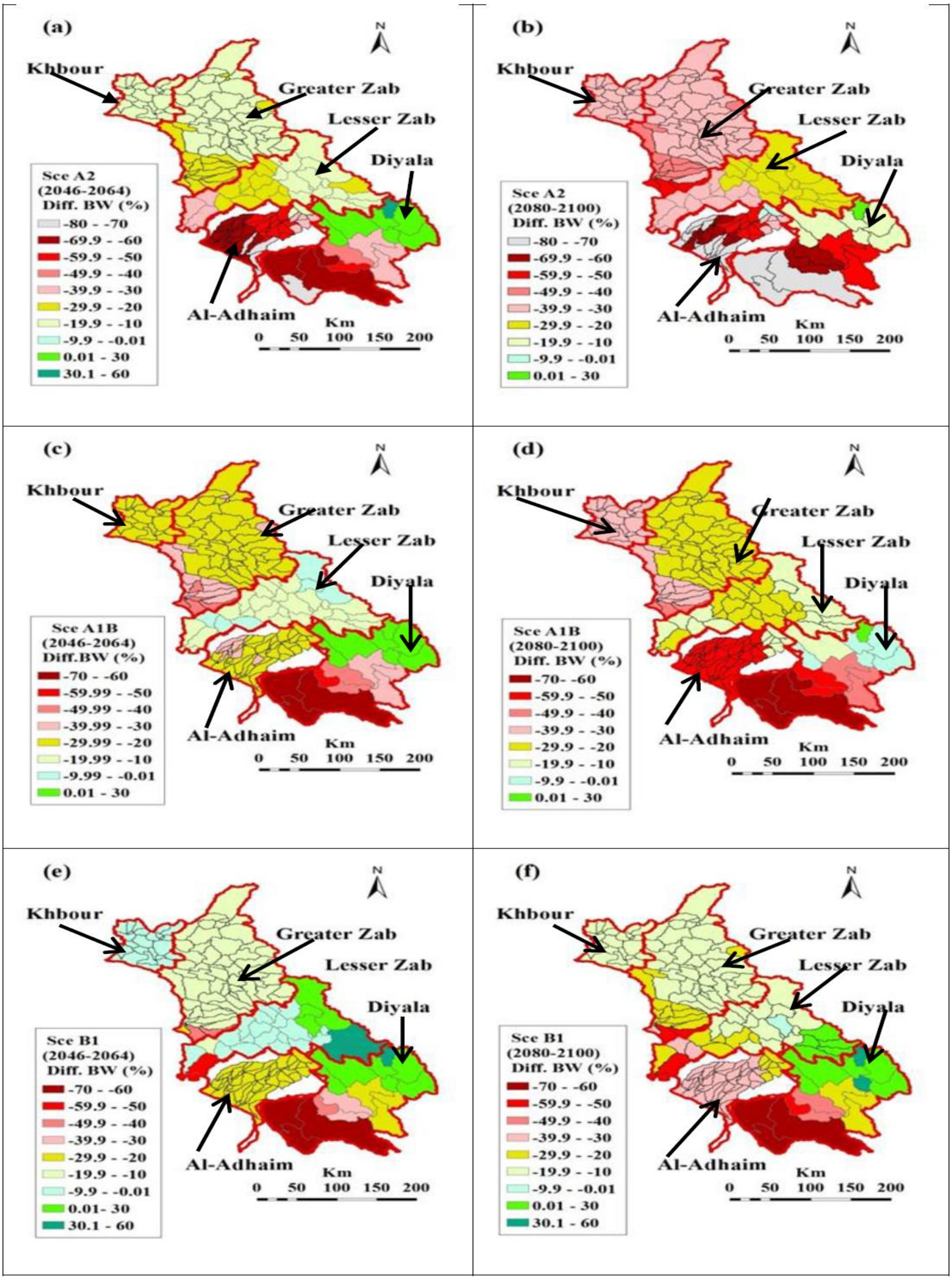

Figure 6.11: Projected impacts of climate change on the blue water of the basin (a) Anomaly based on scenario A2 for the period of 2046-2064, (b) Anomaly based on A2 for 2080-2100, (c) Anomaly based on A1B for 2046-2064, (d) Anomaly based on A1B for 2080–2100, (e) Anomaly based on B1 for 2046-264, and (f) Anomaly based on B1 for 2080–2100 (Source: original work created for this thesis)

6.2.4 Green water storage forecasts

In a similar analysis to blue water, green water storages may also decrease under the three emission scenarios for the two future periods, which are captured in Figure 6.12 and Table 6.6. Green water flow calculations (maps not shown) indicated a slight decrease in evapotranspiration due to the assumption that land cover would not significantly change from the period of the 1980s to the 2100s.

Table 6.6: Projected relative changes (in percent) in green water storages for the five basins under A2, A1B, and B1 scenarios for the periods 2046-2064 and 2080-2100.

	Scenarios					
	A2	A2	A1B	A1B	B1	B1
Basin	(2046-64)	(2080-00)	(2046-64)	(2080-00)	(2046-64)	(2080-00)
Khbour	-8	-16	-10	-14	-6	-5
Greater Zab	-23	-31	-22	-27	-11	-16
Lesser Zab	-21	-24	-9	-12	-4	-14
Al-adhiam	-31	-42	-18	-28	-15	-18
Diyala	-17	-21	-14	-17	-7	-10

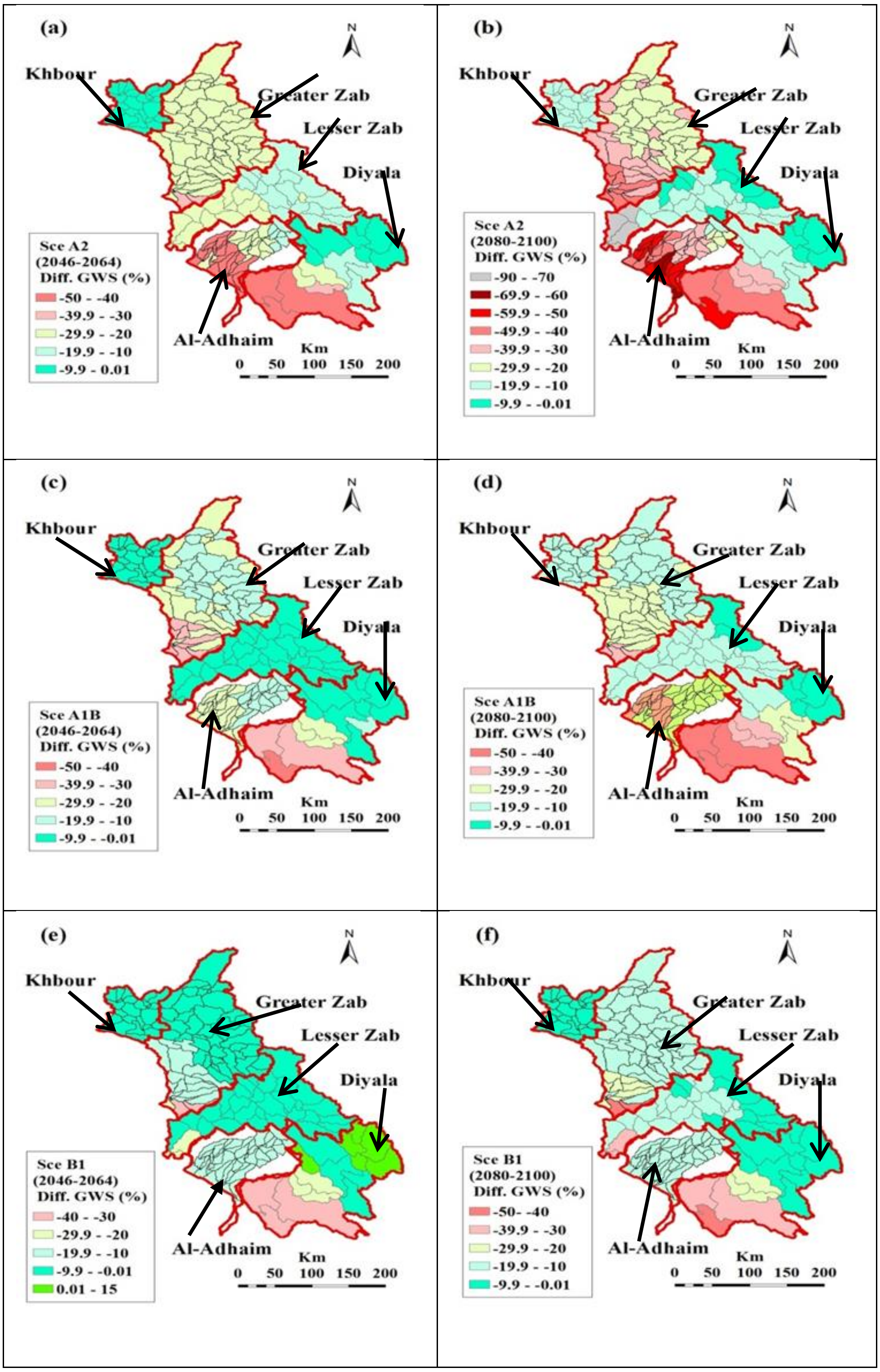

Figure 6.12: Projected impacts of climate change on the green water storages of the basin (a) Anomaly based on scenario A2 for the period of 2046-2064, (b) Anomaly based on A2 for 2080-2100, (c) Anomaly based on A1B for 2046-2064, (d) Anomaly based on A1B for 2080–2100, (e) Anomaly based on B1 for 2046–2064, and (f) Anomaly based on B1 for 2080-2100 (Source: original work created for this thesis)

6.2.5 Deep aquifer recharge forecasts

Figure 6.13 captures the anomaly maps of deep aquifer recharge (maps of percent deviation from historical data, 1980-2010) for the A2, A1B, and B1 scenarios for the periods 2046-2064 and 2080-2100 from the average change of the multi-GCM ensemble. The Khbour Basin will experience a decrease of up to 50% under A2 for the half-century and end-of-century projections. However, deep aquifer recharge in Greater Zab is more variable: most of the basin will see decreases ranging from 10% to 80%, and the most affected areas are the mountainous zone; the middle of the basin, however, will experience increases of up to 30%. Lesser Zab, Al-Adhiam and Diyala will see decreases ranging from 10% to 90%. A1B and B1 show the same trends of A2 but with less variation, as shown in Figure 6.13.

6.2.6 Streamflow forecasts

The results from the hydrological modelling for annual stream flow are shown in Figure 6.14. Khbour, Al-Adhiam and Diyala streamflow will significantly decrease in the six models for all scenarios (A2, A1B, B) for both time periods. Except for GCM outputs of MRI, Greater Zab streamflow will experience decreases for all scenarios for both periods. Lesser Zab streamflow will decrease under A2 and A1B but will experience increases under B1 for both periods.

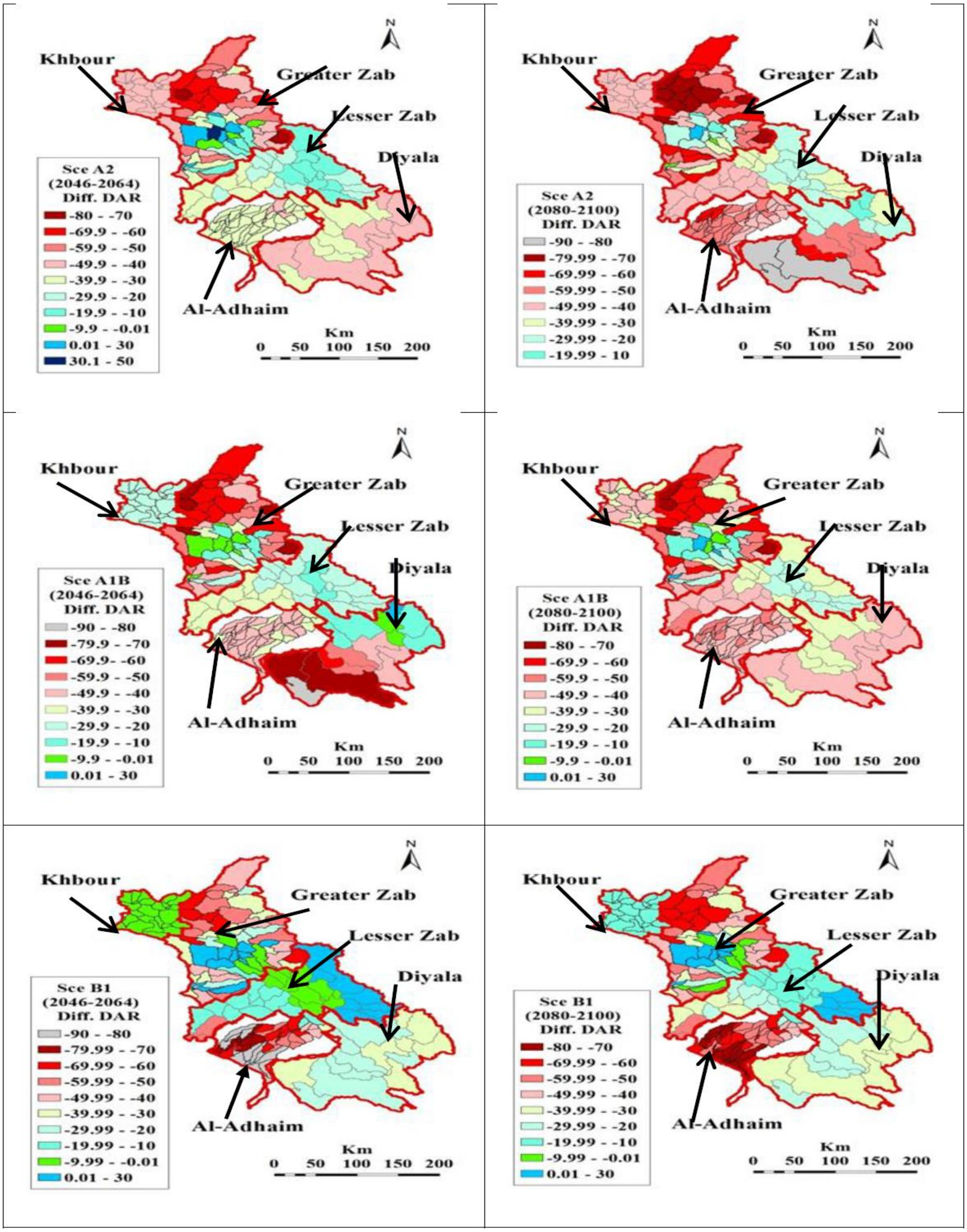

Figure 6.13: Projected impacts of climate change on the deep aquifer recharge of the basin (a) Anomaly based on scenario A2 for the period of 2046-2064, (b) Anomaly based on A2 for 2080-2100, (c) Anomaly based on A1B for 2046-2064, (d) Anomaly based on A1B for 2080–2100, (e) Anomaly based on B1 for 2046–2064, and (f) Anomaly based on B1 for 2080-2100 (Source: original work created for this thesis)

Khbour

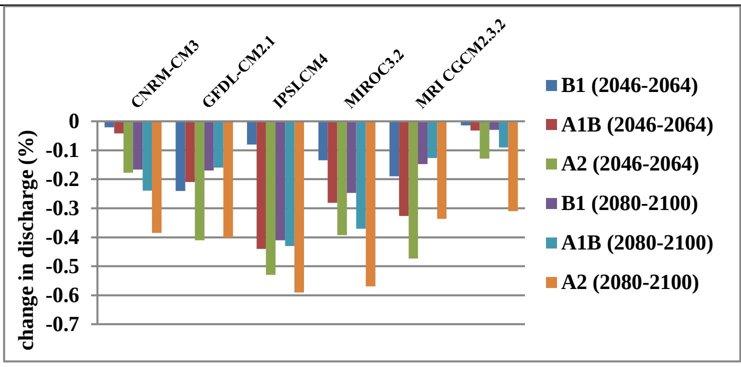

Greater Zab

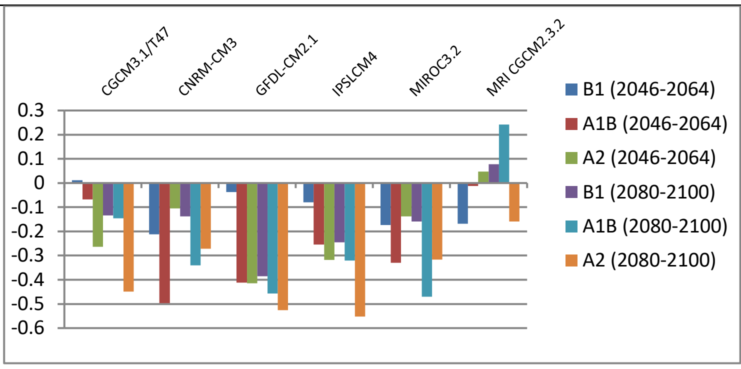

Lesser Zab

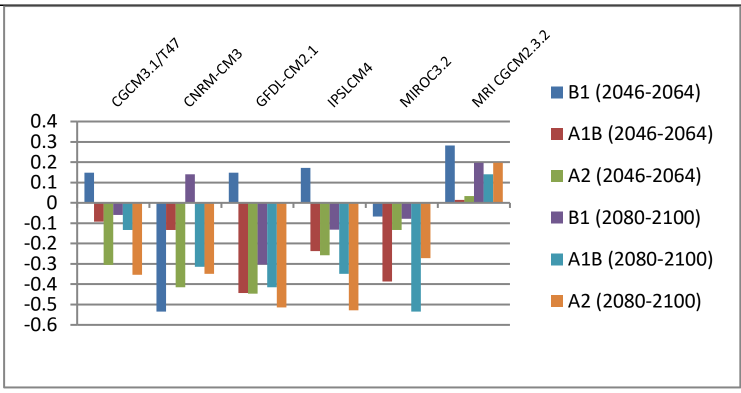

Al-Adhiam

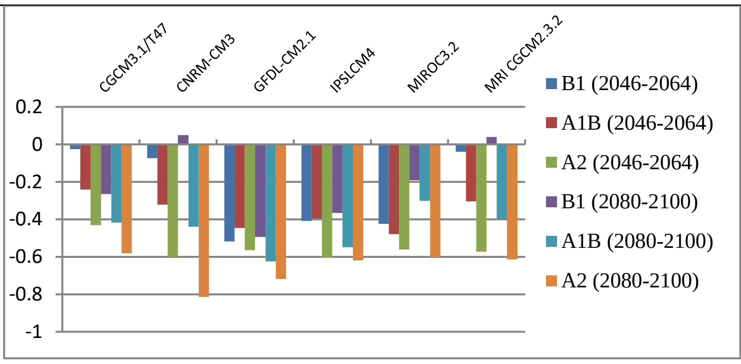

Figure 6.14 continues to next page.

Diyala	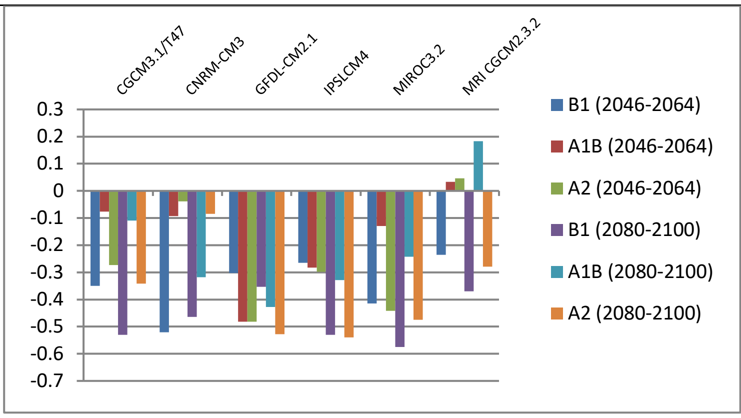

Figure 6.14: Projected changes in streamflow in the five basins compared to the base-period 1982-2000, for 2046-2064 and 2080-2100 for B1, A1B and A2 scenarios (Source: original work created for this thesis)

6.3 Impacts of climate change on the Fitzroy Basin using CMIP3

6.3.1 Temperature forecasts

Table 6.7 captures the projected changes in mean annual temperature for two future periods (2046-2064) and (2080-2100) relative to the base period (1980-2010). All the models showed consistent increasing trends in temperature across the Fitzroy Basin under the three scenarios (A2, A1B, B1). As anticipated, the B1 scenario showed the lowest increases, which are expected to be up to 0.71^{0}C and 1.15^{0}C for the near future and the distant future, respectively. The A2 scenario projected the highest increases, up to 1.05^{0}C and 2.60^{0}C for the period of 2046 to 2064 and 2080 to 2100, respectively. The MRI model projected the lowest average annual temperature while GFDL projected the highest temperature (Table 6.7). These results are consistent with results of Chambers et al. (2005) who found that, in Australia by 2070, projected average annual temperature may rise by 1.0°C to 2.5°C for low greenhouse gas emissions and 2.2°C to 5°C for high emissions.

Table 6.7: GCM predicted changes in the mean annual temperature of the future under A2, 1B and B1 scenarios.

Periods	Annual change in mean temperature (^{0}C)					
	CGCM3.1/T47	CNRM-CM3	GFDL-CM2.1	PSLCM4	MIROC3.2	MRI CGCM2.3.2
			A2			
2046-2064	1.08	1.13	1.24	1.11	0.91	0.83
2080-2100	2.47	2.47	3.37	2.76	2.2	2.2
			A1B			
2046-2064	1.12	1.29	1.35	1.26	0.86	0.76
2080-2100	1.67	1.95	2.16	2.39	1.89	0.83
			B1			
2046-2064	0.64	0.72	0.99	0.86	0.53	0.51
2080-2100	1.16	1.28	1.28	1.12	1.16	0.94

6.3.2 Precipitation forecasts

Figure 6.15 shows the anomaly maps of precipitation distribution (maps of percent deviation from historical data, 1980-2010) for the A2, A1B and B1 scenarios for the periods 2046-2064 and 2080-2100 for the average change of multi-GCM ensemble. All scenarios show an increase in precipitation trend for the near and distant futures for most basins except for a small part of the Nogoa Basin, which will experience reduction of up to 10% under the A2 scenario for the period 2046-2064. The B1 scenario projected the highest increases in the near and distant futures of 11% and 23%, respectively. A1B projected increases of 8% and 12% for the period of 2046-2064 and 2080-2100. A2 showed increases of 3% and 6% for near and distant futures. The Isaac Basin will experience the highest increase under the B1 scenario for both periods.

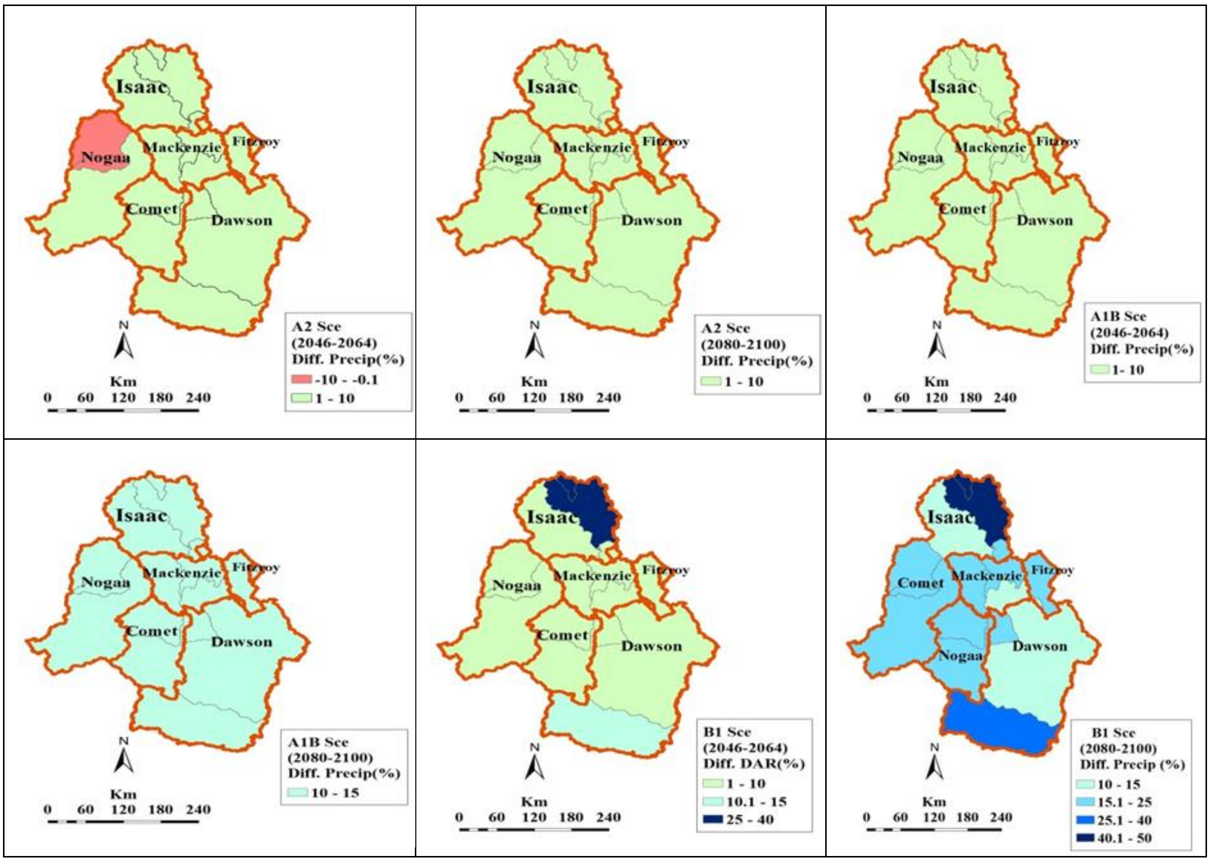

Figure 6.15: Projected impacts of climate change on precipitation of the basin (a) Anomaly based on scenario A2 for the period of 2046-2064, (b) Anomaly for A2 to 2080-2100, (c) Anomaly for A1B to 2046-2064, (d) Anomaly for A1B to 2080–2100, (e) Anomaly for B1 to 2046–2064, and (f) Anomaly for B1 to 2080-2100 (Source: original work created for this thesis)

6.3.3 Blue and green water storage forecasts

Blue and green water patterns generally follow precipitation patterns. Blue and green water tend to be high where precipitation is high. Figure 6.16 shows the anomaly maps of blue water distribution (maps of percent deviation from historical data, 1980-2010) for the A2, A1B and B1 scenarios for the periods 2046-2064 and 2080-2100 for the average change of multi-GCM ensemble. Similar to the precipitation trend, all scenarios show an increase in the blue water trend for the near and distant futures for most basins, except for a small part of the Nogoa Basin, which will experience a reduction of up to 10% under the A2 scenario for the period 2046-2064. A2 showed increases of 7% and 27% for near and distant futures, respectively. A1B projected increases of 35% and 52% for the period of 2046-2064 and 2080-2100, respectively. The B1 scenario projected increases in near and distant futures of 50% and 110%, respectively. The Isaac Basin will experience the highest increase under B1 scenario for the both periods.Green water storage has a similar trend to blue water trend (Figure 6.17).

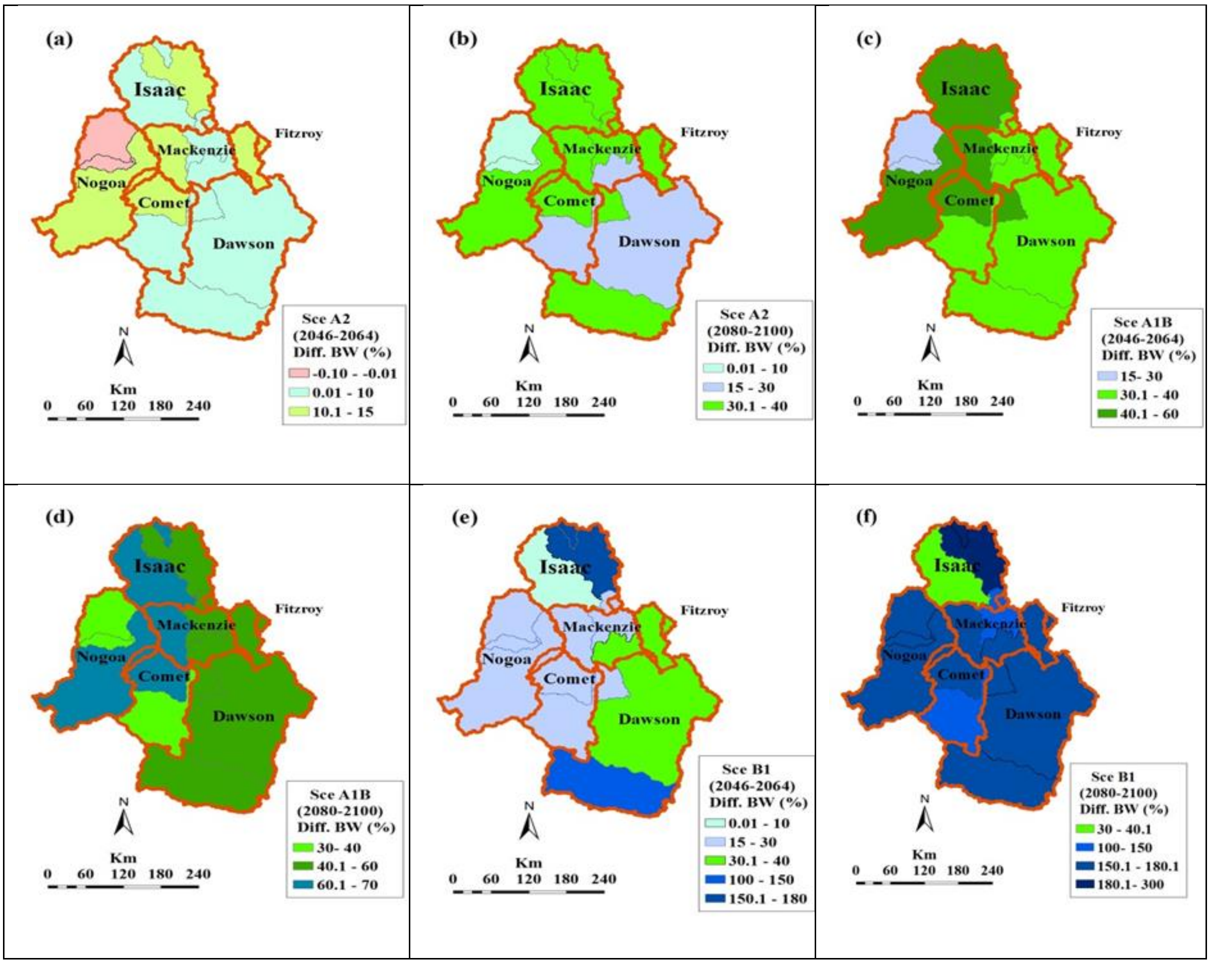

Figure 6.16: Projected impacts of climate change on the blue water of the basin (a) Anomaly based on scenario A2 for the period of 2046-2064, (b) Anomaly for A2 to 2080-2100, (c) Anomaly for A1B to 2046-2064, (d) Anomaly for A1B to 2080–2100, (e) Anomaly for B1 to 2046–2064, and (f) Anomaly for B1 to 2080-2100 (Source: original work created for this thesis)

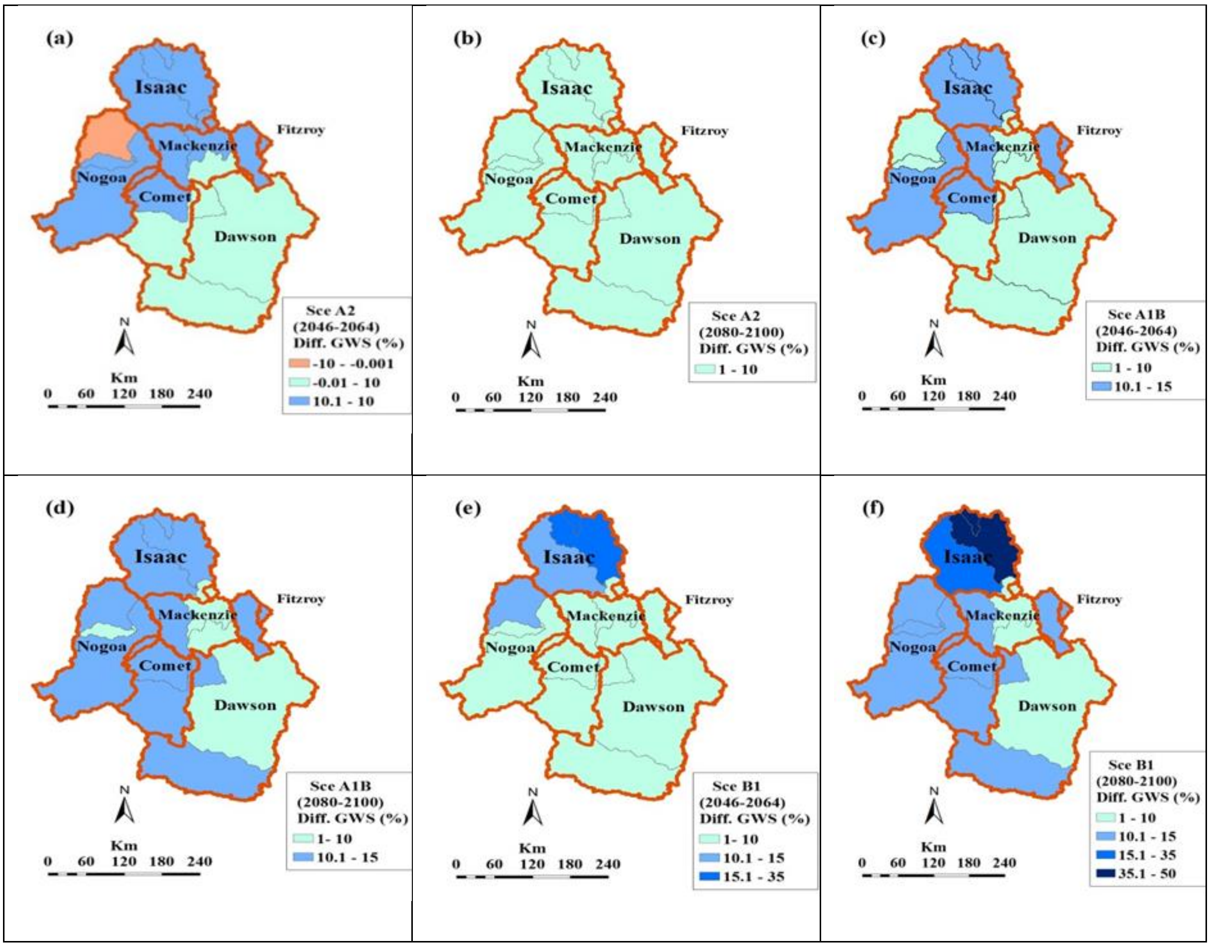

Figure 6.17: Projected impacts of climate change on the green water storage of the basin (a) Anomaly based on scenario A2 for the period of 2046-2064, (b) Anomaly for A2 to 2080-2100, (c) Anomaly for A1B to 2046-2064, (d) Anomaly for A1B to 2080–2100, (e) Anomaly for B1 to 2046–2064, and (f) Anomaly for B1 to 2080-2100 (Source: original work created for this thesis)

6.3.4 Deep aquifer recharge forecasts

Figure 6.18 captures the anomaly maps of deep aquifer recharge (maps of percent deviation from historical data, 1980-2010) for the A2, A1B, and B1 scenarios for the periods 2046-2064 and 2080-2100 from the average change of the multi-GCM ensemble. All basins will experience increases except for a small part of the Nogoa Basin, which will experience a decrease of up to 20% under the A2 scenario for the period of 2046-2064. The B1 scenario projected the highest increases, ranging from 0.01% to 150% in the near future and 40% to 250% in the distant future; the highest increases will occur in the Isaac Basin due to its proximity to the ocean. Under A1B scenario, the increases in deep aquifer recharge will reach up to 40% in the near future and 50% in the distant future. For the A2 scenario, the increases will range between 0.01 and 20% in the near future and between 0.01 and 40% in the distant future.

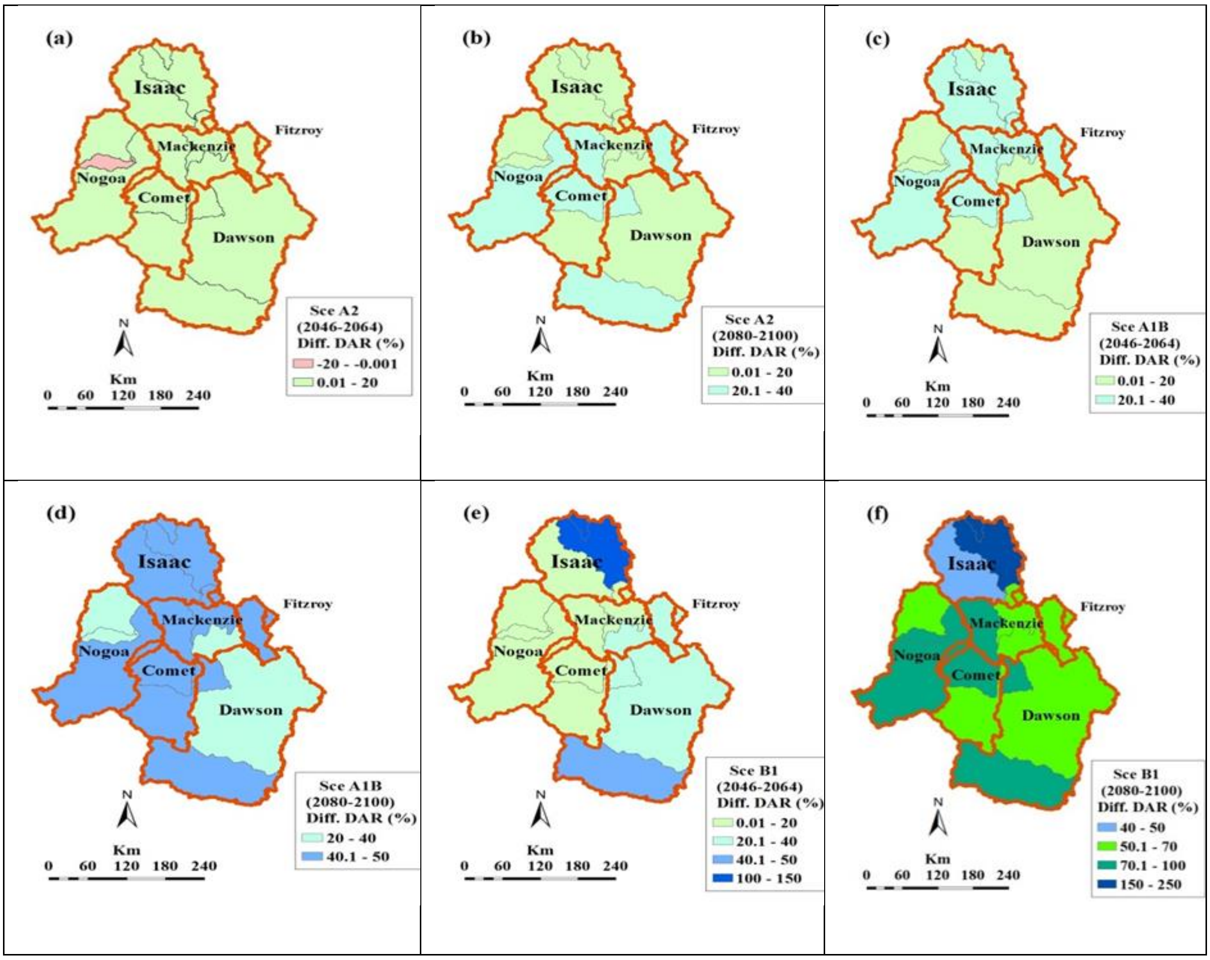

Figure 6.18: Projected impacts of climate change on the deep aquifer recharge of the basin (a) Anomaly based on scenario A2 for the period of 2046-2064, (b) Anomaly for A2 to 2080-2100, (c) Anomaly for A1B to 2046-2064, (d) Anomaly for A1B to 2080–2100, (e) Anomaly for B1 to 2046–2064, and (f) Anomaly for B1 to 2080-2100 (Source: original work created for this thesis)

6.3.5 Stream Flow Forecasts

The results from the hydrological modelling for annual stream flow are shown in Figure 6.19. The six sub-basins will experience increases under CGCM3 and MIROC 3.2 for the A2, A1B and B1 emission scenarios, except that Comet will experience a decrease under A1B for both periods midand end- century. Under CNRM-CM3, the Isaac River will see increases for B1 and A1B, but decreases under A2 for both periods. Nogoa will see decreases under B1 and A2 for 2046-2064. Comet will experience decreases under B1 (2046-2064), A1B (2080-2100) and A2 (2080-2100) but increases in the rest of the scenarios. Dawson will see increases under A2 (2080-2100) only. Mackenzie will only experience increases under A1B (2046-2064), B1 (2080-2100) and A2 (2080-2100). Fitzroy will experience increases under A1B (2046-2064 and 2080- 2100) and A2 (2080-2100). For GFDL-CM2-1, the Isaac River will experience increases under B1 (2046-2064) and (2080-2100) only. Nogoa will experience increases under A1B (2046-2064) and A2 (2080-2100). Comet will experience increases under all emission scenarios for both periods. The Dawson River will experience decreases under B1 (2080-2100) and A1B (2080-2100) only. Mackenzie will experience decreases under B1 and A2 (2046-2064) and A1B (2080-2100). Fitzroy will see increases only under A1B and A2 (2080-2100). For IPSL-CM4, Isaac will experience decreases only under A1B (2080-2100). Nogoa will see increases under A1B (2046-2064) and B1 (2080-2100). Comet will experience decreases only under A1B (2046-2064). Dawson will decrease under A1B and A2 (2080-2100). Mackenzie will experience decreases under A1B (2080-2100). Fitzroy will experience decreases under A1B and A2 (2080-2100). For MRI, Isaac will see decreases under A2 (2046-2064). Nogoa will experience decreases under B1 (2046-2064). Comet will experience decreases under A1B (2046-2064). Dawson will decreases under A2 (2046-2064). Mackenzie will experience decreases under B1 (2046-2064). Fitzroy will experience decreases under B1and A2 (2046-2064).

Isaac	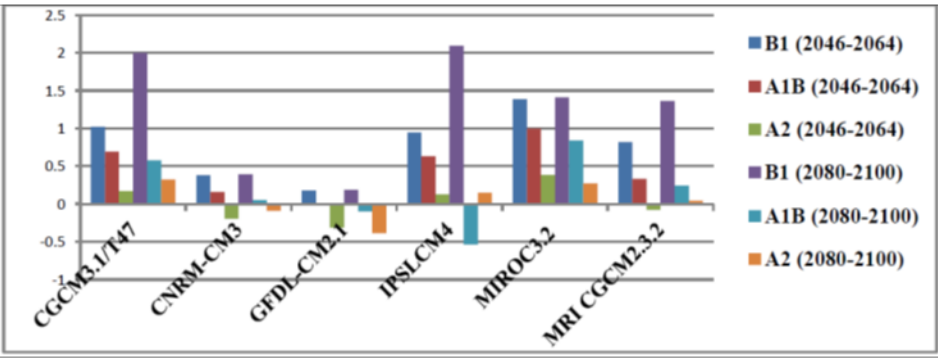

Nogoa

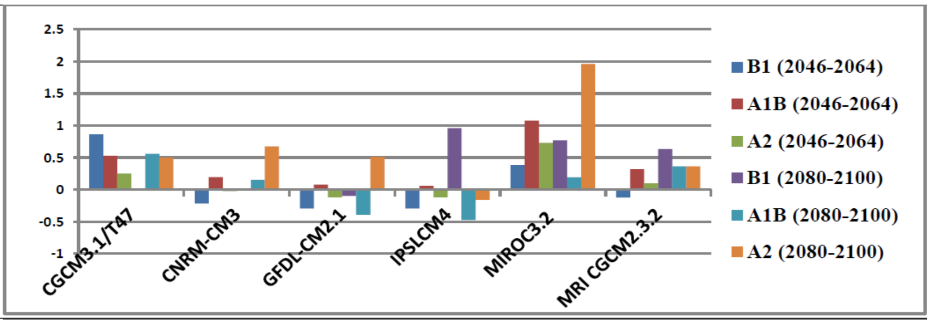

Comet

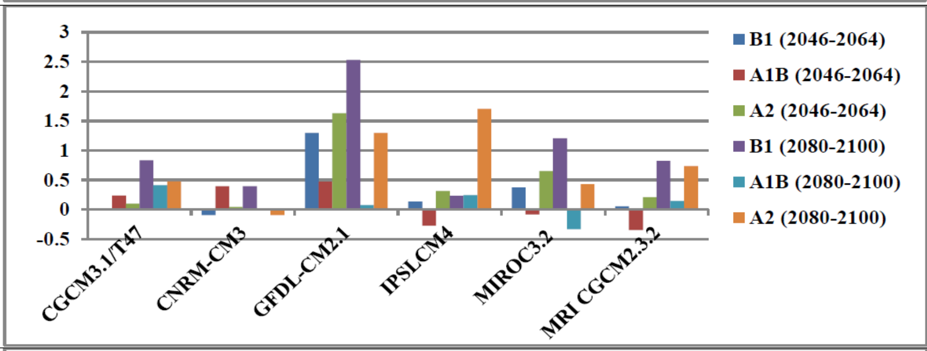

Dawson

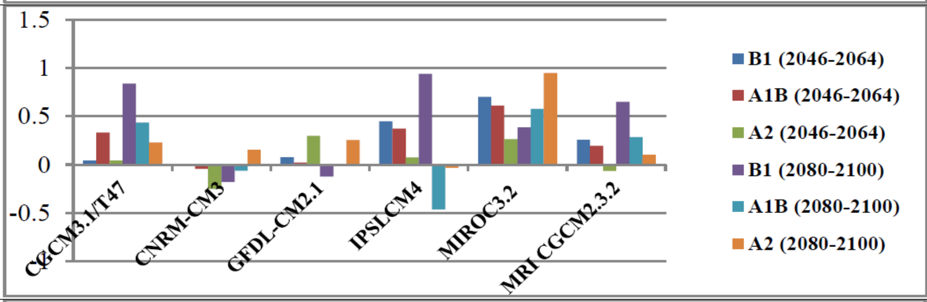

Mackenzie

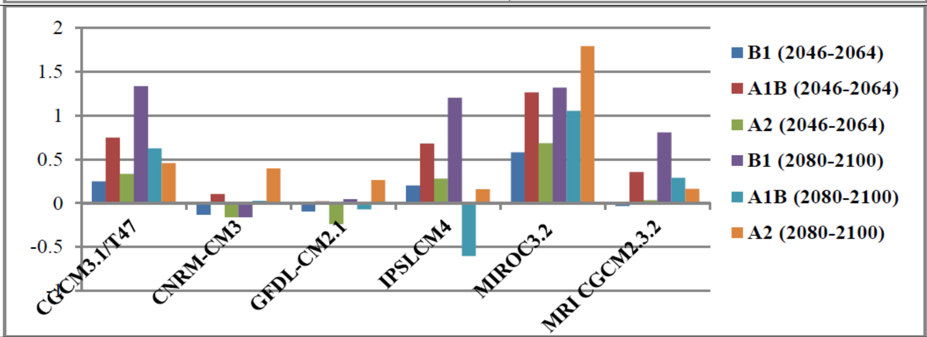

Fitzroy

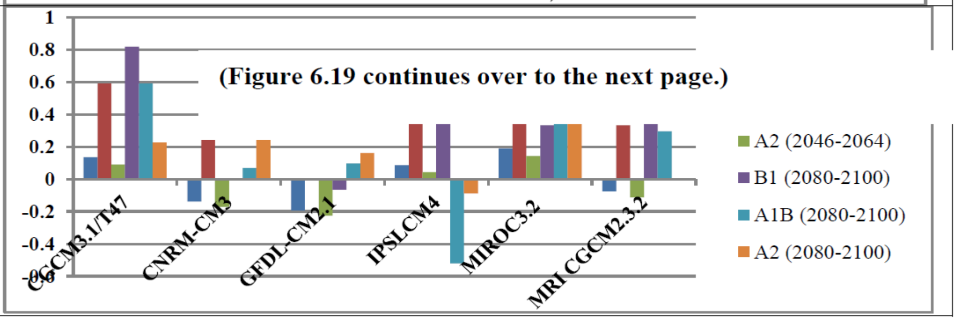

(Figure 6.19 continues over to the next page.)

Figure 6.19: Projected changes in streamflow in the six sub-basins compared to the base period 1982-2000, for 2046-2064 and 2080-2100 for B1, A1B and A2 scenarios. (Source: original work created for this thesis).

6.4 Impacts of climate change on Tigris Basin using CMIP5

6.4.1 Precipitation Forecasts

Overall, all selected GCMs predicted a decrease in the mean annual precipitation at about a half-century lead time (2046-2064) and about a one-century lead time (2080-2100) for the five basins. Figure 6.20 shows the anomaly maps of precipitation distribution (maps of percent deviation from historical data, 1980-2010) for RCP 2.6, RCP 4.5 and RCP 8.5 scenarios for the periods 2049-2069 and 2080-2099 for the average change from the multi-GCM ensemble. RCP 8.5 produced the same decreases for the half-century ahead forecast in the five basins, while for the end of the century, apart from Lesser Zab which will experience decreases of about 18%, Diyala, Al-Adhiam, Khbour and Greater Zab will experience reductions of about 23%. RCP 4.5 produced nearly the same reduction (average -18%) for all basins in the mid-century, whereas at the end of the century, apart from Greater Zab which will see a reduction of about -15%, the rest of the basins will experience nearly the same decline of 26%. Under the RCP 2.6, Diyala Basin is expected to experience the highest reduction in precipitation (average 28%). The south of Diyala will experience a reduction of about 55%, while the north of the basin may experience about a 16% decrease; about 5% of the basin located in the basin’s far north will experience increases of about 14%. Al-Adhiam will experience a decrease of 26%, followed by Greater Zab 17%, Khbour 7% and Lesser Zab 3% for the mid-century. At the end of the century, Khbour and Greater Zab will experience the same reduction (15%), while Al-Adhiam, Diyala and Lesser Zab will experience reductions of 38%, 36% and 10%, respectively. It is clear that Diyala and Al-Adhiam will experience the highest reductions for both periods under the three scenarios. This is a reasonable result, because Diyala and Al-Adhiam experience higher air temperatures and lower precipitation amounts compared to those of Khbour, Greater Zab and Lesser Zab Basins (Table 6.8).

Table 6.8: The projected relative changes in precipitation for the five basins under RCP 8.5, RCP 4.5, and RCP 2.6 scenarios for the periods 2046-2064 and 2080-2100.

	Scenarios					
	RCP 8.5	RCP 8.5	RCP 4.5	RCP 4.5	RCP 2.6	RCP 2.6
Basin	(2049-69)	(2080-99)	(2049-69)	(2080-00)	(2049-69)	(2080-99)
Khbour	-12	-25	-18	-25	-7	-15
Greater Zab	-12	-22	-17	-15	-17	-15
Lesser Zab	-12	-18	-18	-26	-3	-10
Al-Adhiam	-13	-25	-19	-26	-26	-38
Diyala	-14	-27	-18	-25	-28	-36

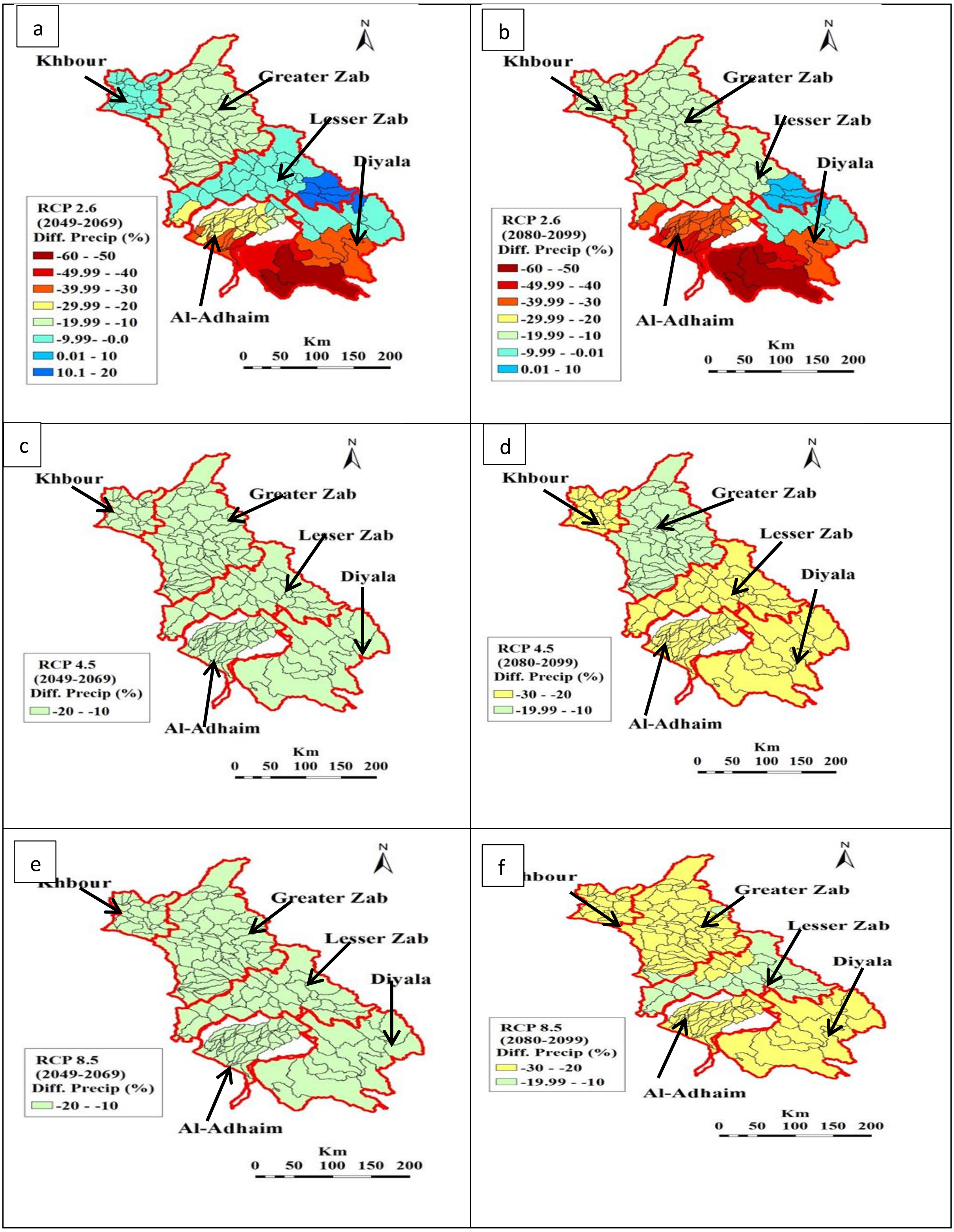

Figure 6.20: Projected impacts of climate change on the precipitation of the five basins (a) Anomaly based on scenario RCP 2.6 for the period 2046-2064, (b) Anomaly based on RCP 2.6 for 2080-2100, (c) Anomaly based on RCP 4.5 for 2046-2064, (d) Anomaly based on RCP 4.5 for 2080–2100, (e) Anomaly based on RCP 8.5 for 2046-264, and (f) Anomaly based on RCP 8.5 for 2080–2100 (Source: original work created for this thesis)

6.4.2 Blue Water and Green Water Forecasts.

Figure 6.21 captures the anomaly maps of blue water distribution (maps of percent deviation from historical data, 1980-2010) for the RCP 2.6, RCP 4.5 and RCP 8.5 scenarios for the periods 2049-2069 and 2080-2099 from the average change of the multi-GCM ensemble. The half-century projection (2049-2069) and the end–of-century (apart from Khbour) projections show a decrease in blue water under all emission scenarios for the whole region. The Al-Adhiam Basin is likely to experience the highest reductions under the three scenarios in both periods, followed by Diyala, Lesser Zab and Gtreater Zab. Khbour will experience an increase of about 8% under RCP 4.5 for the end of the century. Table 6.9 provides the estimated values. Green water has the same trend as blue water (Figure 6.22, Table 6.10).

Table 6.9: The projected relative changes in blue water for the five basins under RCP 8.5, RCP 4.5, and RCP 2.6 scenarios for the periods 2049-2069 and 2080-2099.

	Scenarios					
Basin	RCP 8.5 (2049-69)	RCP 8.5 (2080-99)	RCP 4.5 (2080-99)	RCP 4.5 (2080-00)	RCP 2.6 (2049-69)	RCP 2.6 (2080-99)
Khbour	-22	-43	8	-44	-16	-24
Greater Zab	-23	-39	-20	-45	-29	-27
Lesser Zab	-23	-43	-33	-48	-22	-28
Al-Adhiam	-23	-48	-35	-49	-70	-65
Diyala	-22	-31	-33	-44	-35	-44

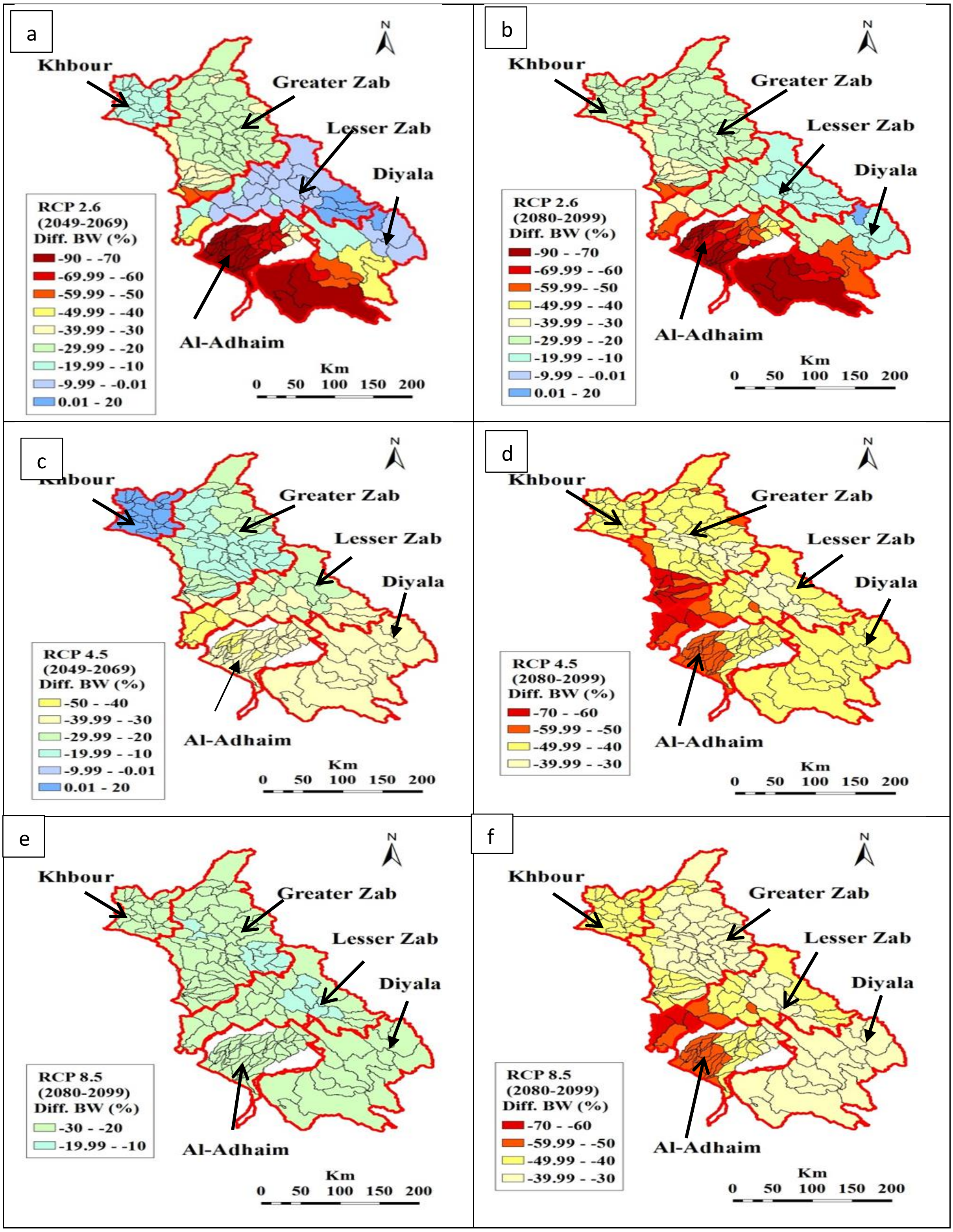

Figure 6.21: Projected impacts of climate change on the blue water of the five basins (a) Anomaly based on scenario RCP 2.6 for the period 2046-2064, (b) Anomaly based on RCP 2.6 for 2080-2100, (c) Anomaly based on RCP 4.5 for 2046-2064, (d) Anomaly based on RCP 4.5 for 2080–2100, (e) Anomaly based on RCP 8.5 for 2046-264, and (f) Anomaly based on RCP 8.5 for 2080–2100 (Source: original work created for this thesis)

Table 6.10: Projected relative changes in green water for the five basins under RCP 8.5, RCP 4.5, and RCP 2.6 scenarios for the periods 2049-2069 and 2080-2099.

	Scenarios					
	RCP 8.5	RCP 8.5	RCP 4.5	RCP 4.5	RCP 2.6	RCP 2.6
Basin	(2049-69)	(2080-99)	(2080-99)	(2080-00)	(2049-69)	(2080-99)
Khbour	-9	-18	-12	-16	-5	-7
Greater Zab	-9	-17	-16	-20	-7	-8
Lesser Zab	-11	-20	-15	-19	-8	-8
Al-Adhiam	-13	-22	-16	-21	-40	-29
Diyala	-11	-21	-15	-21	-19	-19

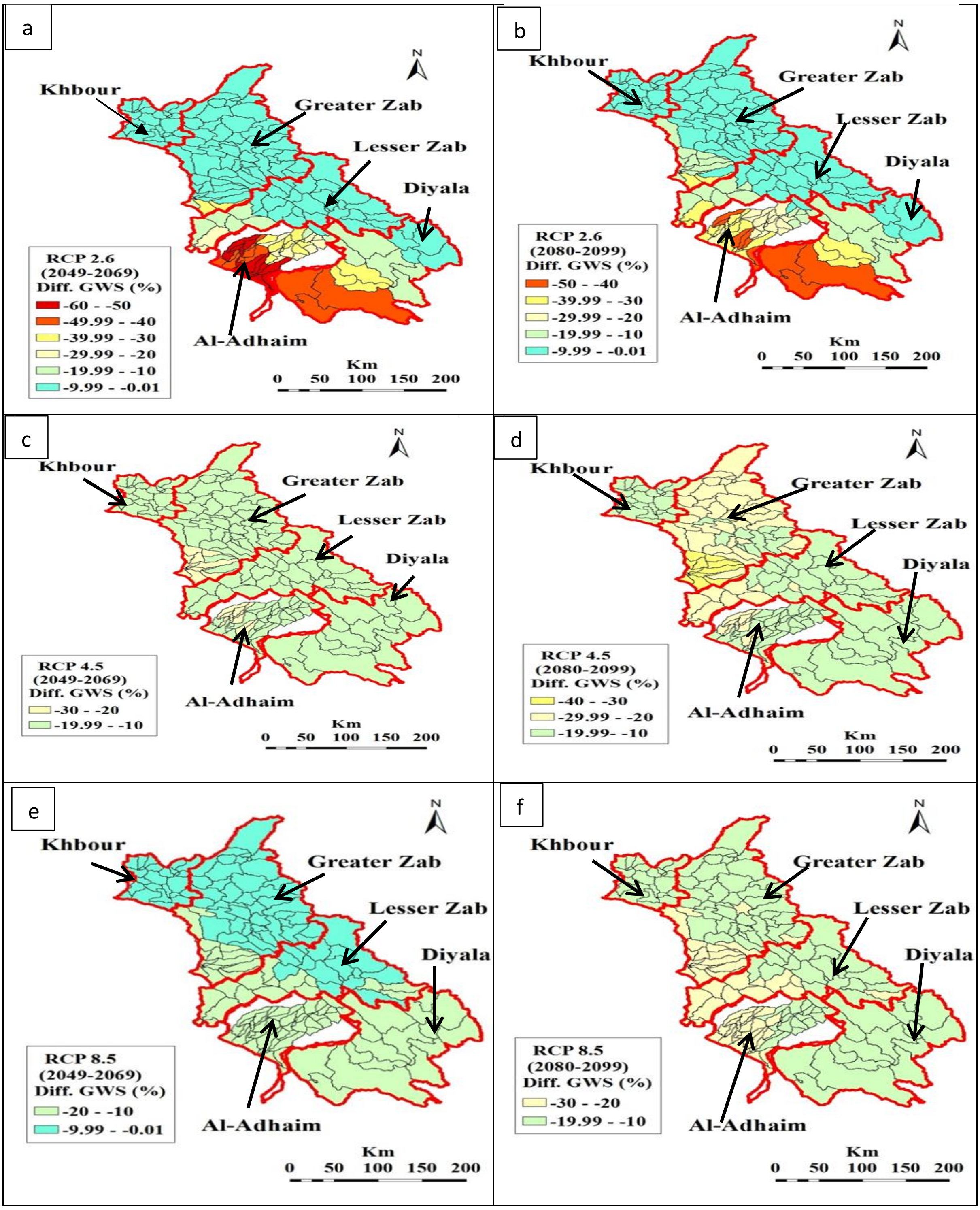

Figure 6.22: The impacts of climate change on the green water of the five basins (a) Anomaly based on scenario RCP 2.6 for the period 2046-2064, (b) Anomaly based on RCP 2.6 for 2080-2100, (c) Anomaly based on RCP 4.5 for 2046-2064, (d) Anomaly based on RCP 4.5 for 2080–2100, (e) Anomaly based on RCP 8.5 for 2046-264, and (f) Anomaly based on RCP 8.5 for 2080–2100 (Source: original work created for this thesis)

In comparing the impacts of climate change using CMIP3 between the Tigris Basin and Fitzroy Basin, Table 6-11 shows that for the Fitzroy Basin the temperature will increase by about 1.16 and 3.2 for near future and distant future, respectively, while in the Tigris Basin the temperature will increase by 2.5°C and 5.5 °C for the near future and far future, respectively. The Fitzroy Basin will experience increases in precipitation by about 8% and 14% for mid-century and end-century, respectively; however, the Tigris Basin will experience severe reductions in precipitation which could reach 15% and 22% for the near and far future, respectively. In the Fitzroy Basin blue water is expected to increase by about 13% and 27% for 2046-2064 and 2080-2100, respectively. The Tigris Basin will experience significant reductions by about 22% and 33% for near and far future, respectively. Green water, deep aquifer and stream flow will have the same trends of blue water for both regions.

Table 6-11: comparison the impacts of climate change on water resources between the two regions.

Factors	Fitzroy		Tigris	
	2046-2064	2080-2100	2046-2064	2080-2100
Temperature	1.16 ^{0}C	3.2^{0}C	2.5^{0}C	5.5^{0}C
Precipitation	+8	+14	-15	-22
Blue water	+13	+27	-22	-33
Green water	+10	+25	-15	-20
Deep aquafer	+20	+27	-18	-30
Streamflow	+26	+43	-35	-57

To summarise the results, precipitation in the last three decades in northeast Iraq show a declining trend that can be considered as deteriorating at an alarming rate. By contrast, in Queensland, the results over the past 30 years show that the Fitzroy River basin has sufficient water, with a depletion rate that is likely to cause minimal adverse effects. Impacts of climate change modelled using the CMIP3 models for both the Australian and Iraqi regions portray a northeast Iraq where the Tigris River will experience increasing temperatures and decreasing annual precipitation that will have far-reaching consequences, with the likelihood of greatest effects being felt in the southern part of the basin and the possibility of air temperatures increasing up to 50^0C. The Fitzroy region is expected to be hotter and wetter compared to current conditions, in particular in the Isaac Basin, due to its location adjacent to the ocean. The adverse effects may not be that consequential if the availability of water increases.

CHAPTER 7

CLIMATE CHANGE ADAPTATION AND MITIGATION

7.1 Background

Although climate change is a physical process linked with alterations in climatic variables, it also involves social processes associated with the way society evolves over time. Climate change has impacts on social, economic, and environmental systems and forms scenarios for water, food and health security (Bryan et al. 2009). Capability for mitigating and adapting to climate change depends largely on proactive approaches adopted by diverse socioeconomic groups that exist in various geographical circumstances (Deressa et al. 2009). Climate change can intensify the vulnerability of society. It may lead to aggravated water scarcity, exposure to diseases and undermining of growth opportunities. The impacts of climate change in northeast Iraq vary geographically. The southern part, which includes Diyalia and Al-Adhiam, is projected to be most impacted by droughts and shortened growing seasons. Extreme droughts have categorized the region in the last three decades, as shown in this research, and the results are in line with the report of UN-ESCWA and BGR (2013). Severe drought has caused a reduction in agricultural production, especially in the areas of rain-fed crop; this in turn has caused a noticeable reduction in farmers' income.

This chapter considers the concept of vulnerability in the context of climate change and its three features (exposure, sensitivity and adaptive capacity) and discusses adaptation and mitigation measures that could be implemented to respond to climate change, and thus secure and sustain water for present and future generations at all levels.

7.2 The concept of vulnerability

IPCC's Third Assessment Report (TAR) defines vulnerability as the level to which a system is prone or at which it is incapable of tackling the adverse impacts of climate change, including climate variability and extremes (IPCC 2014). Vulnerability in the context of climate change has three components: exposure, sensitivity, and adaptive capacity (Fellmann 2012) (Figure 7.1). For example, farming vulnerability to climate change can arise through exposure to increased temperatures and decreased rainfall, and thus reduction in water resources. The sensitivity of crop yields is described as how they are affected because of these changes. Adaptive capacity is expressed as the capability of farmers to adjust to the impacts of that exposure and sensitivity – for instance, by growing plant varieties that are more drought-resistant.

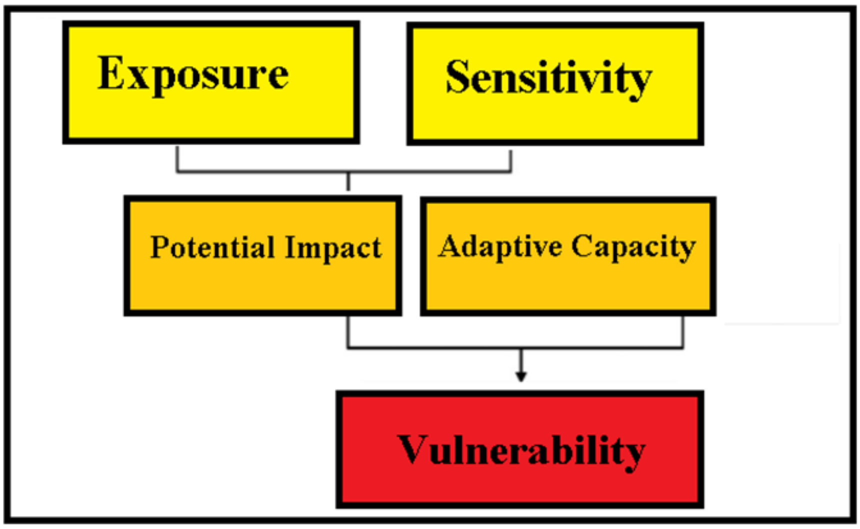

Figure 7.1: Vulnerability and its components. (Source: original diagram created using data from Fellmann (2012

The possible impacts of climate change on any system can be described by both exposure and sensitivity factors. Nevertheless, it has been established that, despite a system being considered as greatly exposed and/or sensitive to climate change, it does not necessarily indicate that it is vulnerable (IPCC 2014; Fellmann 2012). The reason is that exposure and sensitivity do not account for the capability of a system to adjust to climate change, while vulnerability is the effect remaining after adaptation has happened (Figure 7.1). Consequently, the adaptive capacity of any system impacts its vulnerability to climate change by controlling exposure and sensitivity (Adger et al. 2007; Fellmann 2012).

7.3 The concept of adaptive capacity

Adaptive capacity has been described by IPCC (2014) as the potential ability of a system to adapt successfully to climate change. Recent studies stress the significance of socio-economic aspects for the adaptive capacity of a system, particularly underlining the essential part played by organizations, authorities and management in defining the capability to respond and adjust to climate change (Williamson et al. 2012). Consequently, the adaptive capacity of any system is essentially determined by socio-economic actions, and it affects both the social features and biophysics of a system (IPCC 2014). The main role of adaptive capacity in prompting vulnerability is shown in Figure 7.2. Higher adaptive capacity, lower sensitivity and exposure result in lower vulnerability, as shown in the lower part of Figure 7.2, whereas lower adaptive capacity, higher sensitivity and exposure lead to higher vulnerability, as shown in the upper part of the figure.

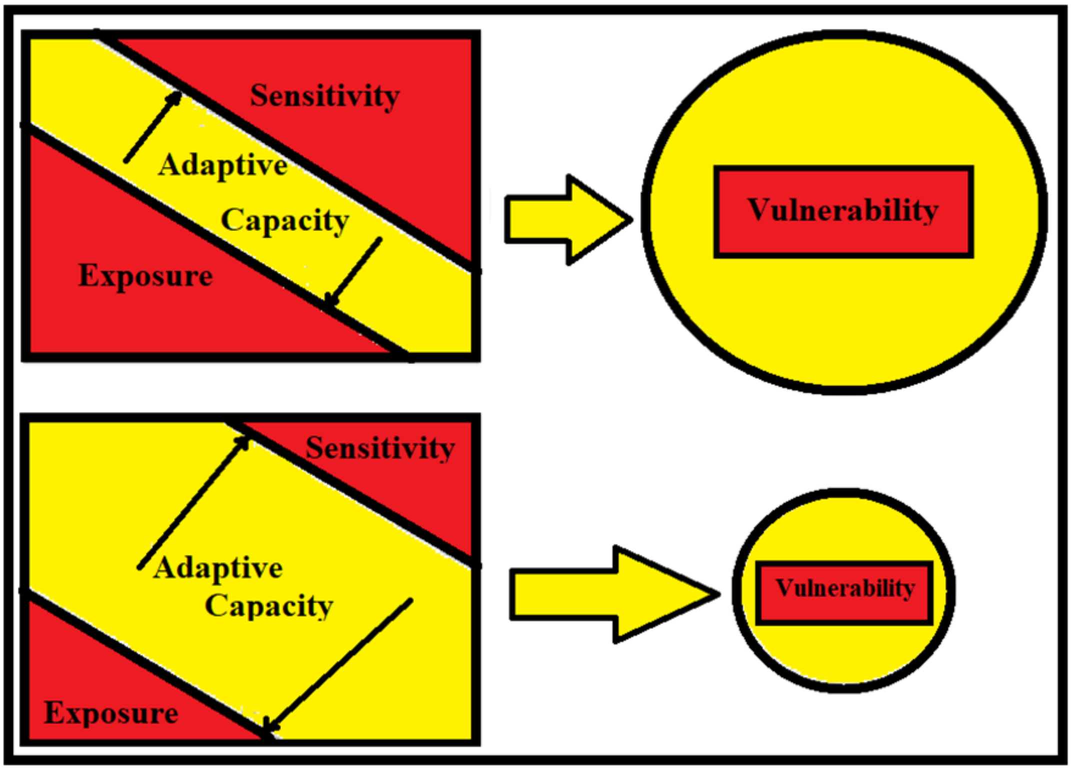

Figure 7.2: The basic role of adaptive capacity in influencing vulnerability (Source: original diagram created using data from Fellmann, 2012)

As discussed earlier, Iraq's agriculture is the country's most fragile sector and is negatively affected by climate change (UN-ESCWA and BGR 2013). Without appropriate adaptation strategies to climate change, there is the potential to stifle economic development and aggravate already persistent socio-economic affliction (Fellmann 2012). Logically, therefore, adaptation is increasingly being considered as one of the possible strategies to diminish the adverse effects of climate change (Adger et al. 2007). In particular, developing countries such as Iraq need to take into consideration the optimal management of water resources and agricultural activities, since climate change is highly likely to affect agricultural production the most.

For the Fitzroy Basin, the politics of strong denial of climate change has to date stifled any action that would deal with its adverse effects (Greg 2020). Some disaster management schemes are in place but these are identified as unrelated to climate change.

7.4 Agricultural adaptation to climate change for the Tigris Basin

Generally, agricultural adaptation includes two forms of amendments in plant production systems. The first strategy is enhanced agricultural diversification through, for example, using drought-tolerant varieties to address temperature stresses. The second policy emphasizes plant management practices, such as managing critical plant growth stages by not coinciding with severe climatic events such as mid-season droughts. According to Orindi and Eriksen (2005), shifting the duration of the plant growth period and altering implanting and harvesting dates are common plant management measures that are used in plant adaptation to climate change. The Iraqi Ministry of Water Resources (2015) and Fadeil (2016) have stated that climate change has already been noticed by the population, and it has been inferred from examining farmers' views on climate change and their actions in responding to its adverse effects. The responses of farmers have included planting trees, crop modification, altering planting dates and soil conservation as the main possible adaptation policies to deal with the effects of climate change for rain-fed crops.

7.4.1 Adaptation to climate change at farm level

In order to adapt and respond efficiently to climate change, farmers must initially recognize that changes are occurring. Most farmers have noticed that the climate has become hotter and drier and that water resources have decreased significantly. The farmers' observations are in line with the results of this study. They have been struggling to adjust to such extreme weather conditions, especially those farmers who live in the south of the northern region of Iraq.

The following are the adaptation measures to climate change that farmers believe to be proper approaches.

Crop Modification – Farmers grow crop varieties that have the ability to survive in harsh weather conditions. In addition, growers plant early-ripening crop varieties and grow drought-tolerant crops and crops that are resistant to temperature stresses. These are significant forms of plant protection against rainfall variations (Orindi and Eriksen 2005). Furthermore, planting diverse crop varieties in the same field or various plots with different crops moderates the risk of whole crop failure, because diverse crops are influenced differently by climate conditions, and this therefore somewhat underpins a minimum level of revenue for livelihood security (Orindi and Eriksen 2005).

Soil Conservation – Soil conservation practices are to increase productivity on-farm (Gebrehiwot and van der Veen 2013). Decreasing rainfall and increasing prolonged periods of drought due to climate change are highly likely to reduce crop yields. Increasing soil health and fertility leads to increased crop productivity, thus serving to moderate the impact of climate change on agricultural productivity.

Irrigation – Improving the usage of water irrigation has proven to be an efficient practice to confront unreliable rainfall conditions. Using irrigation is likely to improve agricultural productivity through complementing rainwater during dry periods (Orindi and Eriksen 2005). In addition, using irrigation systems may enable framers to grow crops such as vegetables in low rainfall fields and during the dry season and drought events. These can be considered a substitute source of food and revenue when rain-fed crops are unsuccessful. In some areas, floodwaters are harvested and utilized for developing crops after the floods have receded (Gebrehiwot and van der Veen 2013). Generally, improvement of irrigation water usage enables farmers to avoid crop losses in areas exposed to frequent drought (Orindi and Eriksen 2005).

Changing Planting Dates – Early- and late-growing plants are another policy measure to adapt to climate change. This approach enables farmers to protect sensitive growth stages to safeguard these critical stages from coinciding with severe climatic conditions.

Planting Trees – This strategy includes growing trees on a farm to function as shade against severe hot weather. Growing trees and afforestation enhance agricultural productivity, because they usually contribute to climate change alleviation through improved carbon sequestration (Gebrehiwot and van der Veen 2013).

7.4.2 Adaptation measures at local government

The local governments in the Tigris Basin region could adopt a multi-step framework to cope with the adverse impacts of climate change, which includes the following.

Water Management Strategy View

1. Consideration of a long-run integrated national water resources management plan by all authorities concerned, including the Ministry of Water Resources, Ministry of Agriculture, Ministry of Environment, and water resources experts at universities.
2. Rehabilitation of the infrastructure of water treatment plants and irrigation and drainage pumping stations.
3. Usage of alternative water resources such as recycled waste water by establishing recycling water plants.
4. Raising public awareness about climate change and its impact. Use of the social media is one of the great ways to educate the population about the adverse impacts of climate change and the importance of water conservation strategies. According to Al-Ansari et

al. (2014), many people, especially in developing countries, are unaware how climate change will affect their lives. Therefore, working with the media, government authorities can spread their message easily and quickly. Conducting effective environmental education campaigns is also of importance for increasing public awareness about climate change issues and mitigation practices. Furthermore, the relevant agencies and authorities can use the classroom to introduce this subject to students. According to UNEP, educating children and the young population about environmental issues is vital to long-term achievement of mitigation goals. This will enable them to acquire a sense of responsibility so that they can play an essential role in educating their community about these issues, since the absence of public awareness of the significance of appropriate water management and the impact of governmental decisions on long-term assurance of water resources are among the major problems in the Middle East (Al-Ansari 2011).

5. Since agriculture is the biggest water consumer in the Iraq's northeast region, educating farmers on the usage of modern irrigation systems that are appropriate for an arid climate can be a great measure to avoid water losses.

Research and Development

1. Creating an inclusive data set that comprises weather, hydrological, topographical, soil and plant cover data that can be utilized by researchers. Hence they can conduct research to introduce new technologies in water resources and agriculture which are suitable for Iraq's environment.
2. Conducting modelling research that predicts the impacts of climate change on various sectors of life.

Regional Cooperation

1. Collaboration amongst riparian countries. Iraq, Turkey, Iran and Syria should organize their efforts to find realistic arrangements among riparian countries on water asset distribution.
2. UN organizations such as UNESCO and international organizations such as FAO, WMO and international universities should be involved to assist the region with their experience and expertise in this domain.

Irrigation and Agriculture

1. Abandoning conventional irrigation systems, such as furrows, to avoid wasting water and adopting effective irrigation systems that are appropriate for the types of the soils, water accessibility and quality and crop yields. For example, sprinkler irrigation is appropriate for grain, whereas drip irrigation is suitable for orchards such as grapes, using saline water, and both practices are much better than furrow irrigation.
2. Improving and maintaining the transmission of water systems to reduce water losses and increase transmission effectiveness. Using closed channels reduces evaporation and infiltration losses and prevents irrigation water from coming into contact with the saline water table.
3. Enhancing the drainage systems of agricultural land to improve soil percolation and reduce soil salinity.
4. Reducing chemical fertilizer and pesticide usage which deteriorates water quality.

To summarise, adaptation measures that have been proposed as being effective through scientific analysis at farmer and government levels were investigated. Farm-level adaptation may include adopting crop modification, soil conservation, irrigation efficiency, changing crop calendars and planting of trees. However, to ensure success of these adaptation measures, help is generally needed in terms of financing and technological support from government bodies or other institutions. The overarching need at the planning level of the government is to formulate a multi-step collaborative framework to cope with the adverse impacts of climate change that involve water management strategy, research and development, regional cooperation, and new irrigation and agricultural technologies.

CHAPTER 8

DISCUSSION AND CONCLUSIONS

8.1 Discussion

To accomplish the first objective of this thesis, the performance and suitability of the three tools – GIS, SWAT and statistical analyses, and SWAT embedded in GIS – were applied to northeast Iraq's Tigris and northeast Australia's Fitzroy Basins. The model was calibrated and validated at nine discharge stations in northeast Iraq and at seven discharge stations in the Fitzroy Basin to simulate the streamflow using the SUFI-2 algorithm. The performance of the model was found to be acceptable with R^2 and ENC indices, as well as visual traces during the calibration and validation periods, although there were under-predictions and over-predictions during some months, especially wet months. The underestimation and overestimation during some months is typical of simulation models which cannot often capture extreme events in the system, but they may also be due to errors in measuring flow, unevenly distributed rainfall stations and spatial variability in soil and land use. In general, the model developed can be described as capable of simulating the streamflow of the two regions. Thus the first objective of this thesis, the performance and suitability of the three tools (GIS, SWAT and statistical analyses), was met.

To achieve the second objective, obtaining better understanding of the existing hydrological systems and investigation how changes in climate (rainfall and temperature) may affect and alter streamflow regimes and other hydrological processes, the impacts of climate change for the last three decades on hydrological system were assessed.

The calibrated models were used to identify the trends of temperature and water components during the last three decades for each region. The air temperature trend has been increasing in the last three decades in both regions. These changes in temperture have led to alteration in precipitation, blue water and green water and hence streamflow for both regions.

For the Tigris Basin, temoprally, there is a significant declining trend in precipitation, blue water and green water over the last three decades. Spatially, precipitation was found to have a decreasing trend from north to south and from east to west, which roughly fits the description that, the more mountainous the terrain is, the higher the precipitation amount. Blue water a has tendency to be high where the runoff from precipitation tends to accumulate. Green water tracks blue water. However, land cover contributes to the forming of the spatial allocation of blue and green water.

These changes in water components have led to severe water scarcity per capita. In general, the region has experienced severe water scarcity in terms of blue water availability. Green water storage availability analysis showed that, apart from the Khbour, which has experienced nine to ten months where groundwater is accessible, the region has experienced five to six months per year of groundwater availability. Therefore, large areas of the region can often experience reduced crop yield due to lack of green water availability, particularly downstream catchments such as the Al-adhiam Basin.

In the Fitzroy Basin, during the last three decades the temporal and spatial scale of precipitation revealed that there was a high variable trend of precipitation over the period, which is a typical for Australian rainfall. Blue water followed precipitation distribution. Green water, however, was nearly stable, because the land cover was assumed to be static.

The blue water availability per capita analysis showed that the entire region can be described as having sufficient water. The green water storage availability analysis showed that most of the basin experienced eight to nine months per year groundwater availability, except for the Fitzroy sub-basin and a small part of Isaac and Dawson, which experienced ten to eleven months per year groundwater availability.

To meet the third objective, which is identification and understanding of the various aspects of implications of climate change in these regions, six GCMs for the CMIP3 were applied for both regions. However, six GCMs from the CMIP5 were applied only to the Tigris region as CMIP5 models did not represent the Fitzroy Basin accurately.

In the Tigris Basin, all models run under the CMIP3 and CMIP5 predicted that the basin will experience increasing temperatures and decreasing annual precipitation that will have far-reaching consequences, with the highest impact in the southern part and likelihood of rising temperatures up to 50^0C in both the near and distant future, respectively.

Overall, all GCMs projected a decrease in the mean annual precipitation for about a half century lead time (2046-2064) and about a one century lead time (2080-2100) for the five basins. Diyala Basin is expected to experience the highest reduction in precipitation, followed by Al-Adhiam. This is a reasonable result because Diyala and Al-Adhiam experience higher air temperatures and lower precipitation amounts compared to those of the Khbour, Greater Zab and Lesser Zab Basins. The latter basins may experience nearly the same reductions under the three scenarios for both periods.

In regard to blue water, the half century projection (2046-2064) shows a decrease in blue water under all emission scenarios for the whole region. The Al-Adhiam Basin is likely to experience the highest reductions under all scenarios in both periods, followed by Diyala. Khbour, Greater Zab and Lesser Zab, which would experience approximately the same reductions under all scenarios for both periods. Green water storages may also decrease under all emission scenarios for the two future periods. Green water flow calculations show a slight reduction in evapotranspiration because of the hypothesis that land cover will not significantly change from the period of the 1980s to the 2100s.

The results from the hydrological modelling for annual stream flow show that in five tributaries streamflow will significantly decrease for all scenarios. These findings may have significant effects, because a large area already suffers from per capita water scarcity. Severe water scarcity also corresponds to areas with high population density, adding more complexity to the problem. Any water resources management and development scheme in the future of the region should carefully consider this aspect.

For the Fitzroy region, all six GCMs models in CMIP3 predicted that the catchment will be hotter and wetter in the near and distant futures, except for a small part in the Nogoa Basin located in the north of the study area. The impact on blue water appears to be more pronounced than on green water, which may imply a higher degree of worsening in flood situations than in drought situations.

All the models demonstrated steadily increasing trends in temperature across the Fitzroy Basin under the three scenarios. All scenarios indicated an increase in precipitation trend for the near and distant futures for most basins, apart from a small portion of the Nogoa basin that would see a reduction for the period 2046-2064: this region will likely experience more rain due to longer and more intense monsoon resulting from more intense atmospheric convection, especially in the Isaac Basin due to its location.

Blue and green water patterns commonly follow precipitation patterns. Blue and green water have a tendency to be high where precipitation is high. Similar to the precipitation pattern, all scenarios show an increase in the blue water trend for the near and distant futures for most of basins except a small part of the Nogoa Basin, which will experience a reduction of up to 10%. For streamflow investigation, the six sub-basins will experience increases under all emission scenarios.

However, in incorporating the findings of this study in any water resources planning or management scheme, it is important to note that some shortcomings could not be avoided in the study. Firstly, there were limited availability of data and uneven distribution of weather and discharge stations, especially in the Tigris Basin, where the measured discharge and weather stations are sparse. Secondly, effects of reservoir operation, land use changes and irrigation water usage were neglected due to non-availability of data. Thirdly, sparse evapotranspiration and soil moisture data restricted proper validation of green water flows. These are in addition to the fact that GCMs are considered reliable in predicting temperatures but are less so in predicting precipitation. Nevertheless, to the best of our knowledge, this is the first initiative in the two regions to provide insight into the blue and green water flows. Hopefully, it will be useful for water resources managers, developers, and planners.

To develop suitable tools which can be used by organizations to incorporate climate change impacts, adaptation and vulnerability into their planning and management strategies, this research further looked into adaptations to climate change. Adaptation to climate change is the modification of a system to mitigate its impacts, take advantage of new opportunities and/or cope with the consequences. It is understood that, even with very strict policies to control emissions, greenhouse gases are likely to continue to grow in concentration. Climate change impacts a whole gamut of sectors, particularly water and agriculture. The effects are also pervasive, affecting national food security and farmers' lives. Therefore, it is imperative that every country draws up mitigation and adaptation policies to cope with the climate change impacts anticipated. Adaptation in the agricultural sector is vital to guarantee food security and to protect the sources of revenue of the poor whose main livelihood is derived from farming.

In this study, adaptation measures at farm and government level were discussed. Farm-level adaptation includes adopting crop modification, soil conservation, irrigation, change in crop calendars and planting trees. However, to ensure success of these adaptation measures, the government should become involved and support farmers financially and technologically. The government should adopt a multi-step framework to cope with the adverse impacts of climate change and this involves water management strategies, research and development, regional cooperation, new irrigation schemes and sustainable agriculture technologies.

It appears that climate change will have different impacts on these two regions: the Tigris Basin is likely to experience higher temperatures and lower rainfalls, whereas the Fitzroy Basin may be wetter and hotter in the long run. To avoid future generations having to pay a premium price to deal with the adverse effects of climate change, it is imperative that these aspects are taken into consideration in formulating climate change policies for both regions. Relevant policies to deal with climate change in the field of water resources may include, for instance, recycling of waste water, steps and measures to mitigate and adapt to these impacts through (for example) water-reuse measures, water-sensitive urban infrastructure design such as rainwater tanks, rain gardens and constructed wetland, and growing plants tolerant to drought.

8.2 Conclusion

The SWAT model was used to identify the impacts of climate change on water resources in two different regions, the Tigris Basin and the Fitzroy Basin. The model was successfully calibrated for both regions. The calibrated model was used to evaluate the climate change impact for the near and distant future periods of 2046-2064 and 2080-2100.

The findings from the SWAT model revealed that the water resources of the Tigris and Fitzroy Basins are likely to undergo alterations due to climate change, and, most likely, for the worse. For the Tigris Basin, forecasts on the availability of water resources show declining trends. The basin will get drier and hotter. For the Fitzroy Basin, the results show that the basin will get wetter and hotter. Since water is a precious resource and limited for the regions, a policy to deal with adversity in the future is warranted. The two basins have vastly different socio-economic settings, population density, infrastructure, and resourcing capabilities, and therefore their optimal planning and strategies are expected to be vastly different. No doubt pre-emptive intervention and pro-active actions will be highly beneficial and cost-efficient in the long run for the future generations. The outcomes of this study may prove useful for supporting decision makers in planning relevant adaptation and mitigation measures, and thus decreasing the adverse impacts on water resources in both basins.

This study built a SWAT Tigris and Fitzroy framework that integrates micro-level data on weather, land use, soil and management obtained from Iraqi and Australian databases. Such a large-scale work involves rigorous analysis and provides justification for more reliable predictions than simple models.

The main objectives of this thesis were met in this research as follows.:

1. Determination of the performance and suitability of the three tool s– GIS, SWAT, and statistical analyses.

   Through the calibration and validation, it has been found that SWAT embedded in GIS and other statistical analysis model performed well. The model was calibrated and validated at nine discharge stations in northeast Iraq and at seven discharge stations in the Fitzroy Basin to simulate the streamflow, using the SUFI-2 algorithm. The performance of the model was found to be acceptable with R^2 and ENC indices (where both indices were higher than 0.5, which is considered satisfactory) during the calibration and validation periods.

2. Improved understanding of the existing hydrological systems and insight as to how changes in climate (rainfall and temperature) may affect and alter streamflow regimes and other hydrological processes under different climatic scenarios.

   The climate change impacts in the last three decades (1978-2014) were analyzed for both regions. The models indicated that in both regions there were trends of increasing temperatures. The precipitation trends showed a negative slope for the Tigris Basin but positive slope for the Fitzroy region, although the precipitation trends were variable. Both regions have already experienced extreme changes in the weather. These changes in temperature and precipitation have led to alteration in stream flow regimes for both regions. The Tigris Basin has already suffered from water scarcity per capita. The five tributaries' flows declined by 15% overall in the last three decades. For the Fitzroy Basin, the analysis showed that almost the whole basin had sufficient water in the last three decades, albeit with highly variable trends.

3. Identification and understanding of the various aspects of implications of climate change in these regions.

   The SWAT model was applied for both regions using the average of six GCMs models to investigate the impacts of climate change on water resources (blue water, green water) in the near future (2046-2064) and distant future (2089-20100) periods. The results were presented in detail in Chapter 6. Overall, the Tigris River will experience severe drought in both periods, and the distant future will be worse. For the Fitzroy River, the study showed that the region will be wetter and hotter and subject to more frequent floods, especially in the Isaac Basin.

4. Development of suitable tools which could be used by organizations to account for climate change impacts adaptations and vulnerability in their planning and management strategies.

   This has been discussed in Chapter 7. That chapter looked into the concept of vulnerability in the context of climate change and its three features – exposure, sensitivity and adaptive capacity – and described adaptation and mitigation measures that could be embraced to respond to climate change.

The novelty of the work in this thesis includes many facets. For the Tigris Basin, many disparate sources of knowledge and information have been brought together to build a cohesive hydrometeorological insight of the basin. Next, the most advanced hydrological models, which have been tried and tested in developed countries, were applied to the basin for the first time, and basin parameters were estimated which can be used in any future modelling scheme. The opinions of farmers, who are the dominant community in the region were explored in regard to their experiences with climate change, and any adaptation measures they were implementing, and these were compared with suggested adaptation measures in published literature from experts. For the Fitzroy River, a distributed model for the entire basin to capture its hydrometeorological characteristics was applied for the first time, although detailed modelling of parts of the basin was undertaken done earlier by other researchers. In that model, outputs from GCMs were inputted to capture the effects of climate change, with particular emphasis on impacts on water resources. All these contributions have expanded the horizon of current knowledge about the two basins.

8.3 Future research

Future Tigris and Fitzroy climate change research should be carried out with up-to-date land use data that can provide better insight into flow patterns and environmental impacts for present and future climatic patterns. These were simplified in the present study due to lack of data.

Further extensive assessment of possible climate change impacts on watershed hydrology should be conducted with a higher combination of different GCMs. As computers become more powerful, higher complexity in problem delineation can be added.

The SWAT model should be assessed for the impacts of ponds and wetlands, which have been ignored in this study because of non-availability of data.

Model uncertainties require further work to better understand the limitations of simulations.

References

Abbaspour, K. C., J. Yang, I. Maximov, R. Siber, K. Bogner, J. Mieleitner, J. Zobrist and R. Srinivasan (2007). "Modelling hydrology and water quality in the pre-alpine/alpine Thur watershed using SWAT." Journal of Hydrology, vol.333, no.2, pp. 413-430.

Abbaspour, K., C. Johnson and M. T. Van Genuchten (2004). "Estimating uncertain flow and transport parameters using a sequential uncertainty fitting procedure." Journal of Vadose Zone, vol. 3, no.4, pp. 1340-1352.

Abdulla, F. and L. Al-Badranih (2000). "Application of a rainfall-runoff model to three catchments in Iraq." Journal of Hydrological Sciences, vol. 45, no.1, pp.13-25.

Adger, W.N., S. Agrawala, M.M.Q. Mirza, C. Conde, K. O'Brien, J. Pulhin, R. Pulwarty, B. Smit and K. Takahashi, (2007). "Assessment of adaptation practices, options, constraints and capacity. Climate Change 2007: Impacts, Adaptation and Vulnerability". Contribution of Working Group II to the Fourth Assessment Report of the Intergovernmental Panel on Climate Change, M.L. Parry, O.F. Canziani,J.P. Palutikof, P.J. van der Linden and C.E. Hanson, Eds., Cambridge University Press, Cambridge, UK, 717-743.

Al-Ansari, N. and S. Knutsson (2011). "Toward prudent management of water resources in Iraq." Journal of Advanced Science and Engineering Research, vol. 1, no.1, pp.53-67.

Al-Ansari, N., A. A. Ali and S. Knutsson (2014). "Present Conditions and Future Challenges of Water Resources Problems in Iraq." Journal of Water Resource and Protection, vol. 6, pp 1066-1098.

Al-Ansari, N., M. Abdellatif, M. Ezeelden, S. S. Ali and S. Knutsson (2014). "Climate Change and Future Long-Term Trends of Rainfall at North-East of Iraq." Journal of Civil Engineering and Architecture, vol. 8, pp.790-805.

Alexander, L. V. and J. M. Arblaster (2009). "Assessing trends in observed and modelled climate extremes over Australia in relation to future projections." International Journal of Climatology, vol. 29, no.3, pp. 417-435.

Al-Faraj, F. A. and M. Scholz (2014). "Incorporation of the flow duration curve method within digital filtering algorithms to estimate the base flow contribution to total runoff." Journal of Water Resources Management, vol.28, no, 15, pp. 5477-5489.

Al-Kadhimi, A. M., L. A. Ahmed and R. Y. A. Al-Mphergee (2011). "Runoff Curves Development for Al-Adhaim Catchment Using Digital Simulation Models." Jordan Journal of Civil Engineering vol.5, no.2.

Al-Mukhtar, M., V. Dunger and B. Merkel (2014). "Assessing the impacts of climate change on hydrology of the upper reach of the spree river: Germany." Journal of Water Resources Management, vol. 28, no.10, pp. 2731-2749.

Ammann, C.M., Joos, F., Schimel, D.S., Otto-Bliesner, B.L. and Tomas, R.A. (2007). “Solar influence on climate during the past millennium: Results from transient simulations with the NCAR climate system model”, Proceedings of the National Academy of Sciences of the United States of America, 104(10), pp. 3713-3718.

Angulo R, Diaz Y and Pardo R, 2016, The Colombian multidimensional poverty index: Measuring poverty in a public policy context. Social Indicators Research 127:1-38, Doi: 10.1007/s11205-015-0964-z

Arnold, J. G., R. Srinivasan, Muttiah, Williams (1998). Large area hydrologic modelling and assessment part I: Model development1, Journal of the American Water Resources Association, vol.34, no.1, pp.73-89.

Arnold, J., J. Kiniry, Williams (2012). Soil and water assessment tool. Theoretical documentation. Version 2012, Agriculture Research Service, USA.

ASCE. (1993). “Criteria for evaluation of watershed models” Journal of Irrigation and Drainage Engineering, vol. 119, no.3, pp. 429-442.

Ashraf Vaghefi, S., Mousavi, S. J., Abbaspour, K. C., Srinivasan, R., & Yang, H. (2014). “Analyses of the impact of climate change on water resources components, drought and wheat yield in semiarid regions: Karkheh River Basin in Iran”. Journal of Hydrological Processes, vol.28, no.4, pp. 2018-2032.

Australian Burreau of statistics (2014). “Australia’s Population”, viewed 23 December 2014, http://www.abs.gov.au/AUSSTATS/abs@.nsf/Web+Pages/Population+Clock?opendocument #from-banner=LN.

Bannwarth, M. A., Sangchan, W., Hugenschmidt, C., Lamers, M., Ingwersen, J., Ziegler, A. D., & Streck, T. (2014). “Pesticide transport simulation in a tropical catchment by SWAT”. Journal of Environmental Pollution, vol.191, no. 70-79.

Bingner, R. L. (1996). “Runoff simulated from Goodwin Creek watershed using SWAT”. Transactions of the ASAE, vol. 39, no.1, pp. 85-90.

Bryan, E., T. T. Deressa, G. A. Gbetibouo and C. Ringler (2009). "Adaptation to climate change in Ethiopia and South Africa: options and constraints." Journal of Environmental Science & Policy, vol. 12, no.4, pp. 413-426.

Cai, W., A. Purich, T. Cowan, P. van Rensch and E. Weller (2014). "Did Climate Change–Induced Rainfall Trends Contribute to the Australian Millennium Drought?" Journal of Climate, vol. 27, no.9, pp. 3145-3168.

Chambers, L. E., L. Hughes and M. A. Weston (2005). "Climate change and its impact on Australia's avifauna." Journal of Bird Life Australia, vol.105, no.1, pp. 1-20.

Cheng, L., Xu, Z. X., Luo, R., & MI, Y. J. (2009). “SWAT application in arid and semi-arid region: A case study in the Kuye River Basin”. Journal of Geographical Research, vol. 1, pp. 008.

Chowdhury, R. K., S. Beecham, Boland, Piantados (2014). "Understanding South Australian rainfall trends and step changes." International Journal of Climatology, vol. 35, no. 3, pp. 348-360.

Church, J. A., J. R. Hunter, K. L. McInnes and N. J. White (2006). "Sea-level rise around the Australian coastline and the changing frequency of extreme sea-level events." Australian Meteorological Magazine, vol. 55, no.4, pp. 253-260.

Cibin, R., K. Sudheer and I. Chaubey (2010). "Sensitivity and identifiability of stream flow generation parameters of the SWAT model." Journal of Hydrological processes, vol. 24, no. 9, pp. 1133-1148.

Clarke, H., C. Lucas and P. Smith (2013). "Changes in Australian fire weather between 1973 and 2010." International Journal of Climatology, vol.33, no. 4, pp. 931-944.

Cobon, D., N. Toombs, Zhang (2007). “Climate change impacts on the sediment load for the Nogoa catchment of the Fitzroy Basin”. MODSIM 2007 International Congress on Modelling and Simulation, Queensland.

Coffey, R., B. Benham, Krometis (2014). "Assessing the Effects of Climate Change on Waterborne Microorganisms: Implications for EU and US Water Policy." International Journal of Human and Ecological Risk Assessment, vol.20, no.3, pp. 724-742.

Delpla, I., A.-V. Jung, Baures, Clement, Thomas (2009). "Impacts of climate change on surface water quality in relation to drinking water production." International Journal of Environment, vol, 35, no. 8, pp. 1225-1233.

Deressa, T. T., R. M. Hassan, C. Ringler, T. Alemu and M. Yesuf (2009). "Determinants of farmers' choice of adaptation methods to climate change in the Nile Basin of Ethiopia." Journal of Global environmental change, vol. 19, no.2, pp. 248-255.

Dougall, C (2014). “Modelling reductions of pollutant loads due to improved management practices in the Great Barrier Reef catchments.” Techincal Report, Department of Natural Resource and Mines, Rockhampton.

Elasha, B. O. (2010). "Mapping of climate change threats and human development impacts in the Arab region." United Nations Development Programme, Arab Human Development report , Report–Research Paper Series, 2010, United Arab Emirates.

Elliot, W. J. and D. E. Hall (1997). “Water erosion prediction project (WEPP) forest applications.” US Department of Agriculture, Forest Service, Intermountain Research Station Ogden, USA.

Falkenmark, M., (1989). “The Massive Water Scarcity now Threatening Africa: Why isn't it being Addressed?.” Ambio, vol. 18, no. 2, pp. 2-118.

Faramarzi, M., Abbaspour, K. C., Schulin, R., & Yang, H. (2009). “Modelling blue and green water resources availability in Iran.” Journal of Hydrological Processes, vol. 23, no.3, pp. 486-501.

Fellmann, T. (2012). "The assessment of climate change-related vulnerability in the agricultural sector: reviewing conceptual frameworks." Building resilience for adaptation to climate change in the agriculture sector, FAO/OECD Workshop , vol.23, no. 37.

Fu, C., A. James, Yao (2012). “SWAT-CS: Revision and testing of SWAT (Soil and Water Assessment Tool) for forested Canadian Shield watersheds.” AGU Fall Meeting Abstracts, Canada.

Gebrehiwot, T. and A. van der Veen (2013). “Farm level adaptation to climate change: the case of farmer’s in the Ethiopian Highlands.” Journal of Environmental Management, vol.52, no.1, pp. 29-44.

Ghaffari, G., Keesstra, S., Ghodousi, J., & Ahmadi, H. (2010). “SWAT - simulated hydrological impact of land-use change in the Zanjanrood basin, Northwest Iran.” Journal of Hydrological processes, vol. 24, no. 7, pp. 892-903.

Githui, F., Gitau, W., Mutua, F., & Bauwens, W. (2009). “Climate change impact on SWAT simulated streamflow in western Kenya. “ International Journal of Climatology, vol. 29, no.12, pp. 1823-1834.

Goodchild, M., R. Haining and S. Wise (1992). “Integrating GIS and spatial data analysis:problems and possibilities.” International Journal of Geographical Information Systems.” Vol. 6, no.5, pp. 407-423.Government of Queensland (2014). “The Critical Decade: Queensland climate impacts and opportunities.” viewed 18 April 2016, https://www.nccarf.edu.au/localgov/resources/critical-decade-queensland-climate-impacts-and-opportunty.

Greater Barrier Reef Marine Park Authority (2017). "Final report: 2016 coral bleaching event on the Great Barrier Reef" viewed 18 June 2020, http://elibrary.gbrmpa.gov.au/jspui/bitstream/11017/3206/1/Final-report-2016-coral-bleaching-GBR.pdf

Green, W. H. and G. Ampt (1911). "Studies on soil physics, 1. The flow of air and water through soils." Journal of Agriculture Science, vol. 4, pp. 1-24.Gregory, J. and P. Huybrechts(2006). "Ice-sheet contributions to future sea-level change." Philosophical Transactions of the Royal Society of London A: Mathematical, Physical and Engineering Sciences, vol. 364, no. 1844, pp. 1709-1732.

Greg. J (2020). "Australia has a problem with climate change denial. The message just isn't getting through." viewed 18 April 2020, https://www.theguardian.com/business/grogonomics/2020/jun/16/australians-arent-worried-about-climate-change-the-message-just-isnt-getting-through.

Güngör, Ö. and S. Göncü (2013). "Application of the soil and water assessment tool model on the Lower Porsuk Stream Watershed." Journal of Hydrological Processes, vol. 27, no,3, pp. 453-466.

Guo, H., Hu, Q., & Jiang, T. (2008). “Annual and seasonal streamflow responses to climate and land-cover changes in the Poyang Lake basin, China.” Journal of Hydrology, vol.355, no. 1, pp. 106-122.

Hargreaves, G.L., Hargreaves, G.H. and Riley, J.P., (1985).”Agricultural benefits for Senegal River basin.” Journal of irrigation and Drainage Engineering, vol. 111, no.2,pp.113-124.

Head, A. M., Helen V.McGregor (2014). "Climate change and Australia." Wiley Interdisciplinary Reviews, vol. 5, no. 22.

Hegerl, G. C., H. voN SToRcH, K. Hasselmann, B. D. Santer, U. Cubasch and P. D. Jones (1996). "Detecting greenhouse-gas-induced climate change with an optimal fingerprint method." Journal of Climate, vol. 9, no.10, pp. 2281-2306.

Higgins, Darin Wayne, and Dan Martin Scott. "System and method for synchronizing raster and vector map images." U.S. Patent 7,161,604, issued January 9, 2007.

Hoegh-Guldberg, O. (1999). "Climate change, coral bleaching and the future of the world's coral reefs." Marine and freshwater research 50(8): 839-866.

Holthaus,E 2014. “Is climate change destabilizing Iraq?” , viewed on 7th October 2016 http://www.slate.com/articles/technology/future_tense/2014/06/isis_water_scarcity_is_climate_change_destabilizing_iraq.html

Huang, Q. H., & Zhang, W. C. (2004). “Improvement and application of GIS-based distributed SWAT hydrological modeling on high altitude, cold, semi-arid catchment of Heihe River Basin.” Journal of Nanjing Forestry University, vol. 2004, no.2.

Hughes, L. (2003). "Climate change and Australia: trends, projections and impacts." Journal of Austral Ecology, vol. 28, no. 4, pp. 423-443.

Fadeil, M. (2016). “Spatial and temporal patterns of climate change in Iraq.” Al-Kufa University, Najaf, Iraq.

IPCC, (2007). “Climate Change 2007: impacts, adaptation and vulnerability”: contribution of Working Group II to the fourth assessment report of the Intergovernmental Panel on Climate Change, Cambridge University Press.

IPCC, (2014). “Climate Change 2014 The Physical Science Basis”: contribution of Working Group I to the fifth assessment report of the Intergovernmental Panel on Climate Change, Cambridge University Press.

Iraqi Ministry of Water Resources (2015), climate change analysis in North of Iraq, viewed on 20 April 2015, https://www.developmentaid.org/#!/donors/view/34731/republic-of-iraq-ministry-of-water-resources.

Issa, I. E., N. Al-Ansari, G. Sherwany and S. Knutsson (2014). "Expected Future of Water Resources within Tigris-Euphrates Rivers Basin, Iraq." Journal of Water Resource and Protection, vol. 6, pp.421-432 2014.

Jakeman, A., I. Littlewood and P. Whitehead (1990). "Computation of the instantaneous unit hydrograph and identifiable component flows with application to two small upland catchments." Journal of hydrology, vol. 117, no1-4, pp. 275-300.

Janabi (2013). “Climate Change Impact on Iraqi Water and Agriculture Sectors”, viewed 18 December 2014,< http://iraqieconomists.net/en/2013/04/05/climate-change-impact-on-iraqi-water-and-agriculture-sectors/>

Jang, J. H., Jung, K. W., & Yoon, C. G. (2012). “Modification of SWAT model for simulation of organic matter in Korean watersheds.” Journal of Water Science and Technology, vol. 66, no.11, pp. 2355-2362.

Jeong, D.I. and Kim, Y.O., 2005. “Rainfall-runoff models using artificial neural networks for ensemble streamflow prediction”. Hydrological Processes: An International Journal, vol. 19, no.19, pp.3819-3835.

Kafia, M. S., G. M. Slaiman and M. S. Nazanin (2009). "Physical and chemical status of drinking water from water treatment plants on greater Zab River." Journal of Applied Sciences and Environmental Management, vol.13, no. 3.

Karoly, D. J. and K. Braganza (2005). "Attribution of recent temperature changes in the Australian 64region." Journal of Climate, vol. 18, no. 3, pp. 457-464.

Karoly, D., J. Risbey, Reynolds (2002). "Global warming contributes to Australia’s worst drought."viewed 8 June 2014, <http://www.wwf.org.au/News_and_information/Publications/PDF/Report/drought_report.pd>

Keenan, T. and H. Cleugh (2011). “Climate science update”: a report to the 2011 Garnaut Review, Centre for Australian Weather and Climate Research, Canberra.

Klosterman, R. E. (1991). “Principles of geographic information-systems for land resource assessment-Burrough.” PA, AMER Planning ASSN 1313 EAST 60 STREET, CHICAGO, IL 60637-2891.

Lange, N. (1999). "New mathematical approaches in hydrological modelling an application of artificial neural networks." Journal of Physics and Chemistry of the Earth, Part B: Hydrology, Oceans and Atmosphere, vol. 24, no.1, pp. 31-35.

Leavesley, G. H. (1994). "Modeling the effects of climate change on water resources-a review." Journal of Climatic Change, vol. 28, no. 1-2, pp. 159-177.

Legates, D. R. and G. J. McCabe (1999). "Evaluating the use of “goodness-of-fit” measures in hydrologic and hydroclimatic model validation." Journal of Water resources research, vol. 35, no.1,pp. 233-241.

Li, X., Li, Z. J., & Dong, J. R. (2009). “Application of SWAT model in runoff simulation in upper reaches of Yihe River.” Journal of Hohai University: Natural Sciences, vol. 37, no. 1, pp. 23-26.

Lough, J. (2008). "Shifting climate zones for Australia's tropical marine ecosystems." Geophysical Research Letters, vol. 35, no. 14.

Lough, J. M. (2007). "Tropical river flow and rainfall reconstructions from coral luminescence: Great Barrier Reef, Australia." viewed 13 August 2914, <http://onlinelibrary.wiley.com/doi/10.1029/2006PA001377/pdf>

Lough, J. M. and A. J. Hobday (2011). "Observed climate change in Australian marine and freshwater environments." Marine and Freshwater Research, vol. 62, no.9, pp. 984-999.

Luo, Y., D. L. Ficklin, Zhang (2013). "Assessment of climate change impacts on hydrology and water quality with a watershed modelling approach." Journal of Science of the Total Environment, vol. 450, pp. 72-82.

Medany, M. (2008). "Impact of climate change on Arab countries." Journal of Europe, vol. 22, no. 22, pp. 8.

Mimikou, M., E. Baltas, Varanou, Pantazis (2000). "Regional impacts of climate change on water resources quantity and quality indicators." Journal of Hydrology, vol. 234, no.1, pp. 95-109.

Monteith, J. (1965). “Evaporation and the environment, the state and movement of water in living organisms”. XIXthe Symposium, Cambridge University Press, Swansea.

Morgan, R., J. Quinton, Smith (1998). "The European Soil Erosion Model (EUROSEM): a dynamic approach for predicting sediment transport from fields and small catchments." Journal of Earth Surface Processes and Landforms, vol, 23, no.6, pp. 527-544.

Moriasi, D., Arnold, J., Van Liew, M., Bingner, R., Harmel, R. & Veith, T. (2007). “Model evaluation guidelines for systematic quantification of accuracy in watershed simulations”, Journal of Soil and Water Division of American Society of Agricultural and Biological Engineers, vol, 50, pp. 885-900.

Mosley, L. M., B. Zammit, Leyden, Heneker. (2012). "The impact of extreme low flows on the water quality of the Lower Murray River and Lakes (South Australia)." Journal of Water Resources management, vol, 26, no.13, pp. 3923-3946.

Murdoch, P. S., J. S. Baron, Miller (2000). "Potential effects of climate change on surface-water quality in North America1." Journal of the American Water Resources Association, vol. 36, no.2, pp. 347-366.

Nancarrow,D. (2011).” 2010: Queensland's wettest year on record.” Viewed on 17th November 2015, https://www.smh.com.au/environment/weather/2010-queenslands-wettest-year-on-record-20110105-19fnx.html.

Nash, J. and J. V. Sutcliffe (1970). "River flow forecasting through conceptual models part I—A discussion of principles." Journal of hydrology, vol.10, no.3, pp. 282-290.

Ndomba, P., Mtalo, F. and Killingtveit, A. (2008). “SWAT model application in a data scarce tropical complex catchment in Tanzania.” Physics and Chemistry of the Earth, Parts A/B/C, 33(8-13), pp.626-632.

Nearing, M., G. Foster, Lane, Finkner (1989). "A process-based soil erosion model for USDA-Water Erosion Prediction Project technology." Journal of American Society of Agriculture Engineer, vol.32, no.5, pp 1587-1593.

Nearing, M., L. Lane, Lopes (1994). "Modelling soil erosion." Soil erosion research methods2, pp.127-156.

Nicholls, N., W. Drosdowsky, Lavery (1997). "Australian rainfall variability and change." Journal of Weather, vol. 52, no. 3, pp. 66-72.

Nielsen, S. A. and E. Hansen (1973). "Numerical simulation of the rainfall-runoff process on a daily basis." Journal of Hydrology Research, vol. 4, no.3, pp. 171-190.

Nietsch, S. L., Arnold, J. G., Kiniry, J. R., & Williams, J. R. (2011). “Soil and water assessment tool theoretical documentation version 2009.” Texas Water Resources Institute. Texas.

Nietsch, S., J. Arnold, Williams (2005). "Soil and water assessment tool theoretical documentation. version 2000." Texas Water Resource Institute, College Station, Texas.

Orindi, V. and S. Eriksen. (2005). “Mainstreaming adaptation to climate change in the development process in Uganda.” Ecopolicy series no. 15, Acts Press, Nairobi, Kenya.

Owor, M., R. Taylor, Tindimugaya (2009). "Rainfall intensity and groundwater recharge: empirical evidence from the Upper Nile Basin." Environmental Research Letters, vol.4, no.3, pp. 035009.

Pechlivanidis, I., B. Jackson, McIntyre (2011). "Catchment scale hydrological modelling: a review of model types, calibration approaches and uncertainty analysis methods in the context of recent developments in technology and applications." Journal of Global NEST, vol. 13, no.3, pp. 193-214.

Petter, P. (1992). "GIS and Remote Sensing for Soil Erosion Studies in Semi-arid Environments." PhD, University of Lund, Sweden.

Priestley, C. and R. Taylor (1972). "On the assessment of surface heat flux and evaporation using large-scale parameters." Journal of American Meteorological Society, vol.100, no.2, pp.81-92.

Pruski, F. and M. Nearing (2002). "Runoff and soil-loss responses to changes in precipitation: A computer simulation study." Journal of soil and Water Conservation, vol.57, no. 1, pp. 7-16.

Queensland Floods Commission (2011).”Summary of weather and flood events.” Viewed on 13th October 2017, http://www.floodcommission.qld.gov.au/__data/assets/pdf_file/0007/8782/QFCI-Interim-Report-Chapter-1-Summary-of-weather-and-flood-events.pdf.

Ragab, R. and C. Prudhomme (2002). "Swt—soil and Water: climate change and water resources management in arid and semi-arid regions: prospective and challenges for the 21st century." Journal of Biosystems Engineering, vol. 81, no.1, pp.3-34.

Raghavan, S. V., V. M. Tue and L. Shie-Yui (2014). "Impact of climate change on future stream flow in the Dakbla river basin." Journal of Hydroinformatics, vol.16, no.1, pp. 231-244.

Rijsberman, F. R. (2006). “Water Scarcity: Fact or Fiction?” Journal of Agricultural Water Management, vol, 80 , no., pp. 5-22.

Risbey, J. S. (2011). "Dangerous climate change and water resources in Australia." Journal of Regional Environmental Change, vol.11, no.1, pp. 197-203.

Risbey, J. S., M. J. Pook, McIntosh (2009). "On the remote drivers of rainfall variability in Australia." Journal of American Meteorological Society, vol.37, no.10, pp.: 3233-3253.

Rolfe, J., K. Alam, Windle (2004). "Overview of the Fitzroy Basin and opportunities for offset trading." Establishing The Potential for Offset Trading in the Lower Fitzroy River Research Reports(1), Queensland.

Rostamian, R., A. Jaleh, Afyuni (2008). "Application of a SWAT model for estimating runoff and sediment in two mountainous basins in central Iran." Hydrological Sciences Journal, vol. 53, no.5, pp. 977-988.

Rotstayn, L. D., W. Cai, Dix (2007). "Have Australian rainfall and cloudiness increased due to the remote effects of Asian anthropogenic aerosols?" Journal of Geophysical Research: Atmospheres, vol. 12, pp.1984–2012.

Saeedrashed, Y. and A. Guven (2013). "Estimation of Geomorphological Parameters of Lower Zab River-Basin by Using GIS-Based Remotely Sensed Image." Journal of Water resources management, vol. 27, no.1, pp. 209-219.

Sanadhya, P., J. Gironás and M. Arabi (2014). "Global sensitivity analysis of hydrologic processes in major snow-dominated mountainous river basins in Colorado." Journal of Hydrological Processes, vol. 28, no. 9, pp. 3404-3418.

Santer, B. D., K. E. Taylor, T. M. Wigley, J. E. Penner, P. D. Jones and U. Cubasch (1995). "Towards the detection and attribution of an anthropogenic effect on climate." Journal of Climate Dynamics, vol. 12, no. 2, pp. 77-100.

Santhi, C., J. G. Arnold, J. R. Williams, W. A. Dugas, R. Srinivasan and L. M. Hauck (2001). "Validation of the swat model on a large rwer basin with point and nonpoint sources1", Journal of the American Water Resources Association, vol, 37, no. 5, pp. 1169-1188.

Schilling, K. E., M. K. Jha, Zhang (2008). "Impact of land use and land cover change on the water balance of a large agricultural watershed: Historical effects and future directions." Journal of Water Resources Research, vol. 44, no. 7, pp.1-12.

Schuol, J. and K. Abbaspour (2007). "Using monthly weather statistics to generate daily data in a SWAT model application to West Africa." Journal of Ecological Modelling, vol. 201, no. 3 pp. 301-311.

Schuol, J., K. C. Abbaspour, H. Yang, R. Srinivasan and A. J. Zehnder (2008). "Modelling blue and green water availability in Africa." Journal of Water Resources Research, vol.44, no.7.

Setegn, S. G. (2010). "Modelling hydrological and hydrodynamic processes in lake Tana basin, Ethiopia.PH.D thesis, Royal Institute of Technology, Sweden"

Setegn, S. G., R. Srinivasan and B. Dargahi (2008). "Hydrological modelling in the Lake Tana Basin, Ethiopia using SWAT model." Journal of Open Hydrology, vol. 2, no.1.

Somville, M. and N. De Pauw (1982). "Influence of temperature and river discharge on water quality of the Western Scheldt estuary." Journal of Water Research, vol. 16, no.8, pp. 1349-1356.

Steffen, W. L., L. Hughes, V. Sahajwalla and G. Hueston (2012). The Critical Decade: Queensland climate impacts and opportunities, Climate Commission Secretariat (Department of Climate Change and Energy Efficiency). Queensland.

Sullivan C, 2002, Calculating a Water Poverty Index. World Development 30: 1195-1210

Tait, M. G. (2005). "Implementing geoportals: applications of distributed GIS." Journal of Computers, Environment and Urban Systems, vol. 29, no.1, pp. 33-47.

Timbal, B. and D. Jones (2008). "Future projections of winter rainfall in southeast Australia using a statistical downscaling technique." Journal of Climatic Change, vol.86, no 1-2, pp. 165-187.

Tingsanchali, T. and M. R. Gautam (2000). "Application of tank, NAM, ARMA and neural network models to flood forecasting." Journal of Hydrological Processes, vol. 14, no. 14, pp. 2473-2487.

UN-ESCWA, B. G. R. (2013). “United Nations economic and social commission for western Asia.” Bundesanstalt für Geowissenschaften und Rohstoffe. *Inventory of Shared Water Resources in Western Asia, Beirut*.

United State Department of Agriculture (2102),” Climate change in Iraq.” viewed 8 January 2015,<

iq.one.un.org/.../Climate%20change%20In%20Iraq%20Fact%20sheet%20- %20English.pdf>

Van Vliet, M. and J. Zwolsman (2008). "Impact of summer droughts on the water quality of the Meuse river." Journal of Hydrology 353(1): 1-17.

Van Vliet, M., F. Ludwig, and Zwolsman (2011). "Global river temperatures and sensitivity to atmospheric warming and changes in river flow." Journal of Water Resources Research, vol.47, no.2, pp. 1-19.

Veith, T., M. Van Liew, D. Bosch and J. Arnold (2010). "Parameter sensitivity and uncertainty in SWAT: A comparison across five USDA-ARS watersheds." Transactions of the ASABE 53(5): 1477-1485.

White, K. L., & Chaubey, I. (2005). Sensitivity analysis, calibration, and validations for a multisite and multivariable SWAT model. JAWRA Journal of the American Water Resources Association, vol. 41, no.5,pp. 1077-1089.

Whitehead, P., R. Wilby, Battarbee (2009). "A review of the potential impacts of climate change on surface water quality." Journal of Hydrological Sciences, vol. 54, no.1, pp. 101-123.

Wieczorek, W. F. and A. M. Delmerico (2009). "Geographic information systems." Wiley Interdisciplinary Reviews: Journal of Computational Statistics. Vol. 1, no.2, pp.167-186.

Williams, J. R. (1975). "Sediment-yield prediction with universal equation using runoff energy factor.", In: Present and Prospective Technology for Predicting Sediment Yields and Sources. U.S. Dept. USA.

Williamson, T., H. Hesseln and M. Johnston (2012). "Reprint of: Adaptive capacity deficits and adaptive capacity of economic systems in climate change vulnerability assessment." Forest Policy and Economics 24: 48-54.

Wilson, C. O. and Q. Weng (2011). "Simulating the impacts of future land use and climate changes on surface water quality in the Des Plaines River watershed, Chicago Metropolitan Statistical Area, Illinois." Journal of Science of the Total Environment, vol. 409, no. 20, pp. 4387-4405.

Winchell, M., R. Srinivasan, M. Di Luzio and J. Arnold (2007). "Arc-SWAT interface for SWAT2005-User’s guide." USDA Agricultural Research Service and Texas A&M Blackland Research Center, Temple, Texas.

Winter, J. M. and E. A. Eltahir (2012). "Modelling the hydroclimatology of the midwestern United States. Part 1: current climate." Journal of Climate dynamics, vol. 38, no. 3-4,pp. 573-593.

Wu, K. and C. A. Johnston (2007). "Hydrologic response to climatic variability in a Great Lakes Watershed: A case study with the SWAT model." Journal of Hydrology, vol. 337, no.1 pp. 187-199.

Wu, Y., S. Liu, Gallant (2012). "Predicting impacts of increased CO 2 and climate change on the water cycle and water quality in the semiarid James River Basin of the Midwestern USA." Journal of Science of the Total Environment, vol. 430, pp. 150-160.

Xiuwan, C.J.C. (2004). “Water Balance of the SWAT Model and Its Application in the Suomo Basin.” Journal of Acta Scicentiarum Naturalum Universitis Pekinesis, vol.2, pp. 15.

Xuan, Z. and N.-B. Chang (2014). "Modelling the climate-induced changes of lake ecosystem structure under the cascade impacts of hurricanes and droughts." Journal of Ecological Modelling, vol.288, pp.79-93.

Yang, J., P. Reichert, K. Abbaspour, J. Xia and H. Yang (2008). "Comparing uncertainty analysis techniques for a SWAT application to the Chaohe Basin in China." Journal of Hydrology, vol. 358, no. 1, pp. 1-23.

Young, P. (1998). “Data-based mechanistic modelling of environmental, ecological, economic and engineering systems.” Journal of Environmental Modelling & Software, vol. 13, no.2, pp.105-122.

Young, R. A., C. Onstad, and Bosch (1989). "AGNPS: A nonpoint-source pollution model for evaluating agricultural watersheds." Journal of soil and water conservation, vol. 44, no.2, pp. 168-173.

YU, B., JOO, M. and Caroll, C (2013). “Land use and water quality trends of the Fitzroy River, Australia.” *Understanding Freshwater Quality Problems in a Changing World Proceedings of H, 4,* pp.1-8, Sweden.

Yu, P.-S., T.-C. Yang, Wu (2002). "Impact of climate change on water resources in southern Taiwan." Journal of Hydrology, vol. 260, no.1, pp. 161-175.

Zakaria, S., N. Al-Ansari and S. Knutsson (2013). "Historical and future climatic change scenarios for temperature and rainfall for Iraq." Journal of Civil Engineering and Architecture, vol. 7, pp. 1574-1594.

Zang, C., J. Liu, M. Velde and F. Kraxner (2012). "Assessment of spatial and temporal patterns of green and blue water flows under natural conditions in inland river basins in Northwest China." Hydrology and Earth System Sciences 16(8): 2859-2870.

Zhang, Xuesong, Raghavan Srinivasan, and Fanghua Hao (2007) "Predicting hydrologic response to climate change in the Luohe River basin using the SWAT model." Transactions of the ASABE 50, no. 3 (2007): 901-910.

Zhou, F., Xu, Y., Chen, Y., Xu, C. Y., Gao, Y., & Du, J. (2013).” Hydrological response to urbanization at different spatio-temporal scales simulated by coupling of CLUE-S and the SWAT model in the Yangtze River Delta region.” Journal of Hydrology, 485, 113-125.